TH60026A

Contract No.: NAS8-39880

TSNE
IN-18-CR
DOT.
93105

TETHERED SATELLITE SYSTEM (TSS) DYNAMICS ASSESSMENTS AND ANALYSES TSS-1R POST FLIGHT DATA EVALUATION

14 June 1996

Submitted to:

GEORGE C. MARSHALL SPACE FLIGHT CENTER
MARSHALL SPACE FLIGHT CENTER, AL. 35812

Prepared by:

John R Glaese

Dr. John R. Glaese
Program Manager

Management Approval:

J. Brooks Moore

F. Brooks Moore
Division Manager

SYSTEMS

Control Dynamics, Div. of bd System
600 Boulevard South, Suite 304
Huntsville, AL 35802
Bus: (205) 882-2650 Fax: (205) 882-2683

TETHERED SATELLITE SYSTEM (TSS)
DYNAMICS ASSESSMENTS AND ANALYSES
TSS-1R POST FLIGHT DATA EVALUATION

FINAL REPORT

Prepared By

bd Systems, Inc.
600 Boulevard South, Suite 304
Huntsville, Alabama 35802

Sponsored By

GEORGE C. MARSHALL SPACE FLIGHT CENTER
MARSHALL SPACE FLIGHT CENTER, AL. 35812

Under:

Contract No.: NAS8-39880

June 14, 1996

Table of Contents

1.0 TSS-1R TELEMETRY MSID'S

The Tethered Satellite System (TSS) Mission 1 Reflight ended on Sunday February 25, 1996 at 7:29:27 PM CST. The mission ended prematurely when the tether broke. The duration of deployed tether operations between flyaway and tether break was 4 hours, 41 minutes and 27 seconds. Preliminary appearances suggested that an electrical arc melted a segment of the tether causing it to fail when exposed to the tension levels normally present between the TSS Lower Tether Control Mechanism (LTCM) and the Upper Tether Control Mechanism (UTCM). An examination of the tension levels measured confirms that no tension transient events immediately preceded the tether break incident. Tension levels simply dropped to zero within seconds after the break. An examination of the tether voltage and current also support an electrical arcing event.

The purpose of this report is to document the analyses performed on the TSS-1R telemetry data after the flight. These analyses addressed the tether dynamics of TSS-1R. The telemetry data was provided in a CD-ROM format. The data contained on the CD-ROM was selected from available Satellite and orbiter MSID's: 264 data items were selected and provided in 58 "TAB" files. The data sets start at 3/00:00:00 and end at 3/05:45:00 mission elapsed time (MET). This range spans the period of tether dynamics. MET can be related to Greenwich Mean Time (GMT) by noting that 0/00:00:00 MET corresponds to 53/20:18:00 GMT. A summary of events and times they occurred is contained in section 2.0. Thanks to NASA/MSFC and NTI for providing the data. The CD-ROM is a very convenient format. Table 1.1 lists the TAB files and the MSID codes.

Table 1.1 TSS-1R Telemetry MSID TAB's

P13V3212.TAB		
1 P13V3212D	CNT	TEMAG X MODE 1 OUT/MODE 2 IN
2 P13V3311D	CNT	TEMAG Y MODE 1 IN/MODE 2 OUT
3 P13V3312D	CNT	TEMAG Y MODE 1 OUT/MODE 2 IN
4 P13V3313D	CNT	TEMAG X MODE 1 IN/MODE 2 OUT

V90H4277.TAB

1	V90H4277C	FT	X-COMP OF FLTRS CURR POS VCTR-TLM
2	V90H4278C	FT	Y-COMP OF FLTRS CURR POS VCTR-TLM
3	V90H4279C	FT	Z-COMP OF FLTRS CURR POS VCTR-TLM
4	V90L4281C	FT/S	X-COMP OF FLTRS CURR VEL VCTR-TLM
5	V90L4282C	FT/S	Y-COMP OF FLTRS CURR VEL VCTR-TLM
6	V90L4283C	FT/S	Z-COMP OF FLTRS CURR VEL VCTR-TLM
7	V90W4285C	S	TIME OF FILTER STATE VECTOR-TLM

V90U2240.TAB

1	V90U2240C	ND	M50 TO BODY QUAT MEASURED ELEM 1
2	V90U2241C	ND	M50 TO BODY QUAT MEASURED ELEM 2
3	V90U2242C	ND	M50 TO BODY QUAT MEASURED ELEM 3
4	V90U2243C	ND	M50 TO BODY QUAT MEASURED ELEM 4

V90U2641.TAB

1	V90U2641C	ND	M50 WRT LVLH QUAT 1
2	V90U2642C	ND	M50 WRT LVLH QUAT 2
3	V90U2643C	ND	M50 WRT LVLH QUAT 3
4	V90U2644C	ND	M50 WRT LVLH QUAT 4

V74H2618.TAB

1	V74H2618J	DEG	KU-BAND A CH1 ROLL WORD 3 WD3
2	V74H2619J	DEG	KU-BAND A CH1 PITCH WORD 4 WD4
3	V74U2623J	KFT	KU-A CH 1 RDR RANGE BITS 01-23

P03V2200A.TAB

1	P03V2200A	VDC	EMP EXPERIMENT DC VOLTAGE	
2	P03C2201A	AMP	EMP EXPERIMENT DC CURRENT	
3	P03Q2716D	CNT	MET-SECS	(E10.5)
4	P03Q2738D	CNT	GMT-DAY	
5	P03Q2739D	CNT	GMT-SECS	(E10.5)
6	P03Q2740D	CNT	GMT-MODE	

P03W2015D.TAB

1	P03W2015D	CNT	SFMDM GMT DAY
2	P03W2016D	CNT	SFMDM GMT MINUTES
3	P03W2017D	CNT	SFMDM GMT SECONDS
4	P03W2018D	CNT	SFMDM GMT MILLISECONDS
5	P03W2019D	CNT	SFMDM GMT MICROSECONDS
6	P03W2020D	CNT	SFMDM GMT HOURS

P13A0139D.TAB

1	P13A0139D	*MILL	SLA X-ACCELERATION

P13A0140D.TAB

1	P13A0140D	*MILL	SLA Y-ACCELERATION

P13A0141D.TAB

1	P13A0141D	*MILL	SLA Z-ACCELERATION

P13A0142A.TAB

1	P13A0142A	*MILL	SLA X-ACCELERATION COARSE
2	P13A0143A	*MILL	SLA Y-ACCELERATION COARSE
3	P13A0144A	*MILL	SLA Z-ACCELERATION COARSE

P13H0025D.TAB

1	P13H0025D	CNT	ALPHA ANGLE A
2	P13H0026D	CNT	BETA ANGLE A
3	P13H0027D	CNT	GAMMA ANGLE A
4	P13H0028D	CNT	SKEW ANGLE A

P13H0029D.TAB

1	P13H0029D	CNT	ALPHA ANGLE B
2	P13H0030D	CNT	BETA ANGLE B
3	P13H0031D	CNT	GAMMA ANGLE B
4	P13H0032D	CNT	SKEW ANGLE B

P13H0065A.TAB

1	P13H0065A	DEG/S	X-GYRO RATE FINE
2	P13H0066A	DEG/S	Y-GYRO RATE FINE
3	P13H0067A	DEG/S	Z-GYRO RATE FINE
4	P13H0068A	CNT	SKEW-GYRO RATE

P13H0389D.TAB

1	P13H0389D	RAD	YAW ANGLE	(F10.5)
2	P13H0390D	RAD	ROLL ANGLE	(F10.5)
3	P13H0391D	RAD	PITCH ANGLE	(F10.5)
4	P13H0392D	RAD	ROLL UPDATING ANGLE	(F10.5)
5	P13H0393D	RAD	PITCH UPDATING ANGLE	(F10.5)

P13H0694D.TAB

1	P13H0694D	RAD	CONSTANT DRIFT X COARSE BYTE 1
2	P13H0695D	RAD	CONSTANT DRIFT X COARSE BYTE 2
3	P13H0696D	RAD	CONSTANT DRIFT X COARSE BYTE 3
4	P13H0697D	RAD	CONSTANT DRIFT X COARSE BYTE 4
5	P13H0698D	RAD	CONSTANT DRIFT X FINE BYTE 1
6	P13H0699D	RAD	CONSTANT DRIFT X FINE BYTE 2

7	P13H0700D	RAD	CONSTANT DRIFT X FINE BYTE 3
8	P13H0701D	RAD	CONSTANT DRIFT X FINE BYTE 4

P13H0702D.TAB

1	P13H0702D	RAD	CONSTANT DRIFT Y COARSE BYTE 1
2	P13H0703D	RAD	CONSTANT DRIFT Y COARSE BYTE 2
3	P13H0704D	RAD	CONSTANT DRIFT Y COARSE BYTE 3
4	P13H0705D	RAD	CONSTANT DRIFT Y COARSE BYTE 4
5	P13H0706D	RAD	CONSTANT DRIFT Y FINE BYTE 1
6	P13H0707D	RAD	CONSTANT DRIFT Y FINE BYTE 2
7	P13H0708D	RAD	CONSTANT DRIFT Y FINE BYTE 3
8	P13H0709D	RAD	CONSTANT DRIFT Y FINE BYTE 4

P13H0710D.TAB

1	P13H0710D	RAD	CONSTANT DRIFT Z COARSE BYTE 1
2	P13H0711D	RAD	CONSTANT DRIFT Z COARSE BYTE 2
3	P13H0712D	RAD	CONSTANT DRIFT Z COARSE BYTE 3
4	P13H0713D	RAD	CONSTANT DRIFT Z COARSE BYTE 4
5	P13H0714D	RAD	CONSTANT DRIFT Z FINE BYTE 1
6	P13H0715D	RAD	CONSTANT DRIFT Z FINE BYTE 2
7	P13H0716D	RAD	CONSTANT DRIFT Z FINE BYTE 3
8	P13H0717D	RAD	CONSTANT DRIFT Z FINE BYTE 4

P13H0718D.TAB

1	P13H0718D	RAD	CONSTANT DRIFT SKEW COARSE BYTE 1
2	P13H0719D	RAD	CONSTANT DRIFT SKEW COARSE BYTE 2
3	P13H0721D	RAD	CONSTANT DRIFT SKEW COARSE BYTE 4
4	P13H0722D	RAD	CONSTANT DRIFT SKEW FINE BYTE 1
5	P13H0723D	RAD	CONSTANT DRIFT SKEW FINE BYTE 2
6	P13H0724D	RAD	CONSTANT DRIFT SKEW FINE BYTE 3
7	P13H0725D	RAD	CONSTANT DRIFT SKEW FINE BYTE 4
8	P13H0730D	*RAD/	REFERENCE SPIN RATE BYTE 1

P13Q0073D.TAB

1	P13Q0073D	INTEG	ALFA1/2 ANGLE
2	P13Q0074D	INTEG	ALFA3/4 ANGLE
3	P13Q0075D	INTEG	BETA1/2 ANGLE
4	P13Q0076D	INTEG	BETA3/4 ANGLE

P13Q0089D.TAB

1	P13Q0089D	INTEG	ES1 CHORD 1 ANGLE
2	P13Q0090D	INTEG	ES1 CHORD 2 ANGLE
3	P13Q0091D	INTEG	ES2 CHORD 1 ANGLE
4	P13Q0092D	INTEG	ES2 CHORD 2 ANGLE

P13T0069A.TAB

1	P13T0069A	DEGC	GYRO PKG 1 TEMP. X
2	P13T0070A	DEGC	GYRO PKG 1 TEMP. Z
3	P13T0071A	DEGC	GYRO PKG 2 TEMP. Y
4	P13T0072A	DEGC	GYRO PKG 2 TEMP. SKEW

P13X0001E.TAB

1	P13X0001E	EVENT	MAIN ISO. V. STATUS	
2	P13P0002A	*KPAS	TANK PRESSURE	
3	P13P0003A	*PASC	REGULATED PRESSURE	(F12.3)

P13X0009E.TAB

1	P13X0009E	EVENT	IN LINE 1 V. STATUS
2	P13X0011E	EVENT	IN LINE 2 V. STATUS
3	P13X0013E	EVENT	IN PL. REAR V. STATUS
4	P13X0015E	EVENT	IN PL. FRONT V. STATUS
5	P13X0017E	EVENT	OUT OF PL. RIGHT V. STATUS

P13X0018E.TAB

1	P13X0018E	EVENT	OUT OF PL. LEFT V. STATUS
2	P13X0020E	EVENT	I/O OF PL. ISO. V. STATUS
3	P13X0022E	EVENT	YAW 1 V. STATUS
4	P13X0023E	EVENT	YAW 2 V. STATUS

P13X0037E.TAB

1	P13X0037E	EVENT	X_WHEEL STATUS A
2	P13X0038E	EVENT	X_WHEEL STATUS B
3	P13X0039E	EVENT	X_MODE STATUS A
4	P13X0040E	EVENT	X_MODE STATUS B
5	P13X0045E	EVENT	Y_WHEEL STATUS A
6	P13X0046E	EVENT	Y_WHEEL STATUS B
7	P13X0047E	EVENT	Y_MODE STATUS A
8	P13X0048E	EVENT	Y_MODE STATUS B

P13X0053E.TAB

1	P13X0053E	EVENT	Z_WHEEL STATUS A
2	P13X0054E	EVENT	Z_WHEEL STATUS B
3	P13X0055E	EVENT	Z_MODE STATUS A
4	P13X0056E	EVENT	Z_MODE STATUS B
5	P13X0061E	EVENT	SKEW_WHEEL STATUS A
6	P13X0062E	EVENT	SKEW_WHEEL STATUS B
7	P13X0063E	EVENT	SKEW_MODE STATUS A
8	P13X0064E	EVENT	SKEW_MODE STATUS B

P13X0077E.TAB

1	P13X0077E	EVENT	A1/2 SELECTED OPTICAL HEAD
2	P13X0078E	EVENT	A3/4 SELECTED OPTICAL HEAD
3	P13X0079E	EVENT	B1/2 SELECTED OPTICAL HEAD
4	P13X0080E	EVENT	B3/4 SELECTED OPTICAL HEAD

P13X0081E.TAB

1	P13X0081E	EVENT	ALFA1/2 DATA VALID
2	P13X0082E	EVENT	ALFA3/4 DATA VALID
3	P13X0083E	EVENT	BETA1/2 DATA VALID
4	P13X0084E	EVENT	BETA3/4 DATA VALID
5	P13X0085E	EVENT	FDS1/FDS2 STATUS
6	P13X0086E	EVENT	FDS3/FDS4 STATUS
7	P13X0087E	EVENT	FDS1/FDS2 SUN PRESENCE
8	P13X0088E	EVENT	FDS3/FDS4 SUN PRESENCE

P13X0093E.TAB

1	P13X0093E	EVENT	ES1 PWR STATUS
2	P13X0094E	EVENT	ES2 PWR STATUS
3	P13X0095E	EVENT	ES1 STATUS
4	P13X0096E	EVENT	ES2 STATUS
5	P13V0103A	VDC	ES1 SUN PRESENCE
6	P13V0104A	VDC	ES2 SUN PRESENCE

P13X0149E.TAB

1	P13X0149E	EVENT	SLA OPERATE STATUS
2	P13X0172E	EVENT	P/L 03 TEMAG PWR STATUS
3	P13C0180D	AMP	SA CURRENT (MAGNITUDE AND SIGN)
4	P13X0219E	EVENT	I/O OF PLANE OPERATIVE MODE--BIT 6
5	P13M0367P	INTEG	AMCS OPERATIVE MODE
6	P13Q0388D	INTEG	NSHOT

P33C4266D.TAB

1	P33C4266D	AMP	TCVM TETHER CURRENT MONITOR	(E12.5)
2	P33V4328D	VDC	TETHER VOLTAGE MONITOR DC	

P33C4419D.TAB

1	P33C4419D	NT	X AXIS MAG FIELD	
2	P33C4420D	NT	Y AXIS MAG FIELD	
3	P33C4421D	NT	Z AXIS MAG FIELD	
4	P33U4427D	SEC	CPU TIME MOST SIGNIFICANT BYTE 1	(F10.0)
5	P33U4428D	SEC	CPU TIME BYTE 2	
6	P33U4430D	SEC	CPU TIME BYTE 3	
7	P33U4431D	SEC	CPU TIME LEAST SIGNIFICANT BYTE 4	

P33C6002D.TAB

1	P33C6002D	*MA	EGA1 TETHER CURRENT
2	P33C6003D	*MA	EGA2 TETHER CURRENT
3	P33C6004D	*MA	EGA1 ANODE CURRENT
4	P33C6005D	*MA	EGA2 ANODE CURRENT
5	P33C6006D	*A	EGA1 FILAMENT CURRENT
6	P33C6007D	*A	EGA2 FILAMENT CURRENT

P33C6008D.TAB

1	P33C6008D	*A	EGA1 COIL CURRENT
2	P33C6009D	*A	EGA2 COIL CURRENT
3	P33C6010D	*MA	EGA1 TETHER CURRENT OFFSET
4	P33C6011D	*MA	EGA2 TETHER CURRENT OFFSET
5	P33M6012P	CNT	DV MEASURE

P33G3017D.TAB

1	P33G3017D	*NEW	OUTBOARD FINE TETHER TENSION
2	P33G3018D	*NEW	OUTBOARD COARSE TETHER TENSION
3	P33G3019D	*NEW	INBOARD TETHER TENSION
4	P33G3022D	*NEW	OUTBOARD FINE TETHER TENSION-CP
5	P33G3023A	*NEW	OUTBOARD BLENDED TETHER TENSION

P33G3020D.TAB

1	P33G3020D	*NEW	OUTBOARD COARSE TETHER TENSION-CP
2	P33G3021D	*NEW	INBOARD TETHER TENSION-CP

P33G3051D.TAB

1	P33G3051D	*NEW	COMMANDED OUTBOARD TENSION	(F10.5)
2	P33G3052D	*NEW	MEASURED OUTBOARD BLENDED TENSION	
3	P33W3054D	*SEC	ELAPSED MANEUVER TIME	

P33G3290D.TAB

1	P33G3290D	*NEW	INBOARD TETHER TENSION-8

P33H3040D.TAB

1	P33H3040D	CNT	TETHER LENGTH RAW ENCODER COUNTS	(F12.1)

P33H3042D.TAB

1	P33H3042D	M	COMMANDED STRETCHED TETHER LENGTH	
2	P33L3043D	*MPS	COMMANDED VELOCITY	(F10.5)
3	P33A3044D	*MSS	COMMANDED ACCELERATION	(E12.5)
4	P33H3045D	M	SPOOLED UNSTRETCHED TETHER LENGTH	
5	P33H3046D	M	CMD UNSTRETCHED TETHER LENGTH	
6	P33L3047D	*MPS	SPOOL TETHER VELOCITY	(F10.5)

P33H3048D.TAB

1 P33H3048D	RAD	CMD IN-PLANE LIBRATION ANGLE	(E12.5)
2 P33H3049D	*RADP	CMD IN-PLANE LIBRATION ANGULAR VEL	(E12.5)
3 P33H3050D	*DEGS	CMD IN-PLANE LIBRATION ANGULAR ACC	(E12.5)

P33H3055D.TAB

1 P33H3055D	*RADP	ESTIMATED RM ANGULAR VELOCITY	(F10.5)
2 P33Q3056D	CNT	MOTOR/GENERATOR PULSEWIDTH	
3 P33H3057D	M	ESTIMATED REEL RADIUS	(F10.5)
4 P33Q3058D	*OHMS	COMMANDED LOADBANK RESISTANCE	
5 P33V3060D	VDC	COMMANDED RM TERMINAL VOLTAGE	(F10.5)

P33H3295D.TAB

1 P33H3295D	M	MEAS TETHER LEN 0.1/0.01'S PLACE
2 P33H3296D	M	CMD TETHER LEN 1000/100'S PLACE
3 P33H3297D	M	CMD TETHER LEN 10/1'S PLACE
4 P33H3298D	M	CMD TETHER LEN 0.1/0.01'S PLACE
5 P33H3299D	DEG	COMMANDED LIBRATION ANGLE (DEG)
6 P33X3300E	EVENT	SAT IN-LINE THRUSTERS NECESSARY

P33L3305D.TAB

1 P33L3305D	*MPS	MEASURED TETHER RATE
2 P33X3306E	EVENT	MEAS TETHER VELOCITY SIGN
3 P33L3307D	*MPS	MEAS TETHER VELOCITY FRACTION
4 P33L3308D	*MPS	MEAS TETHER VELOCITY INTEGER PART
5 P33X3309E	EVENT	CMD TETHER VELOCITY SIGN
6 P33L3310D	*MPS	CMD TETHER VELOCITY INTEGER PART

P33L3311D.TAB

1 P33L3311D	*MPS	CMD TETHER VELOCITY FRACTION	
2 P33L3312D	DEG/S	CMD LIBRATION VEL (DEG/S)	(E10.5)
3 P33V3313D	VDC	BLENDED TENSION FILTER (VOLTS)	
4 P33V3314D	VDC	TETHER LENGTH FILTER (VOLTS)	
5 P33V3315D	VDC	REG VOLTAGE/PROP CNTRL (VOLTS)	
6 P33V3316D	VDC	REGULATORY VOLTAGE (VOLTS)	

P33Q3153D.TAB

1 P33Q3153D	CNT	GMT DAYS MSB
2 P33Q3154D	CNT	GMT DAYS LSB
3 P33Q3155D	CNT	GMT HOURS
4 P33Q3156D	CNT	GMT MINUTES
5 P33Q3157D	CNT	GMT SECONDS

P33Q3158D.TAB

1 P33Q3158D	CNT	GMT 1/100 SECONDS

P33Q3318D.TAB

1	P33Q3318D	CNT	CURRENT SEGMENT NUMBER IN PROFILE
2	P33Q3319D	PCT	PERCENT OF TIME ELAPSED IN SEGMENT
3	P33W3320D	*SEC	TIME REMAINING IN SEGMENT
4	P33X3325E	EVENT	MOTOR/GENERATOR MODE
5	P33Q3331D	CNT	REEL MOTOR COMMAND (PULSEWIDTH)
6	P33X3332E	EVENT	TALK BACK MONITOR

P33U4203D.TAB

1	P33U4203D	SEC	GMT SECONDS 1	
2	P33U4204D	SEC	GMT SECONDS 2	(F10.1)
3	P33U4238D	SEC	GMT SECONDS 3	
4	P33U4239D	SEC	GMT SECONDS 4	

P33U9220D.TAB

1	P33U9220D	DAYS	GMTD
2	P33W9221D	HOURS	GMTH
3	P33U9222D	MINUT	GMTM
4	P33U9223D	SECON	GMTS

P33V4471D.TAB

1	P33V4471D	VDC	TETHER VOLTAGE MONITOR DC X 10	(E12.5)
2	P33V4472D	VDC	TETHER VOLTAGE MONITOR DC X 100	(E12.5)

P33W3061D.TAB

1	P33W3061D	*SEC	CURRENT SEGMENT DURATION TIME
2	P33H3062D	DEG	CURRENT SEGMENT INIT LIBR ANGLE
3	P33H3063D	DEG	CURRENT SEGMENT FINAL LIBR ANGLE
4	P33Q3064D	*CNTS	CURRENT SEGMENT TYPE

P33X3066E.TAB

1	P33X3066E	EVENT	U1 SEPARATION PWR STATUS
2	P33X3100E	EVENT	U1 RETRACTED 1 STATUS
3	P33X3119E	EVENT	U1 SEPARATION RLY CMD STATUS

P33X3160E.TAB

1	P33X3160E	EVENT	MOTOR/GENERATOR MODE STATUS
2	P33C3219D	AMP	MCA-REEL MOTOR CURRENT
3	P33C3220D	AMP	MPC-MCA CURRENT

P33X3288E.TAB

1	P33X3288E	EVENT	U1 SEPARATION STATUS
2	P33A3289D	*MSS	CMD TETHER ACCELERATION (M/S/S) (E12.5)
3	P33G3291D	*NEW	COMMANDED OUTBOARD (UTCM) TENSION

4 P33H3292D	M	MEASURED UNSTRETCHED TETHER LENGTH	
5 P33H3293D	M	MEAS TETHER LEN 1000/100'S PLACE	
6 P33H3294D	M	MEAS TETHER LEN 10/1'S PLACE	

P33Y4401D.TAB

1 P33Y4401D	DB	LANGMUIR PROBE OUTPUT	
2 P33C4402D	AMP	DEP CURRENT	
3 P33C4403D	AMP	TCVM CURRENT	
4 P33C4404D	AMP	SRPA CURRENT	
5 P33C4405D	AMP	AMAG CURRENT	(E12.5)
6 P33C4406D	AMP	CCP CURRENT	
7 P33C4407D	AMP	FPEG CURRENT	
8 P33C4408D	AMP	SPIB CURRENT	

W33H3040D.TAB

1 W33H3040D	M	TETHER LENGTH ENCODER

2.0 TETHER DEPLOYMENT EVENTS HISTORY

The reconstructed events history of for TSS-1R tether deployment dynamics activities is shown in table 2.1.

Table 2.1 TSS-1R Deployment Events History

EVENT	TIME OF OCCURRENCE (MET)	TIME OF OCCURRENCE (from flyaway)
Data Starts	3/00:00:00	-1620.0
IL1 On	3/00:25:38	-82
IL2 On	3/00:25:29	-91
Flyaway	3/00:27:00	0.00
IL1 Off	3/00:30:08	188.0
Yaw Hold Enabled	3/00:30:40	220.0
IL2 Off	3/01:53:02	5162.0
ARD Test Begins	3/01:24:07	3427.0
ARD Test Ends	3/01:53:02	5162.0
Passive Mode	3/01:53:02	5162.0
Spin Mode	3/03:33:49	11209.0
Tether Breaks	3/05:11:27	17067.0
Data Ends	3/05:45:00	18450.0

Deployer Profile Control

Seg 1 - Seg 2	3/01:59:44	5564.0
Seg 2 - Seg 3	3/02:45:41	8321.0
Seg 3 - Seg 4	3/04:04:04	13024
Seg 4 - Seg 5	3/05:54:45	19665.0
Sunrise / Sunset		
Sunset 1	3/00:42:54	954.0
Sunrise 1	3/01:17:18	3018.0
Sunset 2	3/02:13:18	6378.0
Sunrise 2	3/02:47:46	8446.0
Sunset 3	3/03:43:42	11802.0
Sunrise 3	3/04:18:08	13868.0
Sunset 3	3/05:14:08	17228.0

3.0 DISCUSSION OF PRE-FLYAWAY DEPLOYER BOOM FREQUENCIES

The lateral frequencies of the TSS Deployer Boom were calculated and tested prior to the flight TSS-1 (original mission). They were also calculated from satellite lateral accelerometer (SLA) data for TSS-1. The assumption here is that the satellite moves rigidly with the boom. The values determined were 0.166 Hertz for x vibration and 0.553 Hertz for y vibration. Satellite accelerometer data for TSS-1R in the time frame immediately prior to flyaway also provide opportunities to determine these frequencies.

The SLA x accelerometer data for the period prior to flyaway is plotted in Figure 3.1. It can be observed that a number of transient events excite the accelerometers. These are apparently due to orbiter thruster firings. These events are numbered for identification purposes. For each event, a set of data points is determined which spans the event for analysis purposes. This data set is a reduced set from the actual telemetry. The data is processed so that it is equally spaced at 0.5 second intervals.

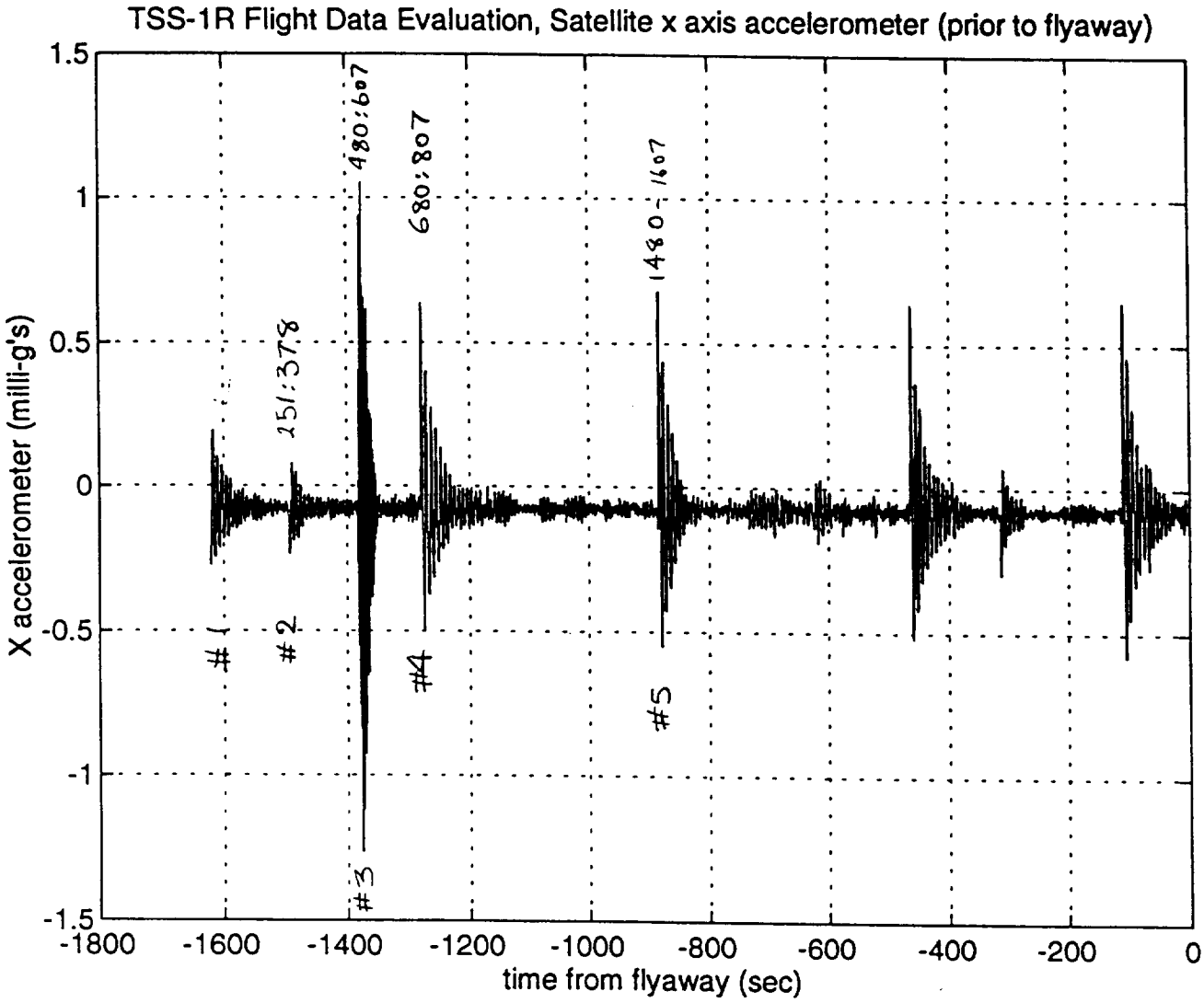
TSS-1R Flight Data Evaluation, Satellite x axis accelerometer (prior to flyaway)
X accelerometer (milli-g's)
time from flyaway (sec)
1.5
1
0.5
0
-0.5
-1
-1.5
-1800
-1600
-1400
-1200
-1000
-800
-600
-400
-200
0
151:378
480:607
680:807
1480:1607
#1
#2
#3
#4
#5

Figure 3-1.

The original data was at approximately 0.640 second intervals with occasional frames missing. The transient events allow several determinations of boom frequencies in the range of 0.13 - 0.15 Hertz. The range seems to be due to a non-linear amplitude dependence of the oscillation, since the frequencies are progressively lower as the amplitude grows higher. This is shown in Figure 3.2 which is a plot of the fourier transforms of the SLA x data over the times of each of the first 5 transient events.

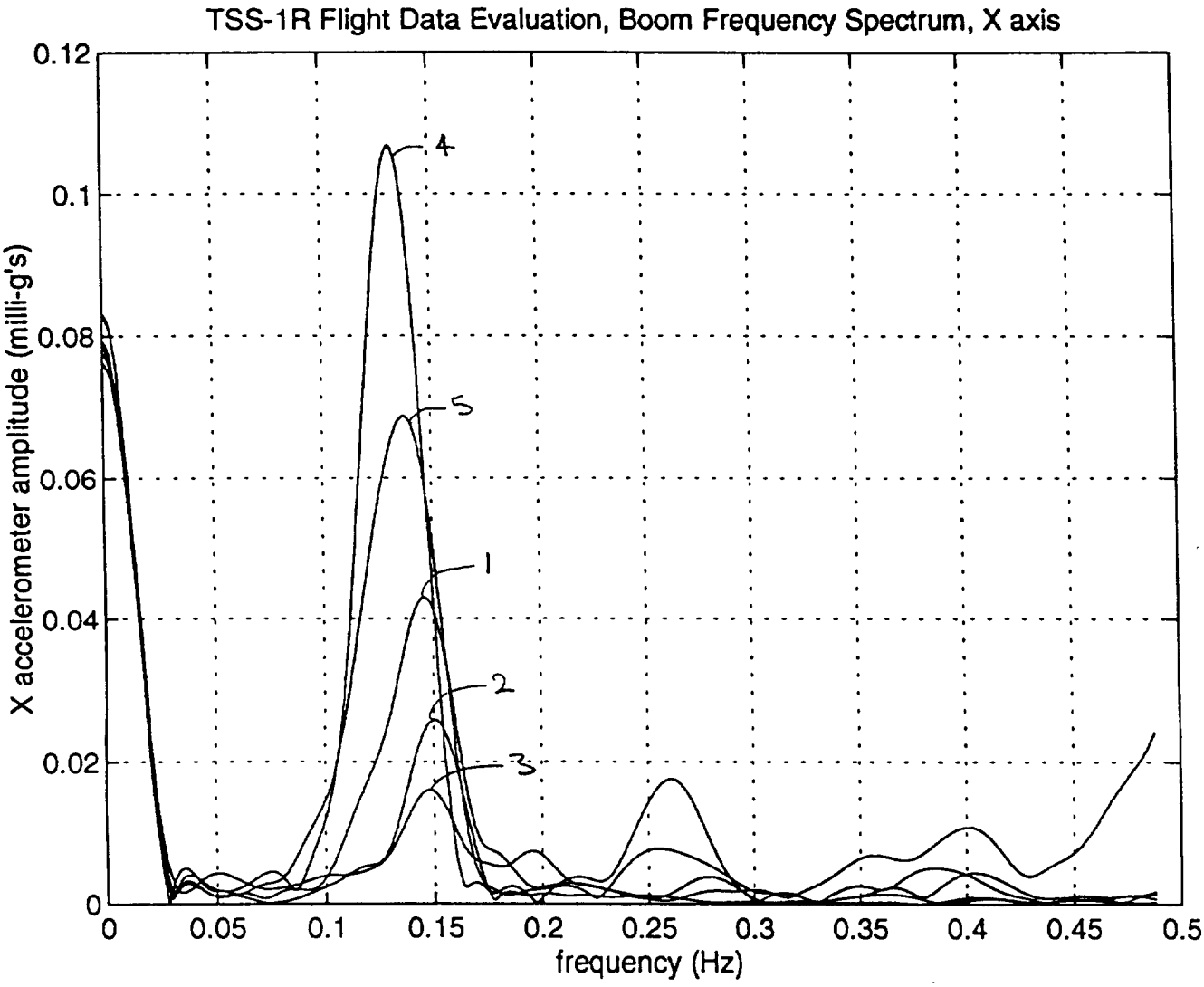

Figure3.2

The SLA y accelerometer data provides just a single, well-defined transient event. This data is plotted in Figure 3.3. It is also biased to a value of 2 milli-g's. The source of this bias has not been determined.

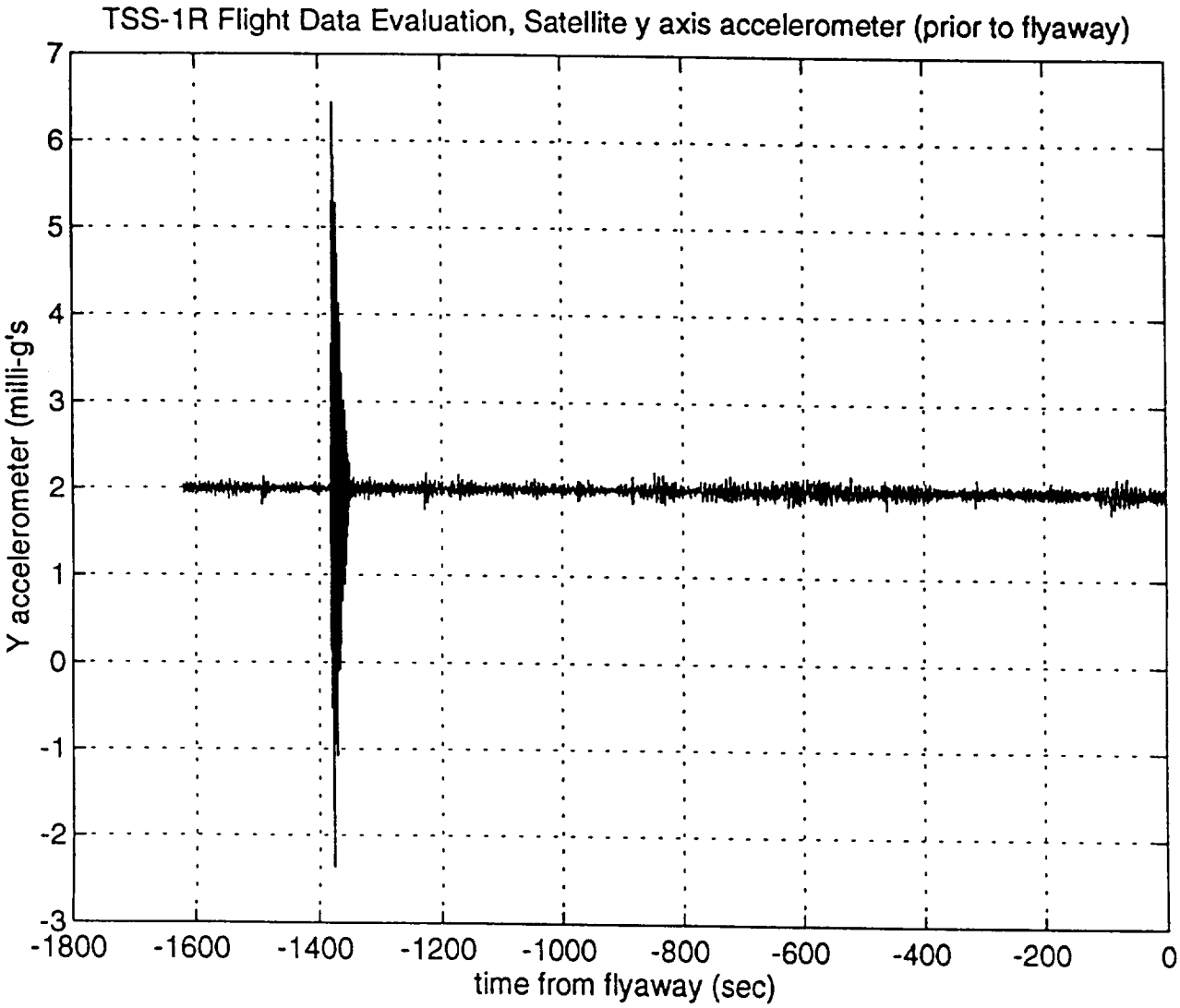

Figure 3.3

For analysis purposes, the bias was subtracted out before the fourier transform operation was performed. Figure 3.4 shows the fourier transform of the data over the transient event. The y axis frequency is observed to be 5.3 Hertz.

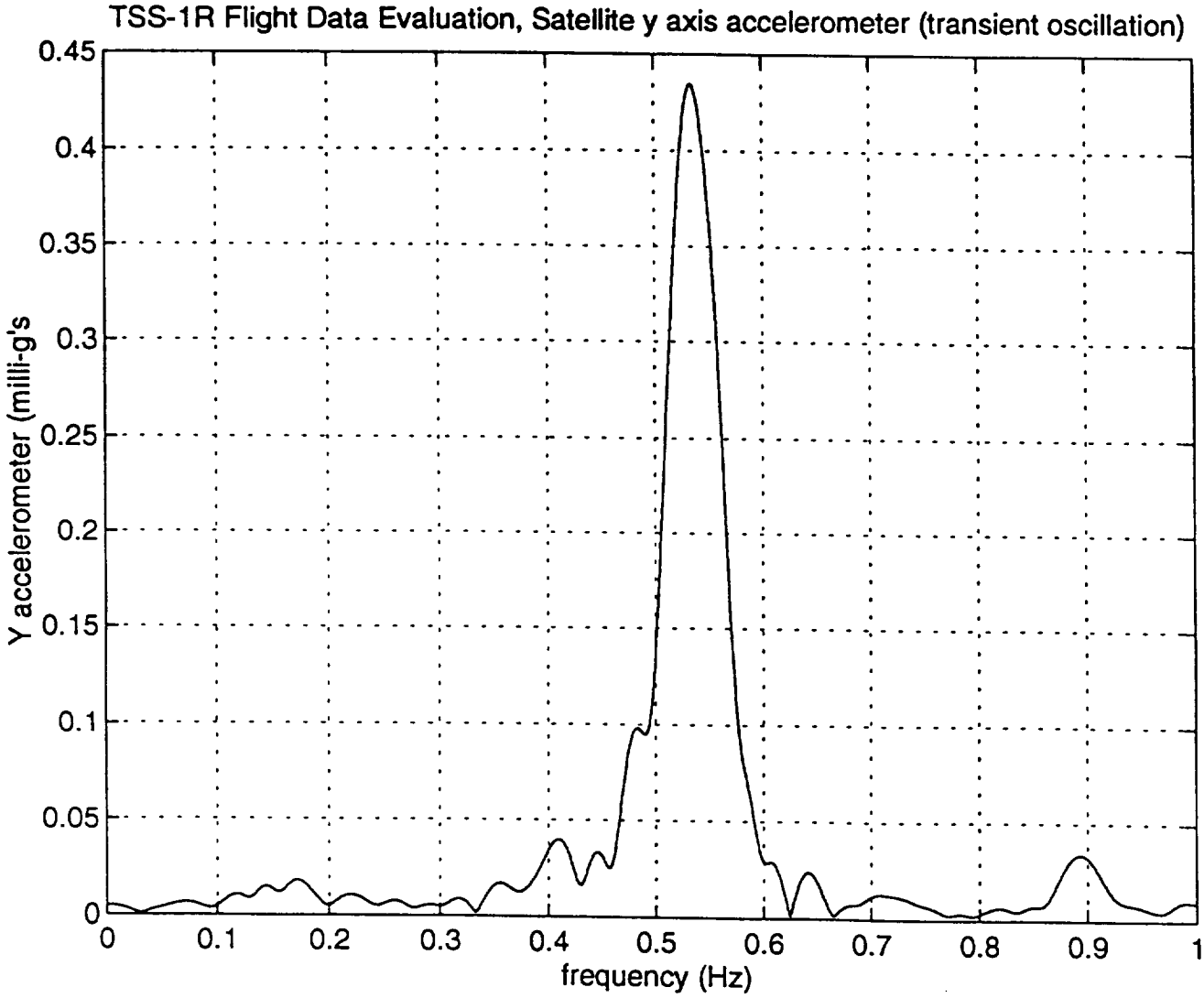

Figure 3.4

This value is significantly higher than was observed in x. No explanation for this phenomena is available yet. Figure 3.5 shows the SLA y data plotted over the pre-flyaway transient. SLA y data for the period following flyaway is shown plotted in Figure 3.6. The tether cut occurs at 17067 seconds. Notice that several transients occur during this period. These are attributed to satellite lateral/attitude thruster firings.

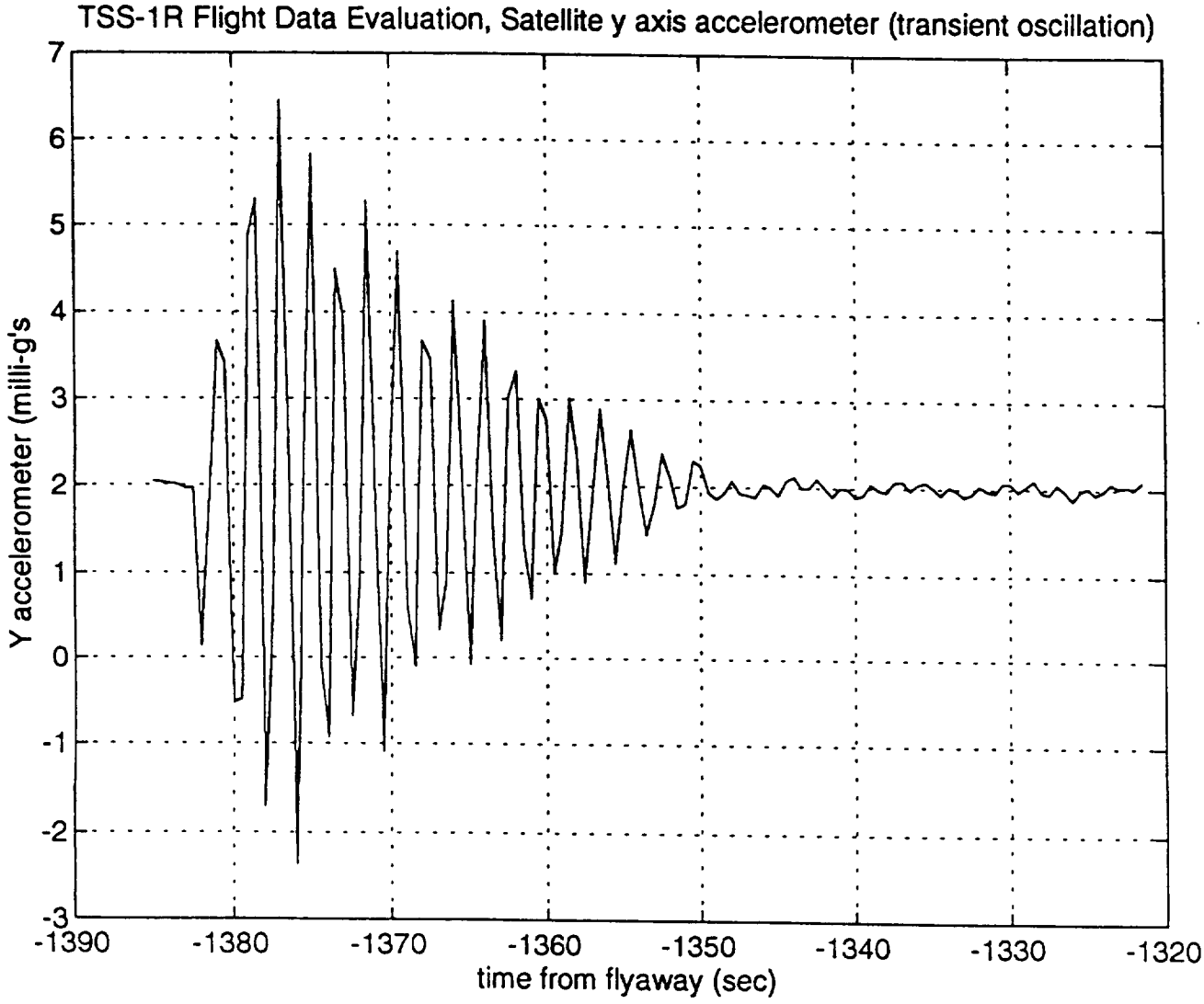

Figure 3.5

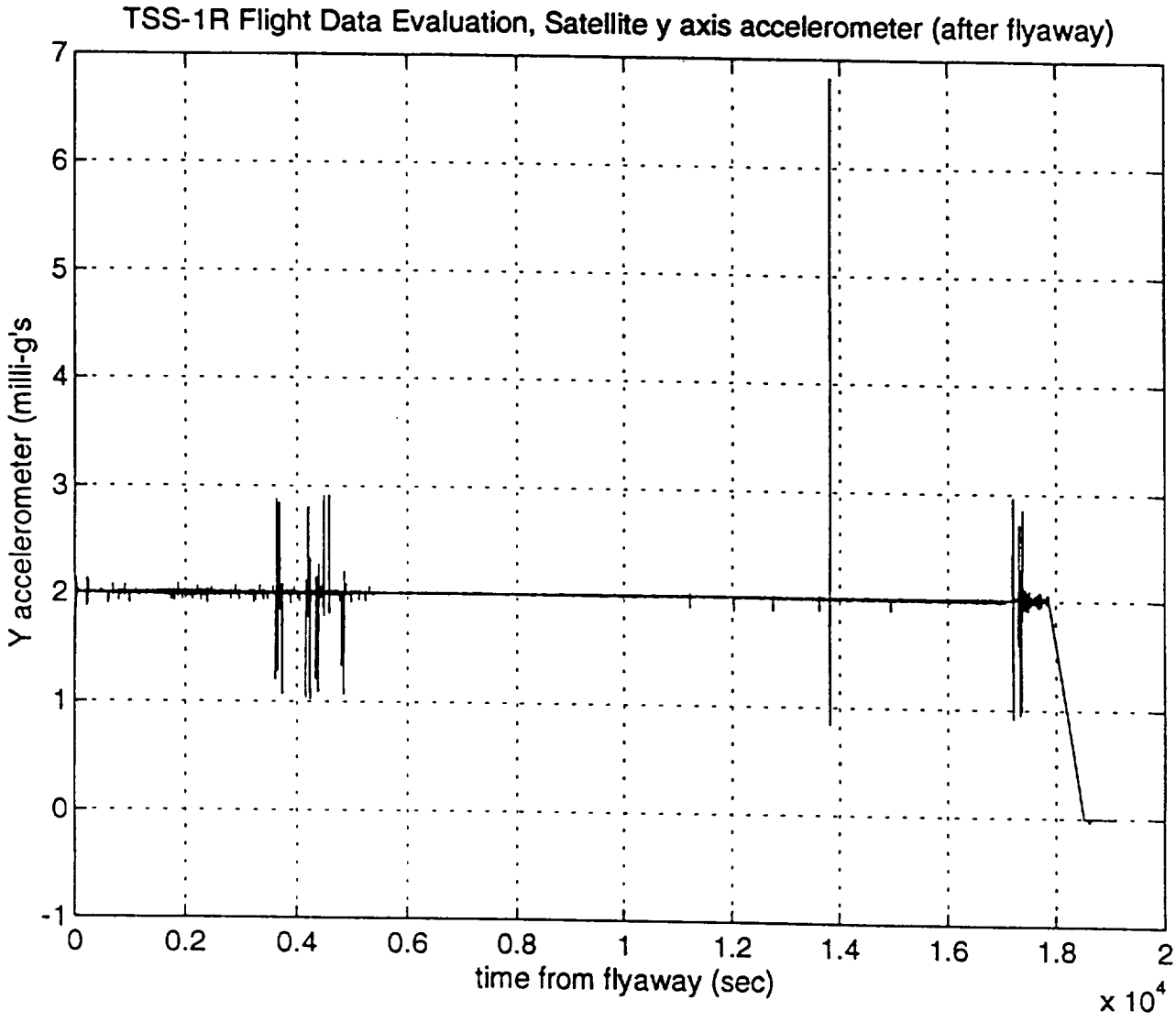
TSS-1R Flight Data Evaluation, Satellite y axis accelerometer (after flyaway)
Y accelerometer (milli-g's
7
6
5
4
3
2
1
0
-1
0
0.2
0.4
0.6
0.8
1
1.2
1.4
1.6
1.8
2
time from flyaway (sec)
x 10^4

Figure 3.6

4.0 OBSERVER RECONSTRUCTION OF SKIP ROPE

The complex, frequency domain skip rope observer (CFDSO) was developed originally for post flight evaluation of data for TSS-1. It was adapted as ground software for use in real-time flight support for the TSS-1R mission. The CFDSO was developed on the assumption that near steady state conditions would prevail during the periods of its operation. In practise this means that tether length rate must be small so that skip rope frequency changes only minimally over a cycle. Also, this means that current must be constant or slowly varying over a skip rope period. It was envisioned that the operating condition during which the skip rope observers (SRO's) would be most needed was on station operations at Station 1, 20.7 km, Creep and Station 2. TSS-1R tether operations included only a period of deployment with relatively large deployment rates and substantial current flowing. Thus, SRO operations were adversely affected. However, the CFDSO estimate of the phase of skip rope motion is more seriously affected than the amplitude. This is due to the fact that the skip rope (SR) frequency is changing and the CFDSO algorithm does not account for this. Hence, its estimate of phase is off. The CFDSO post flight determination of SR amplitude is considered to be reasonably accurate and is constructed somewhat differently from the real-time CFDSO algorithm. The post flight procedure reconstructs the SR over the interval of the rate data, while the real-time algorithm uses the same procedure but projects from this data to the most recent time in the data set.

The reconstructed skip rope is computed from the satellite rate data which has been processed from the TSS-1R telemetry so that the update rate is one per second with no gaps. Any missing data is filled in through linear interpolation. The algorithm reconstructs SR over the period corresponding to the data window. Discrete intervals of time have been selected for processing. The first interval is the period from 4000-4800 seconds after flyaway. This interval was chosen to allow the satellite to get sufficiently far from the boom for SR motion to develop and for any transients due to flyaway to abate. Figure 4.1 shows the variation in tether length measured over the observation interval while, Figure 4.2 contains the 3 body rate components over the same period. The average length is approximately 600 m. This is well outside the 224 m range where the CFDSO was shown to work for TSS-1.

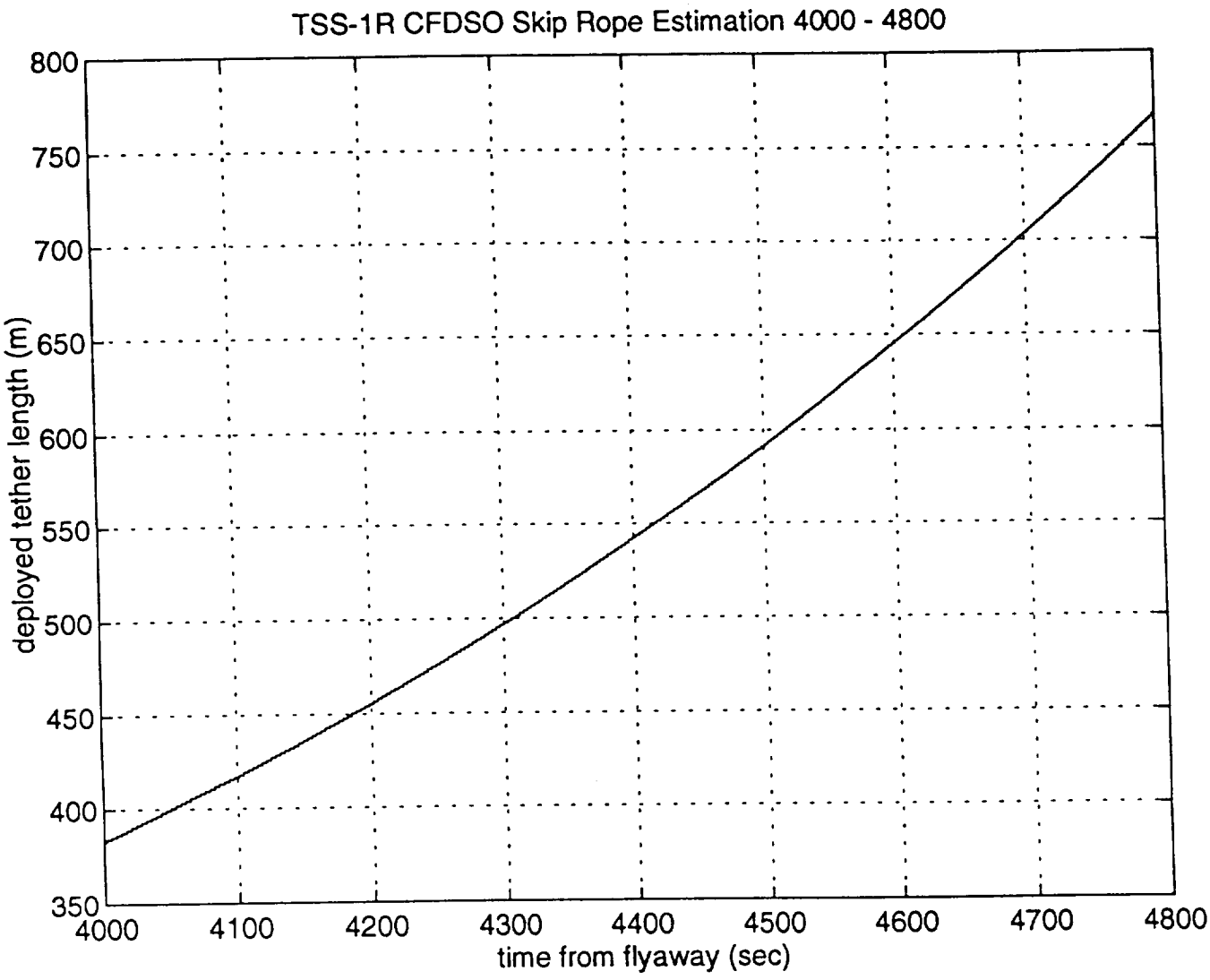
TSS-1R CFDSO Skip Rope Estimation 4000 - 4800
deployed tether length (m)
800
750
700
650
600
550
500
450
400
350
4000
4100
4200
4300
4400
4500
4600
4700
4800
time from flyaway (sec)

Figure 4.1

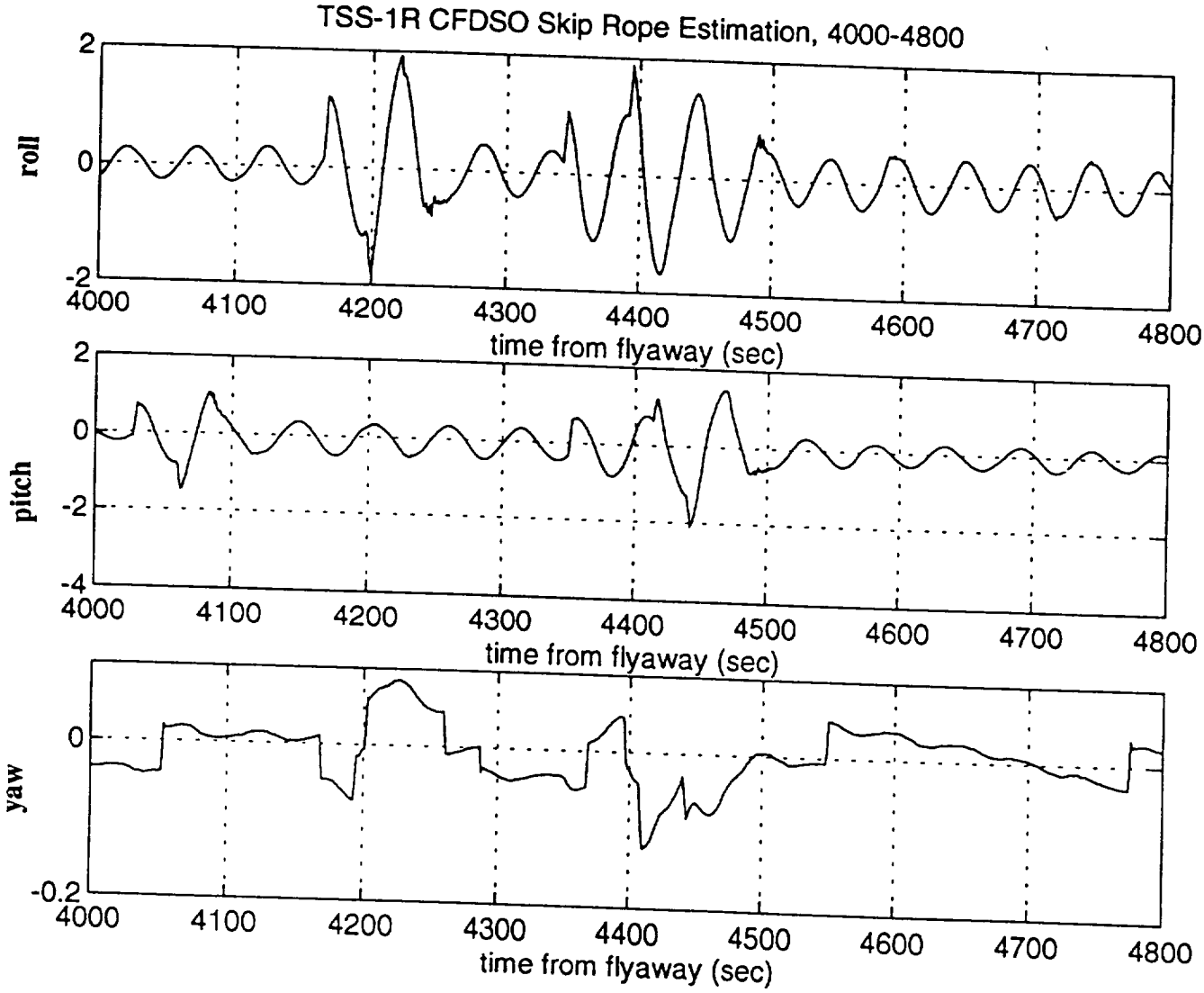
TSS-1R CFDSO Skip Rope Estimation, 4000-4800
SATELLITE ATTITUDE RATES - DEG/SEC.
roll
pitch
yaw
time from flyaway (sec)
4000
4100
4200
4300
4400
4500
4600
4700
4800

Figure 4.2

This data is processed by the CFDSO algorithm and produces the estimate of SR motion shown in Figure 4.3. The estimated motion amplitude in and out of plane are approximately 6 m.

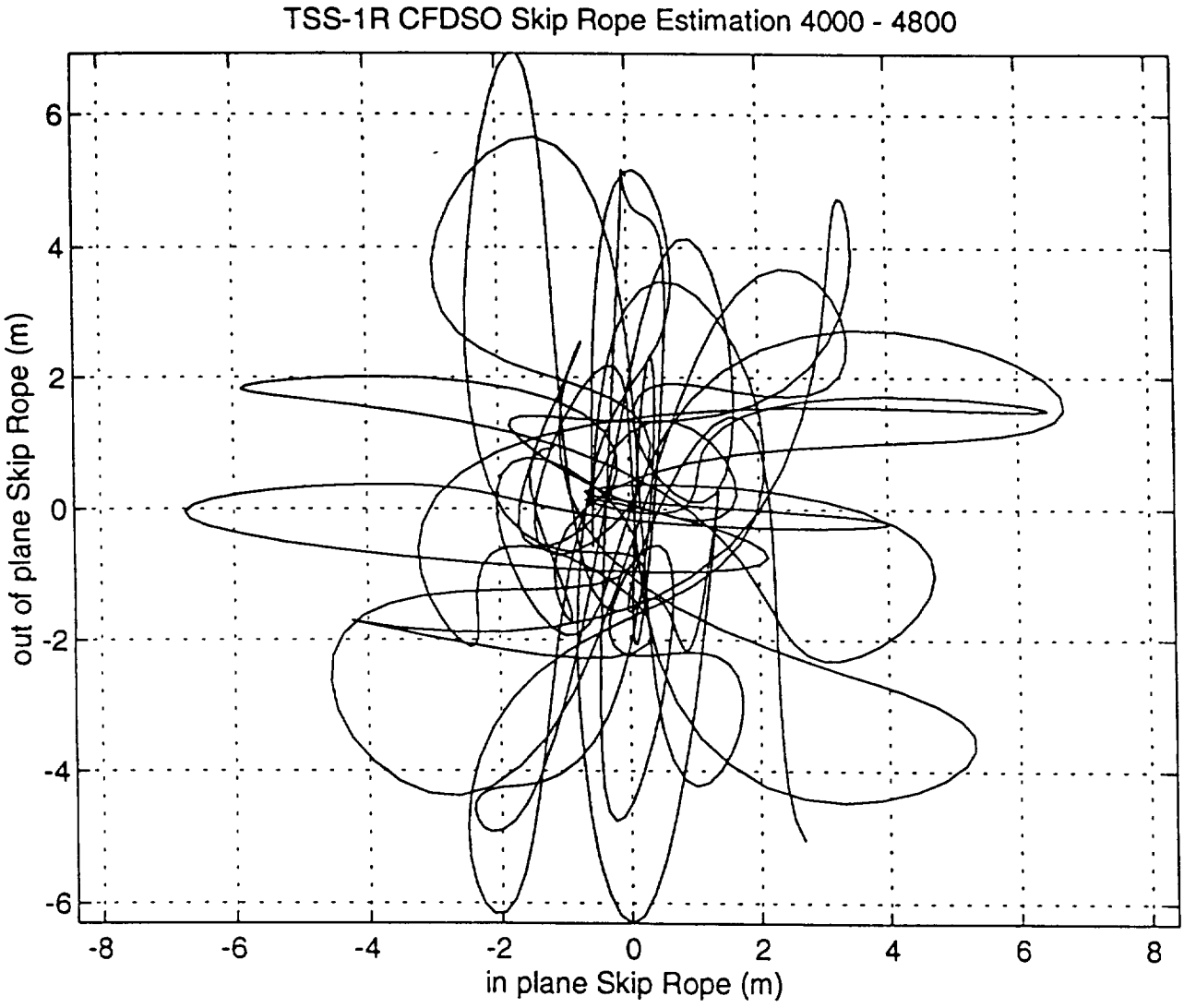

Figure 4.3

The next interval considered is 5160-6000 seconds. This interval was selected to put it beyond the cutoff of the in line 2 thruster set so that the tension in the tether would not be changing significantly. Figure 4.4 shows the tether length variation. The average length is approximately 1600 m. Figure 4.5 presents the satellite rates over this interval. Note that the spin rate is changing over this interval. The satellite has been placed in passive spin mode which means that yaw control is no longer active and the twist torque in the tether is causing the yaw rate to build up slowly. Figure 4.6 is the reconstructed SR for this period and reveals the presence of higher order modes. The amplitudes of the motion are approximately 2 m which is minimal for this location.

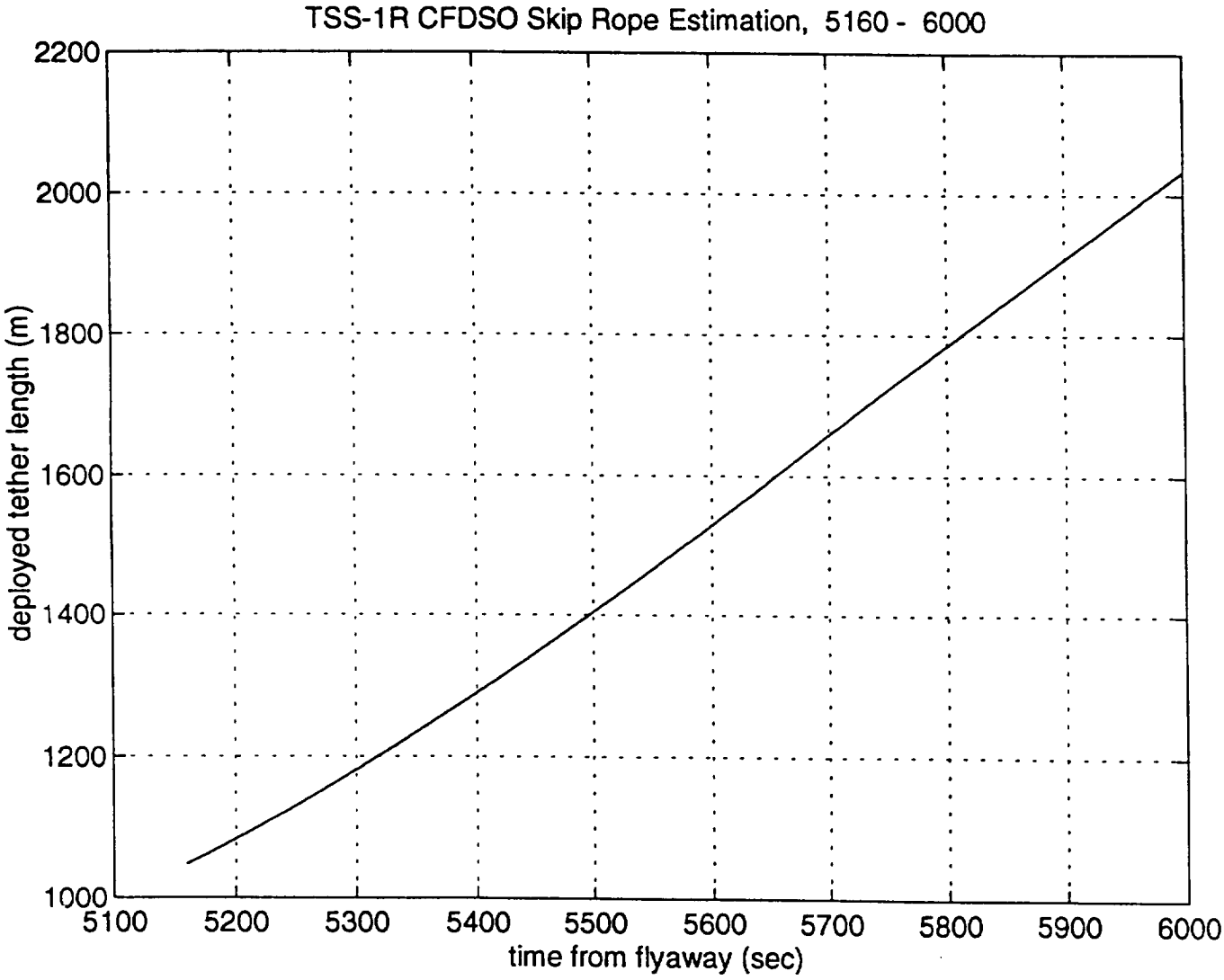

Figure 4.4

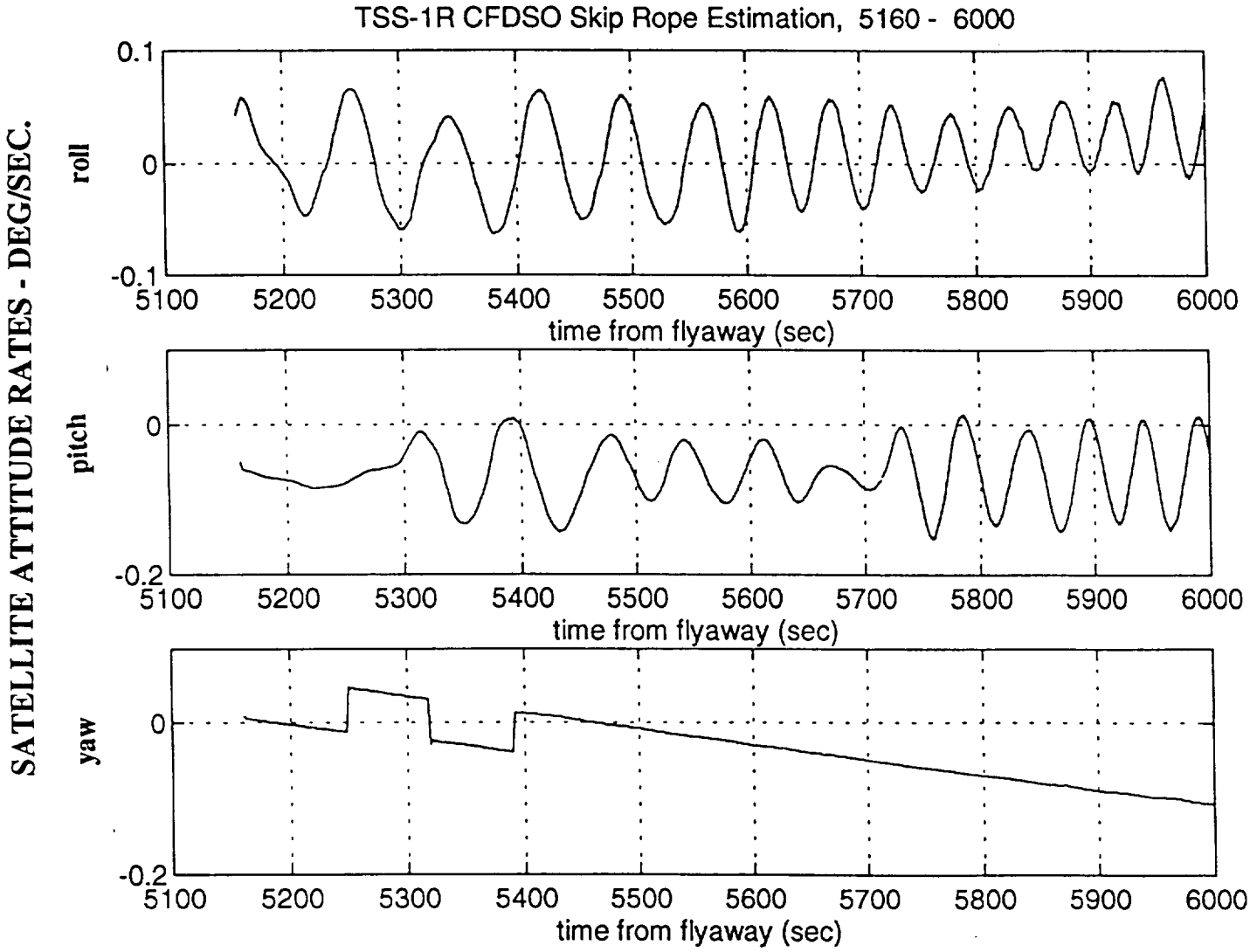
TSS-1R CFDSO Skip Rope Estimation, 5160 - 6000
SATELLITE ATTITUDE RATES - DEG/SEC.
roll
pitch
yaw
0.1
0
-0.1
-0.2
5100
5200
5300
5400
5500
5600
5700
5800
5900
6000
time from flyaway (sec)

Figure 4.5

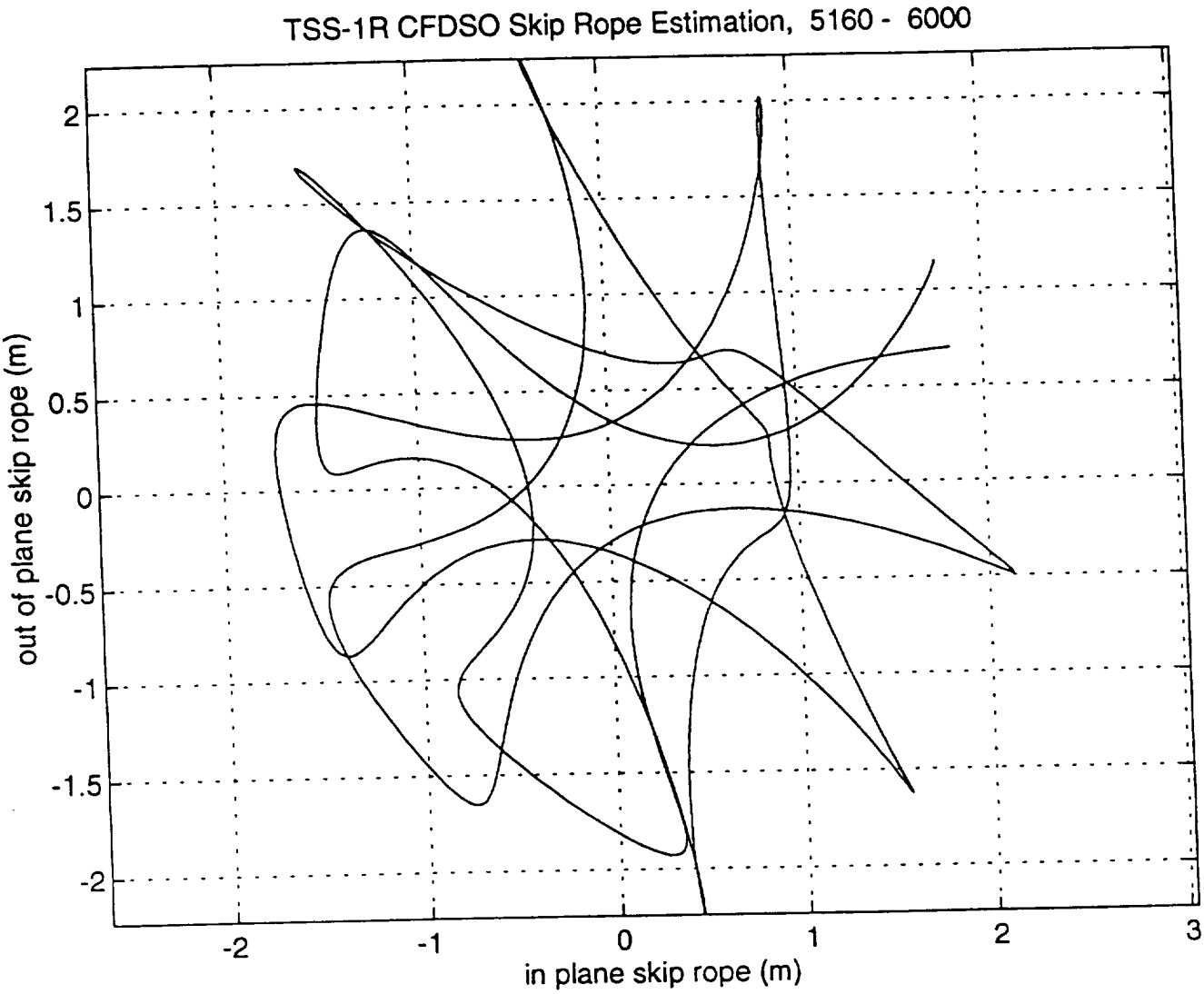
TSS-1R CFDSO Skip Rope Estimation, 5160 - 6000
out of plane skip rope (m)
in plane skip rope (m)
2
1.5
1
0.5
0
-0.5
-1
-1.5
-2
-2
-1
0
1
2
3

Figure 4.6

The next interval is 6000-6800 seconds. Figures 4.7-4.9 show the pertinent results. The average length is 2600 m.. The yaw rate is continuing to build in the negative yaw direction. This is causing the CFDSO to lose lock on its estimate of the satellite yaw angle. However, the SR amplitudes should still be approximately correct. Note that the SR motion amplitudes are still under 2 m.

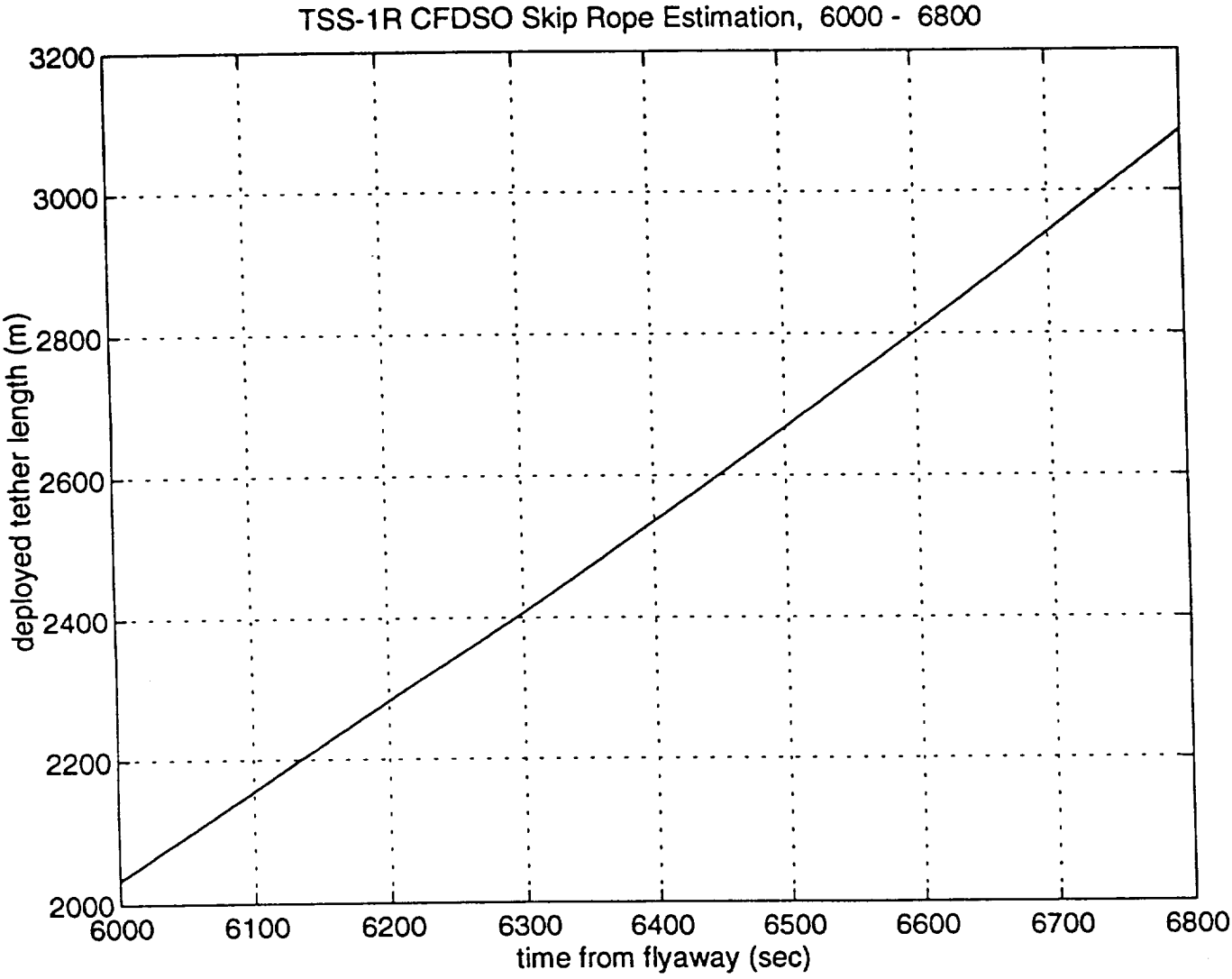

Figure 4.7

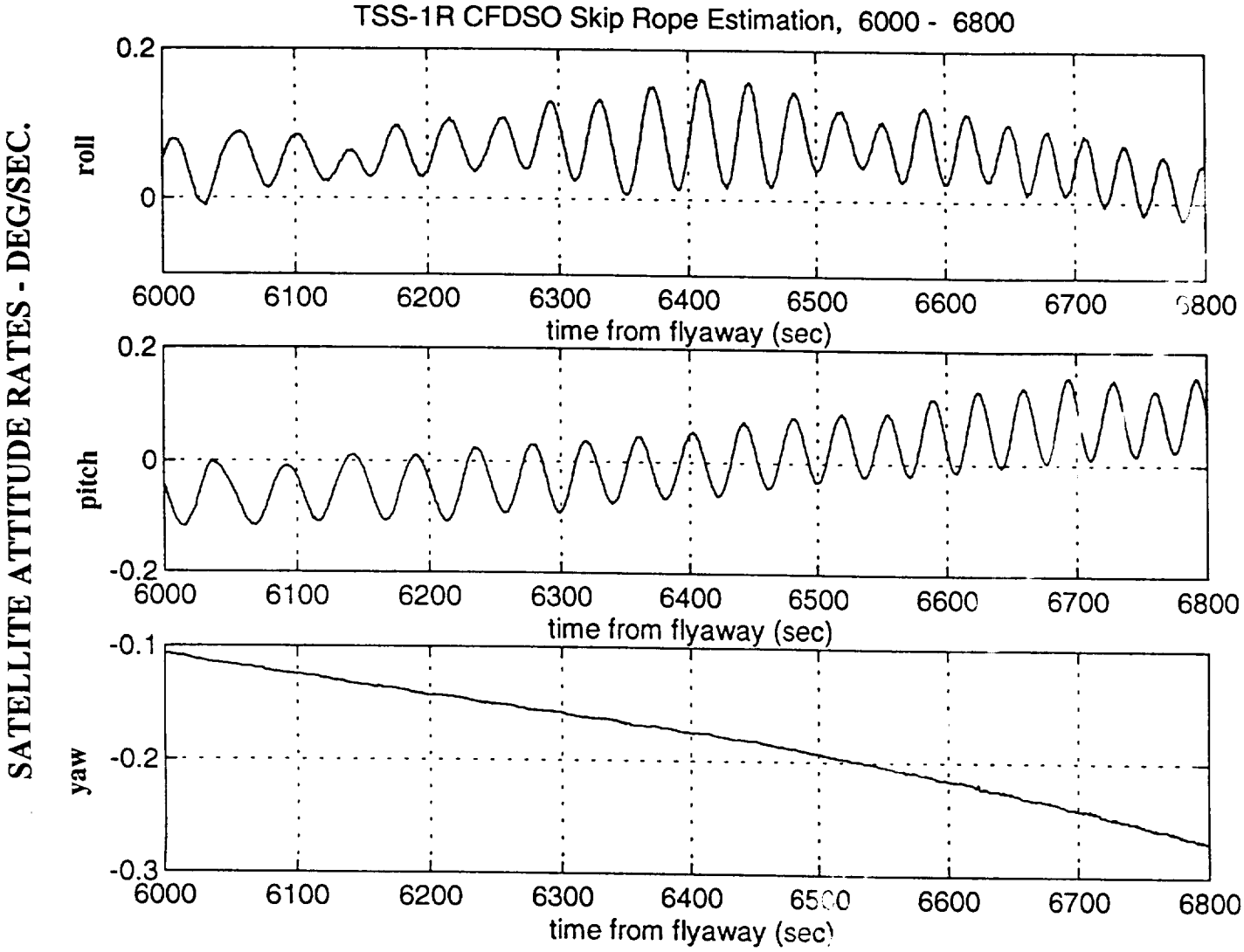
TSS-1R CFDSO Skip Rope Estimation, 6000 - 6800
SATELLITE ATTITUDE RATES - DEG/SEC.
roll
pitch
yaw
0.2
0
-0.2
-0.1
-0.3
6000
6100
6200
6300
6400
6500
6600
6700
6800
time from flyaway (sec)

Figure 4.8

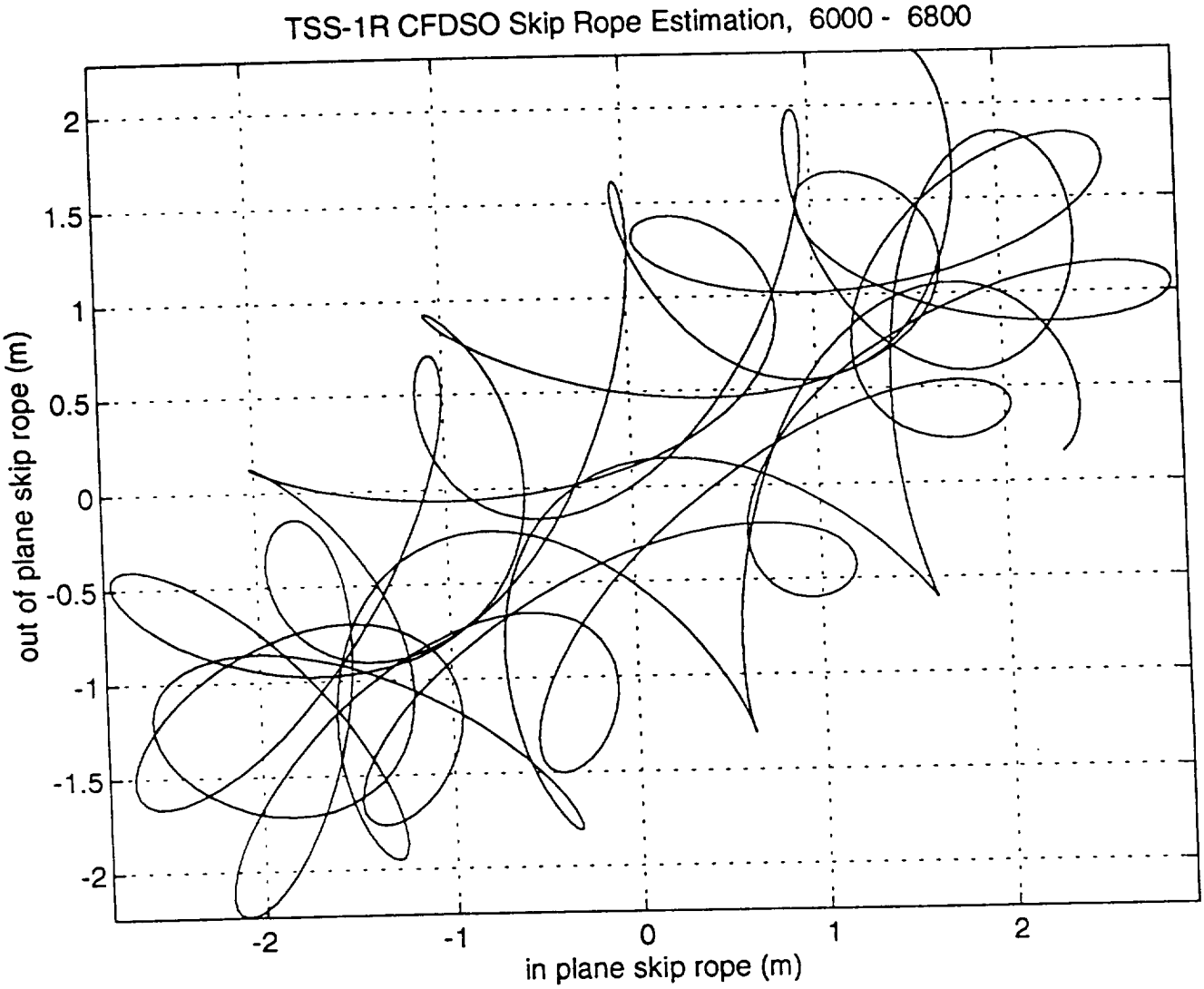
TSS-1R CFDSO Skip Rope Estimation, 6000 - 6800
out of plane skip rope (m)
in plane skip rope (m)
2
1.5
1
0.5
0
-0.5
-1
-1.5
-2
-2
-1
0
1
2

Figure 4.9

The next interval is 7000-8000 seconds. The trend previously described is continuing. This data is shown in Figures 4.10-4.12. The SR motion has simplified and the amplitude is now in the 2-3 m range.

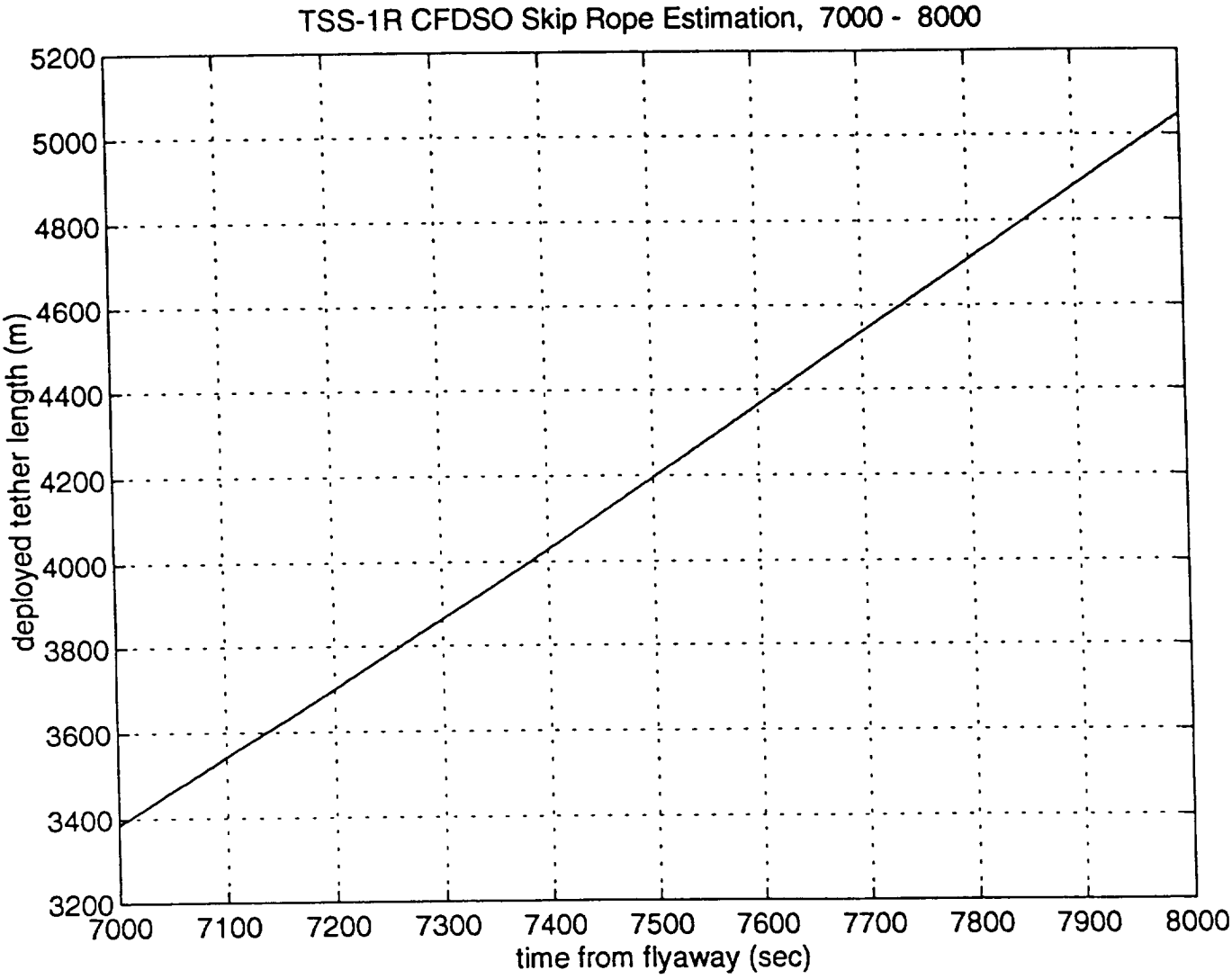

Figure 4.10

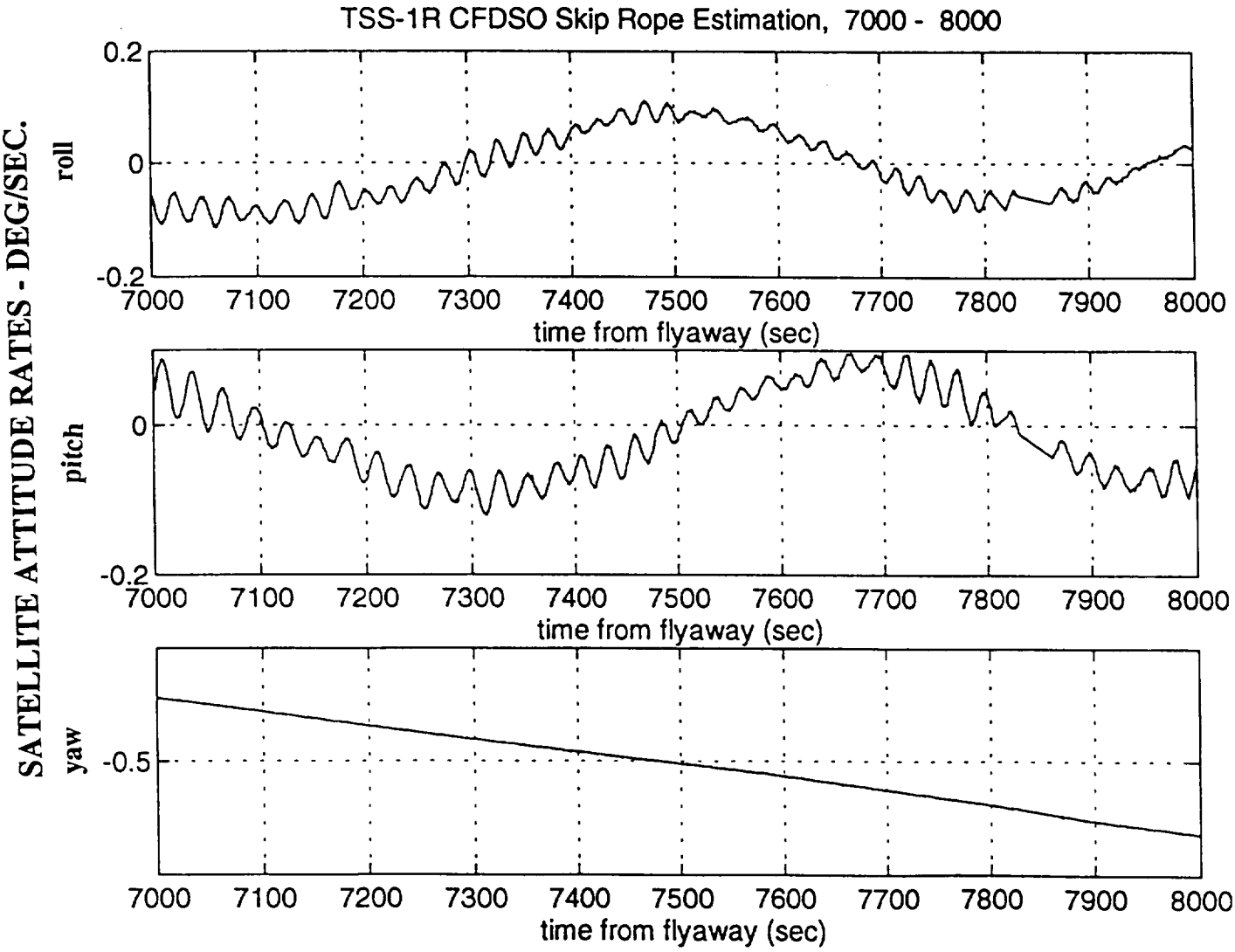
TSS-1R CFDSO Skip Rope Estimation, 7000 - 8000
SATELLITE ATTITUDE RATES - DEG/SEC.
roll
pitch
yaw
0.2
0
-0.2
-0.5
7000
7100
7200
7300
7400
7500
7600
7700
7800
7900
8000
time from flyaway (sec)

Figure 4.11

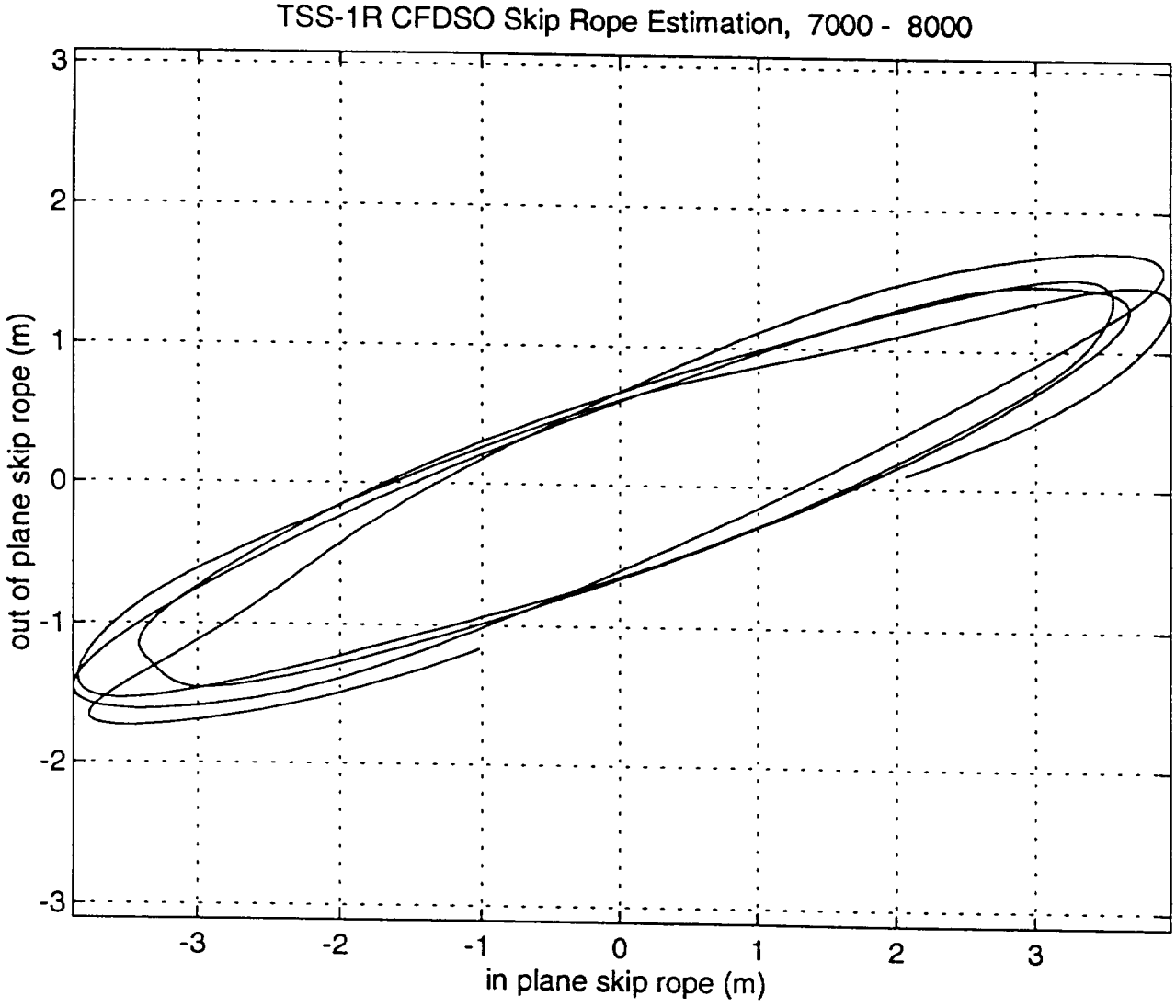
TSS-1R CFDSO Skip Rope Estimation, 7000 - 8000
out of plane skip rope (m)
in plane skip rope (m)
3
2
1
0
-1
-2
-3
-3
-2
-1
0
1
2
3

Figure 4.12

The interval from 8000-9000 seconds after flyaway shows a significant growth in SR amplitude. This data is shown in Figures 4.13-4.15. This trend may be due to the current flow which is starting to be effective in driving SR.

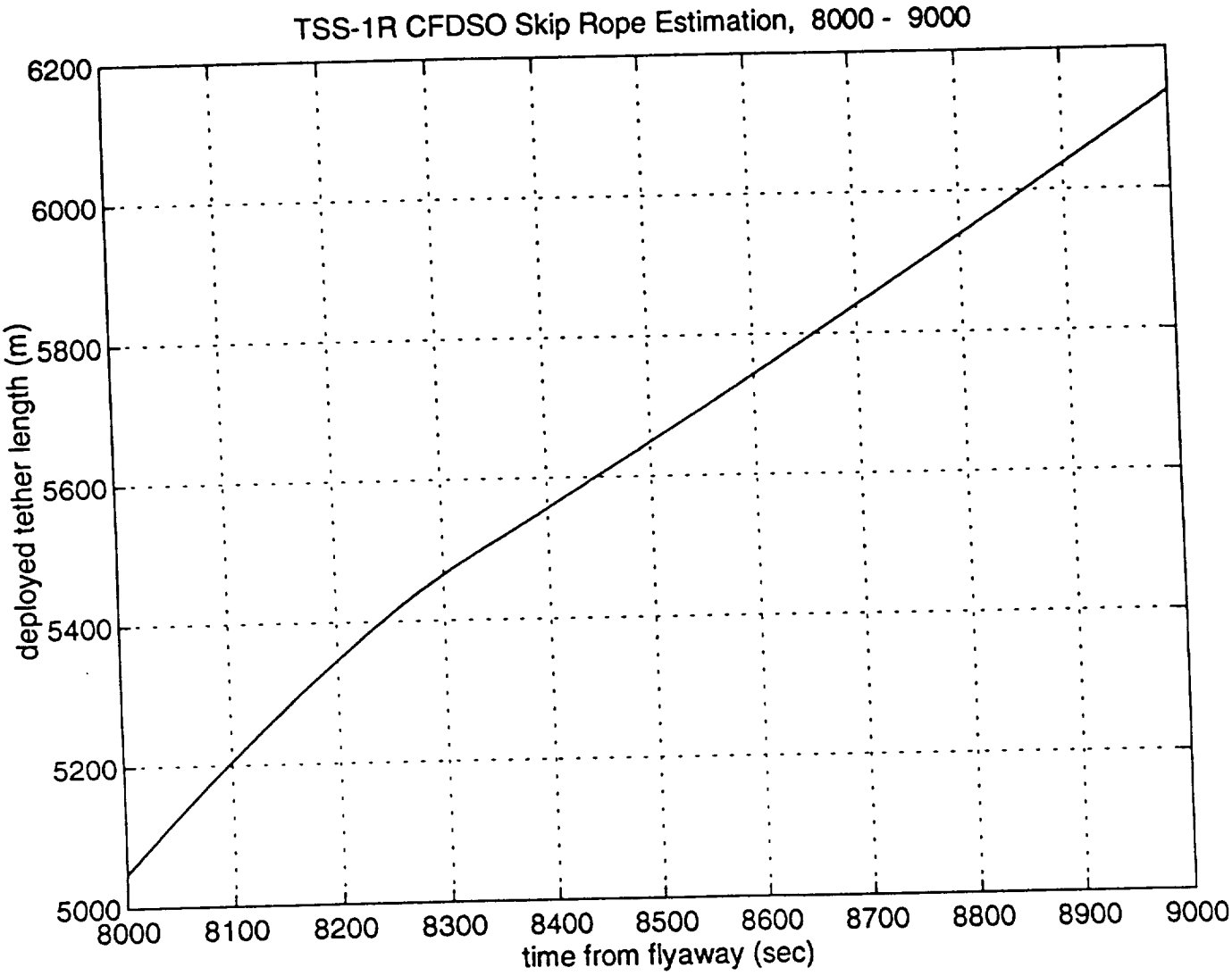

Figure 4.13

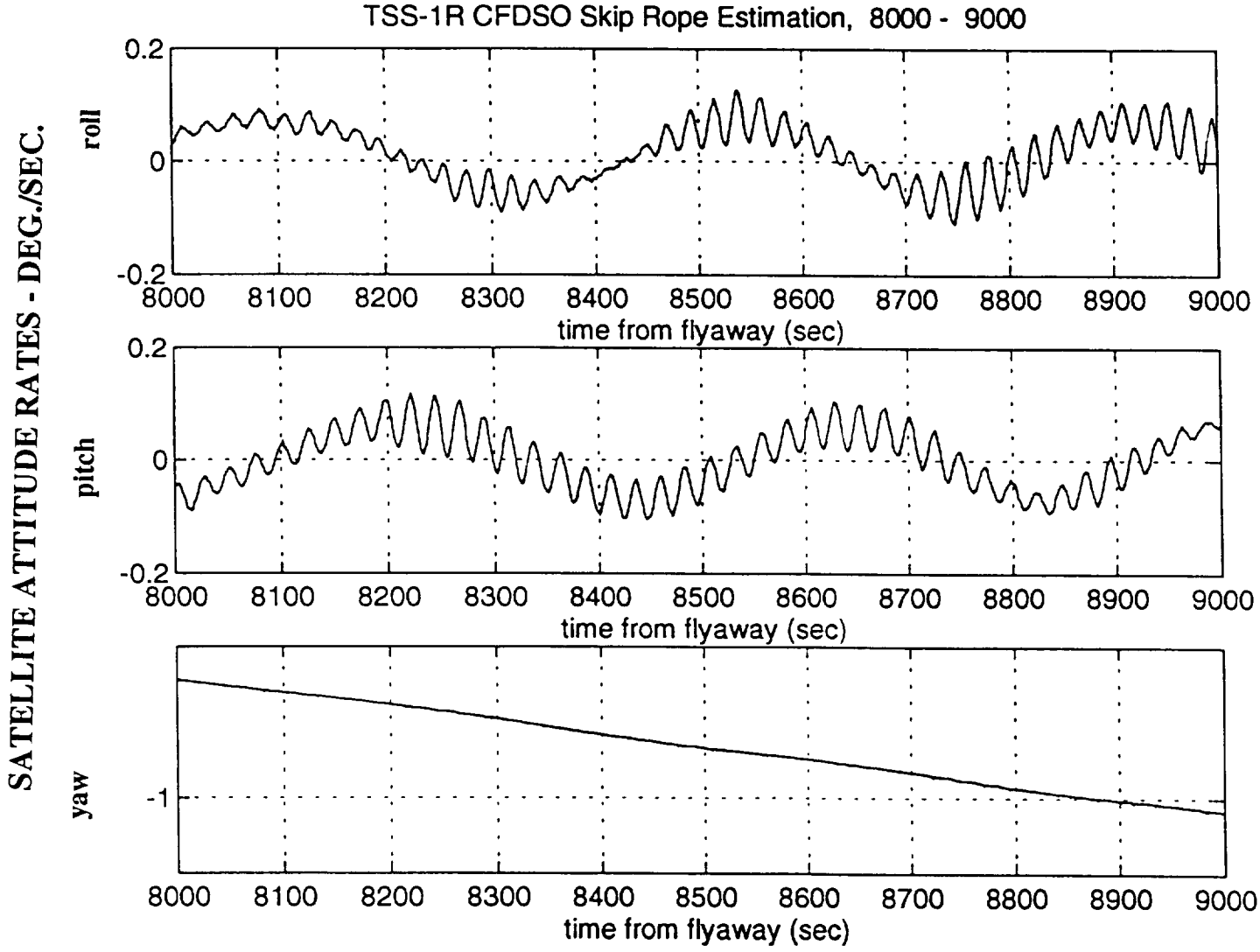
TSS-1R CFDSO Skip Rope Estimation, 8000 - 9000
SATELLITE ATTITUDE RATES - DEG./SEC.
roll
pitch
yaw
0.2
0
-0.2
-1
8000
8100
8200
8300
8400
8500
8600
8700
8800
8900
9000
time from flyaway (sec)

Figure 4.14

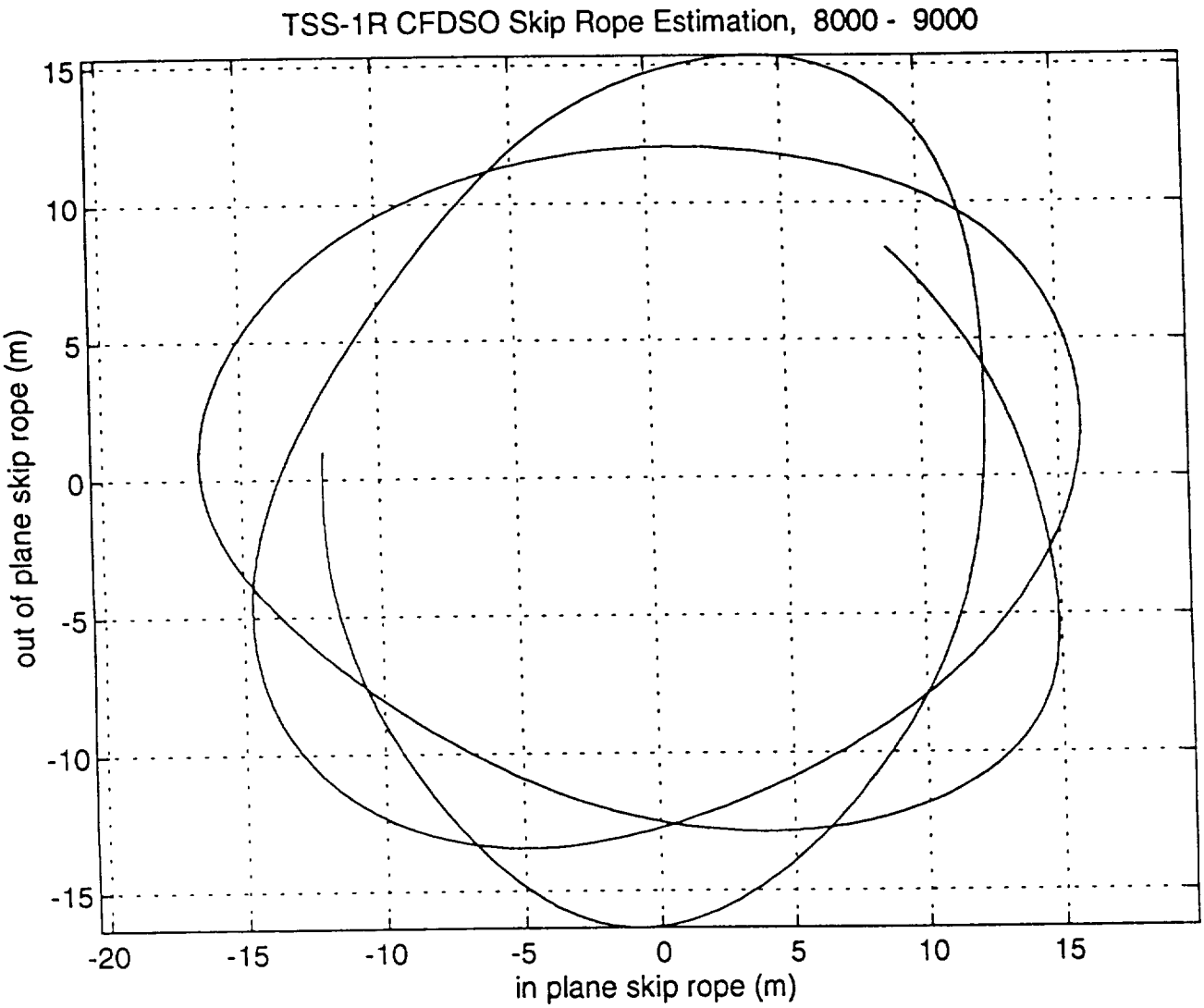
TSS-1R CFDSO Skip Rope Estimation, 8000 - 9000
out of plane skip rope (m)
in plane skip rope (m)
15
10
5
0
-5
-10
-15
-20
-15
-10
-5
0
5
10
15

Figure 4.15

The interval from 10000-11000 seconds (Figures 4.16-4.18) shows a continued buildup in SR amplitude and a significant change in shape but since phase information is unreliable, the shape should not be taken very seriously. The shape is interesting in that it has a small amount of angular momentum relative to the amplitude and results from significant contributions from higher order SR modes.

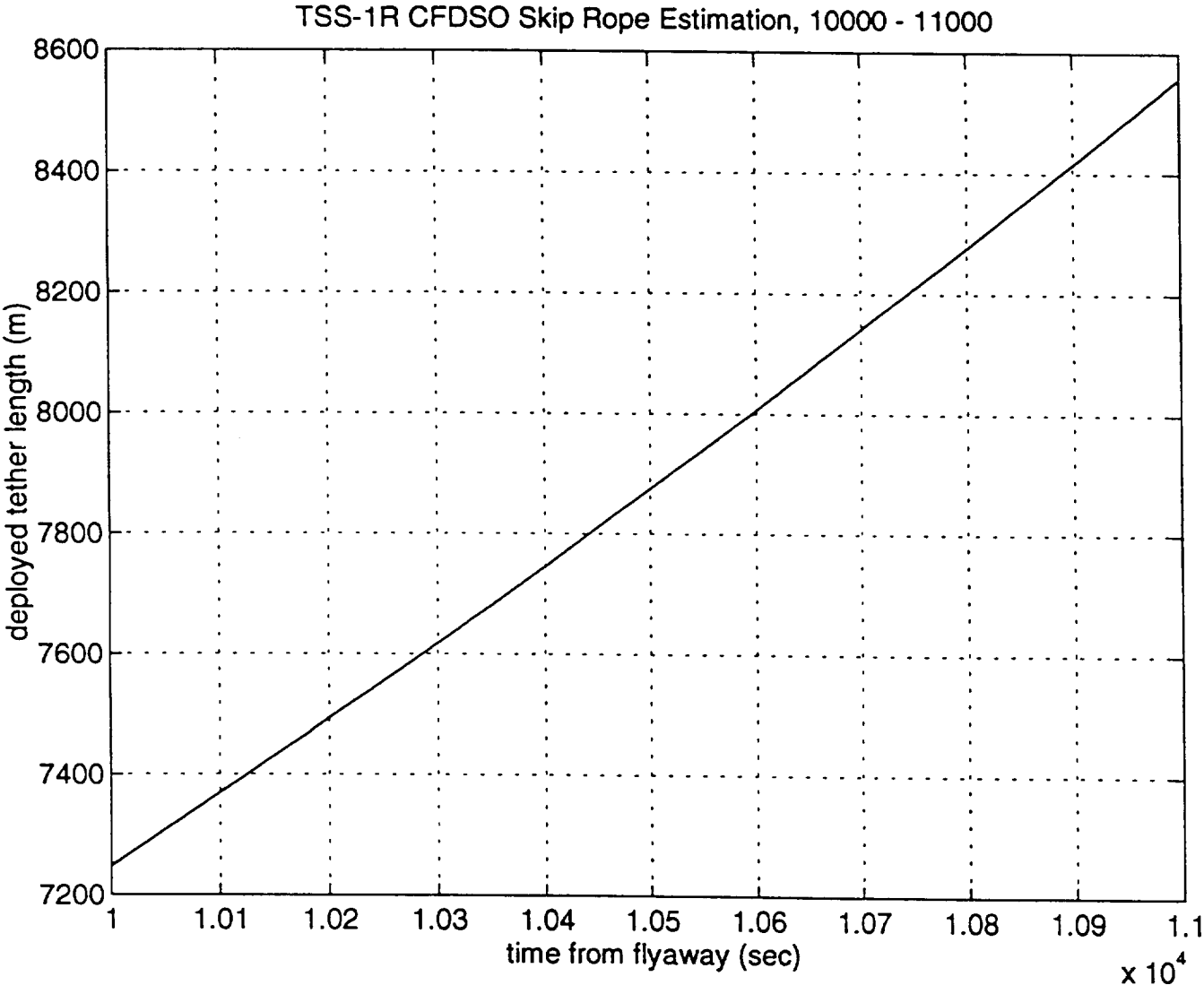

Figure 4.16

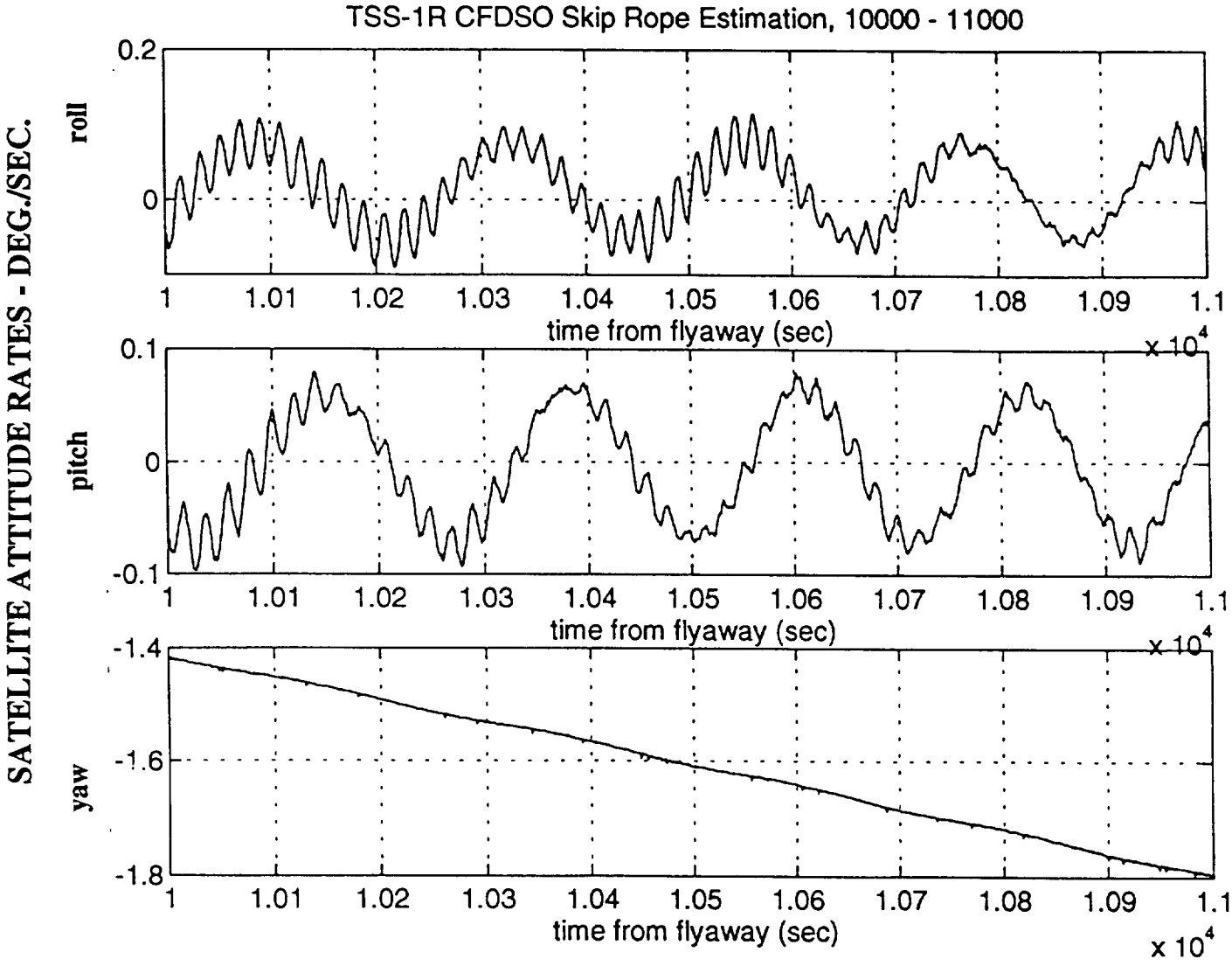
TSS-1R CFDSO Skip Rope Estimation, 10000 - 11000
SATELLITE ATTITUDE RATES - DEG./SEC.
roll
pitch
yaw
time from flyaway (sec)
x 10^4

Figure 4.17

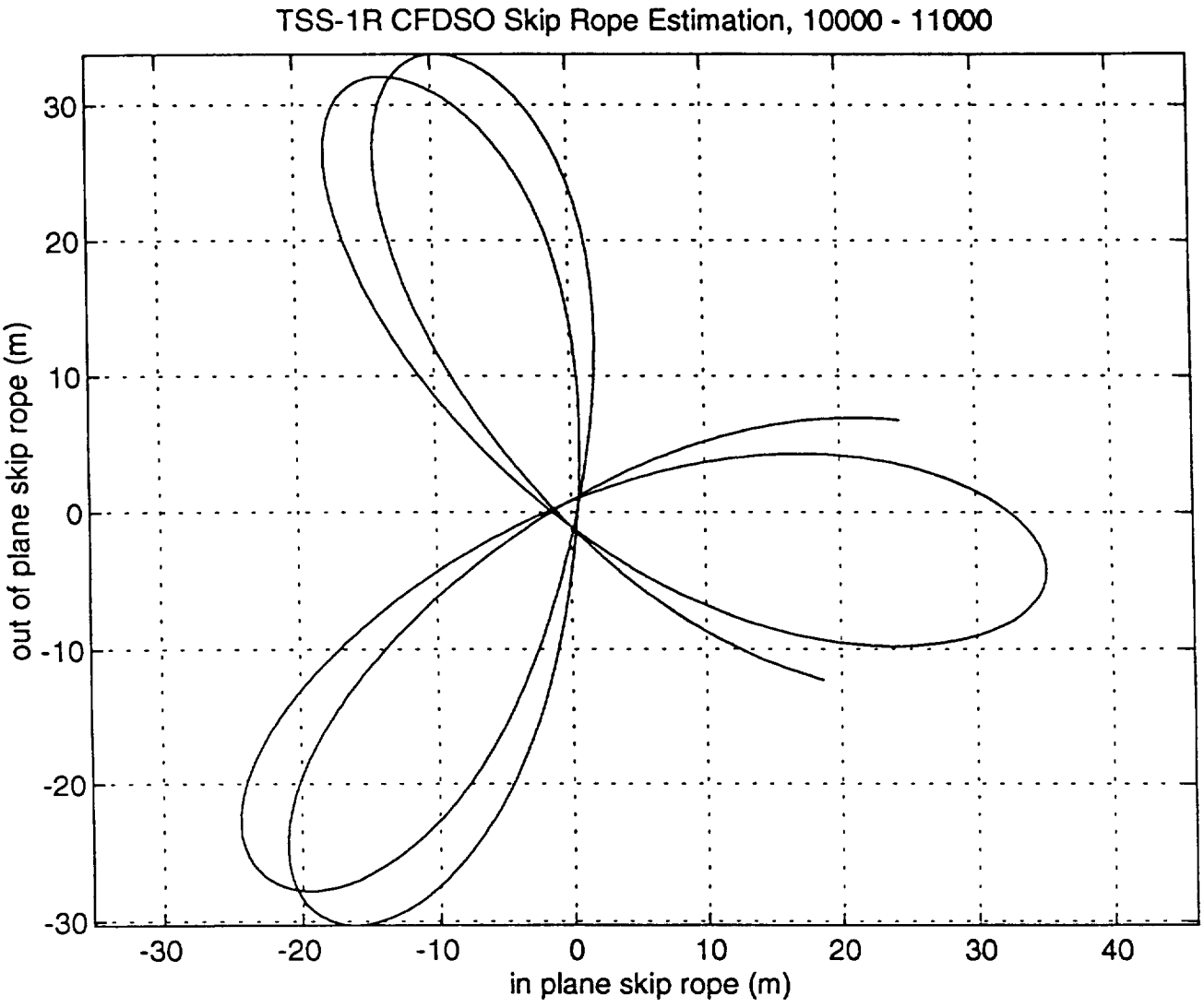
TSS-1R CFDSO Skip Rope Estimation, 10000 - 11000
out of plane skip rope (m)
in plane skip rope (m)
30
20
10
0
-10
-20
-30
-30
-20
-10
0
10
20
30
40

Figure 4.18

The interval from 12000-13000 seconds (Figures 4.19-4.21) covers a period when yaw control has been re-enabled. This should allow improved accuracy for the CFDSO estimates of SR motion.

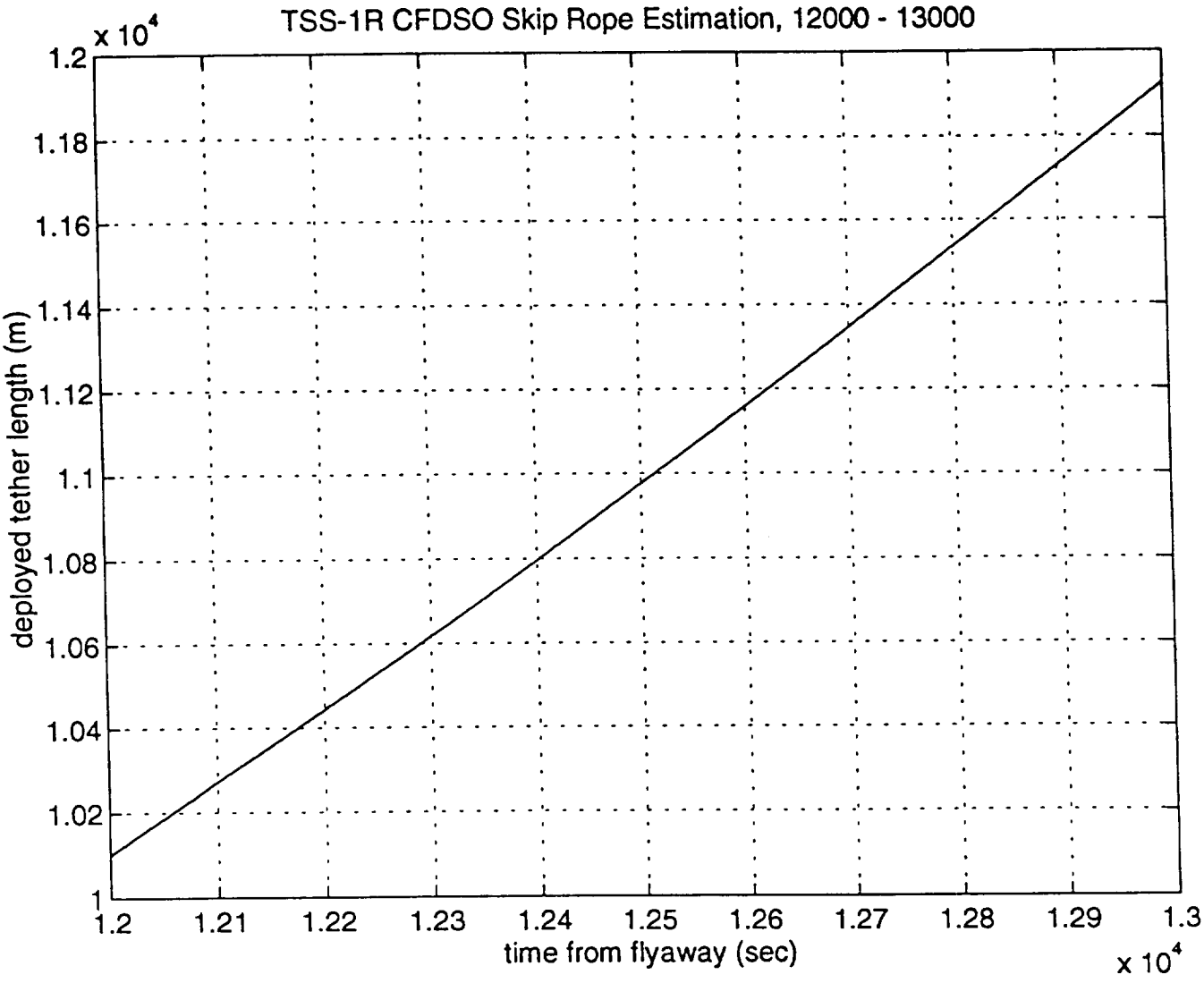

Figure 4.19

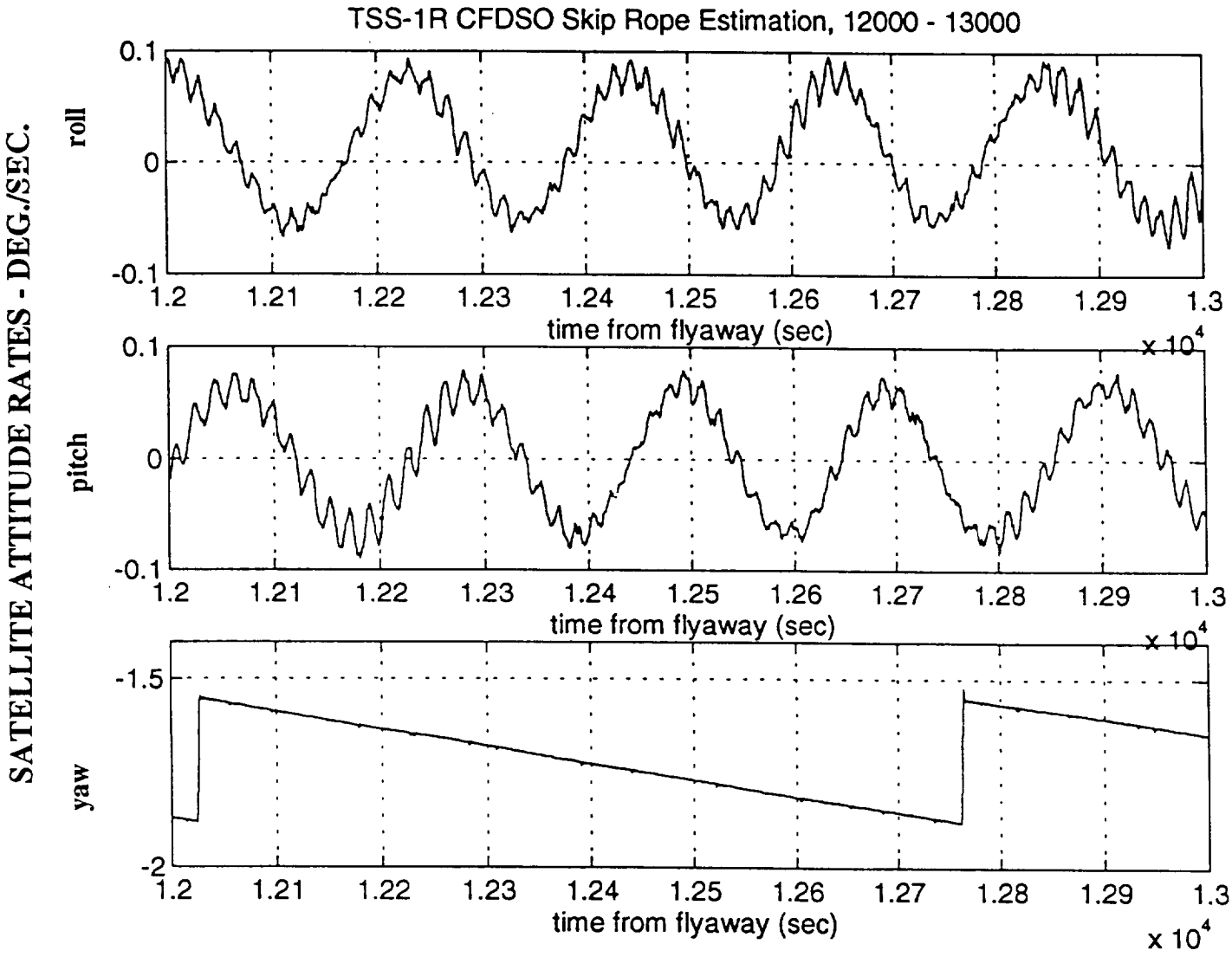
TSS-1R CFDSO Skip Rope Estimation, 12000 - 13000
SATELLITE ATTITUDE RATES - DEG./SEC.
roll
pitch
yaw
0.1
0
-0.1
-1.5
-2
1.2
1.21
1.22
1.23
1.24
1.25
1.26
1.27
1.28
1.29
1.3
time from flyaway (sec)
x 10^4

Figure 4.20

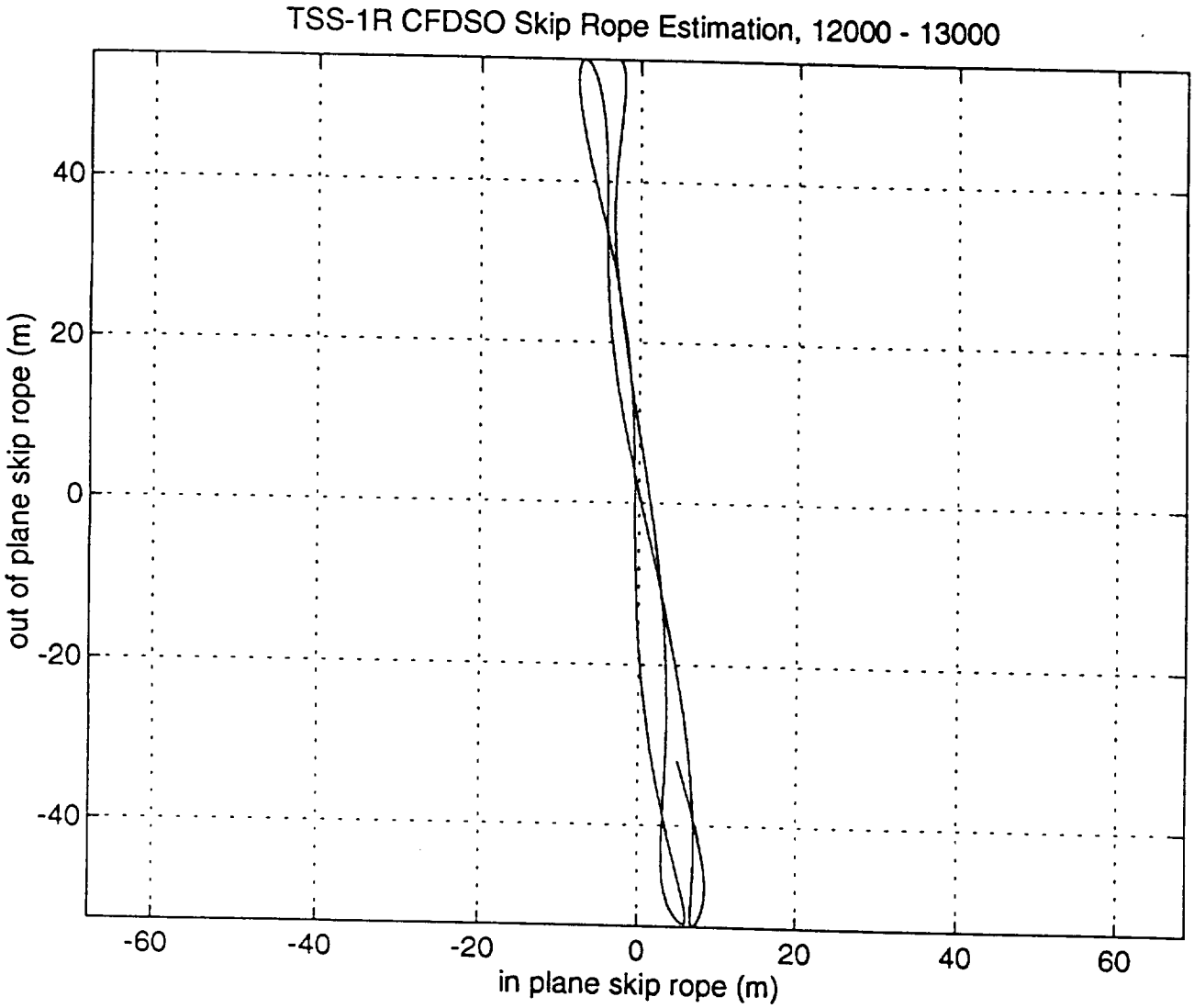
TSS-1R CFDSO Skip Rope Estimation, 12000 - 13000
out of plane skip rope (m)
40
20
0
-20
-40
-60
-40
-20
0
20
40
60
in plane skip rope (m)

Figure 4.21

The resulting SR motion shows nearly 50 m of mostly out of plane skip rope motion. The trend is continued for the period 14000-15200 seconds (Figures 4.22-4.24). The SR motion remains mostly out of plane motion with an amplitude of nearly 70 m.

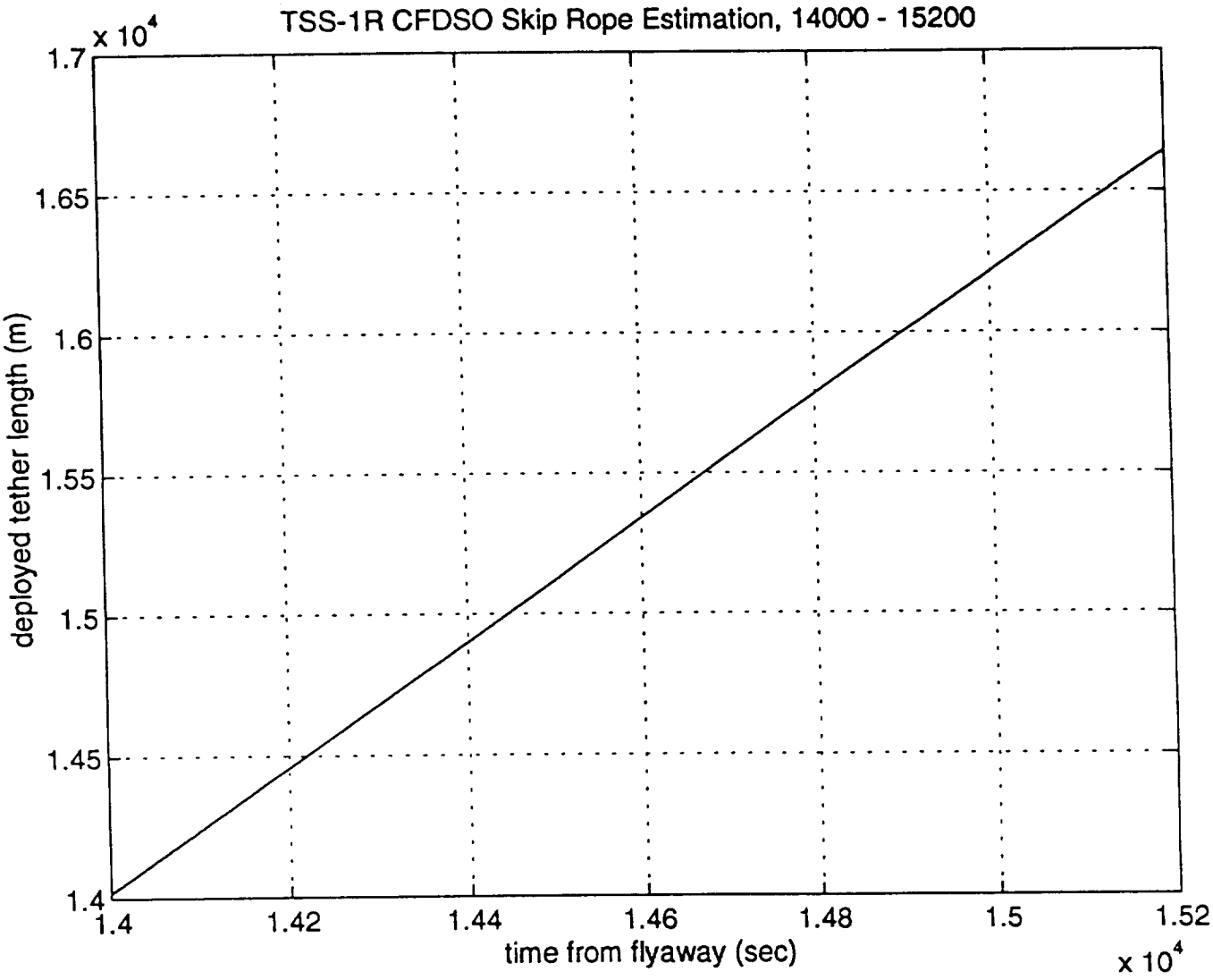

Figure 4.22

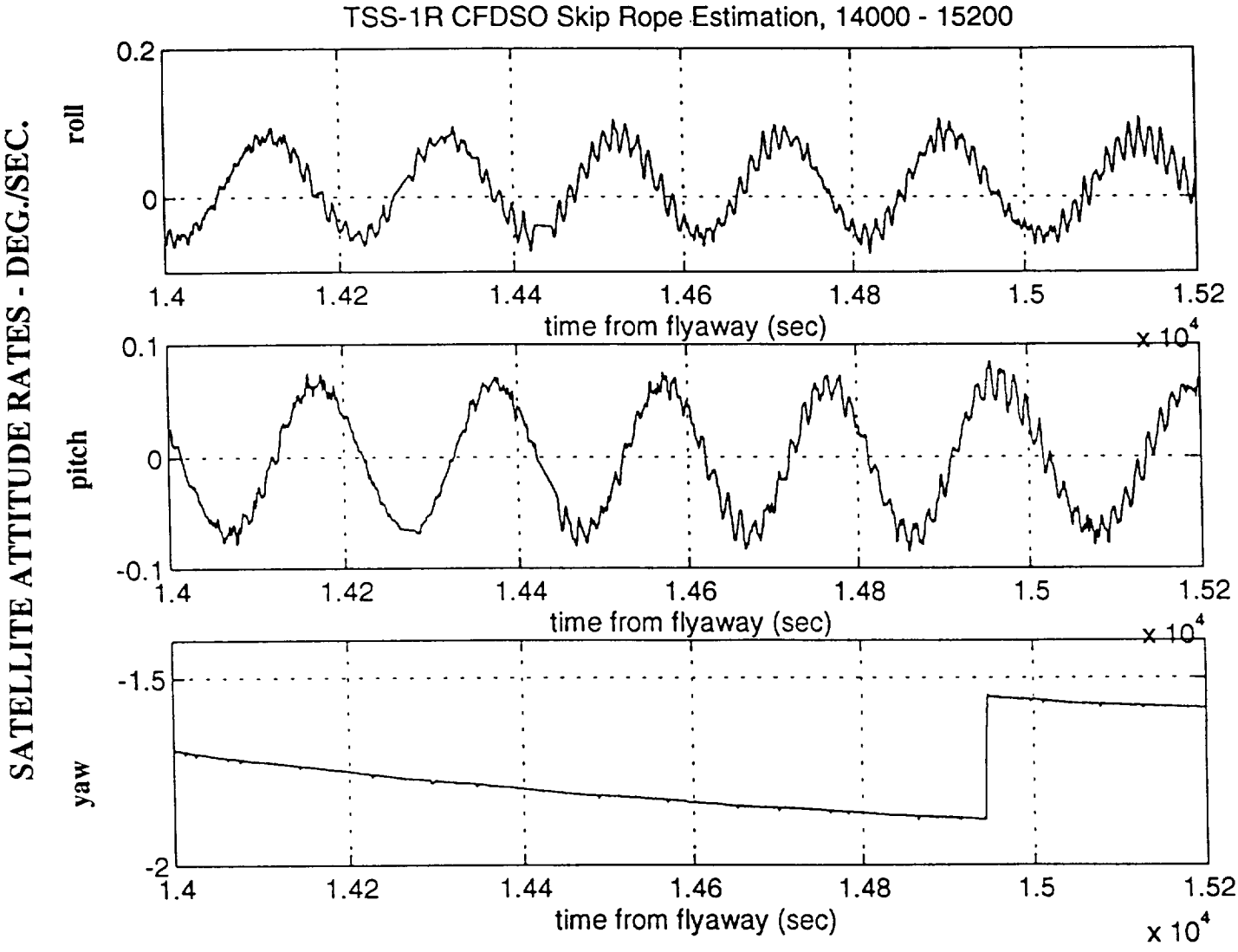
TSS-1R CFDSO Skip Rope Estimation, 14000 - 15200
SATELLITE ATTITUDE RATES - DEG./SEC.
roll
pitch
yaw
0.2
0
0.1
-0.1
-1.5
-2
1.4
1.42
1.44
1.46
1.48
1.5
1.52
time from flyaway (sec)
x 10^4

Figure 4.23

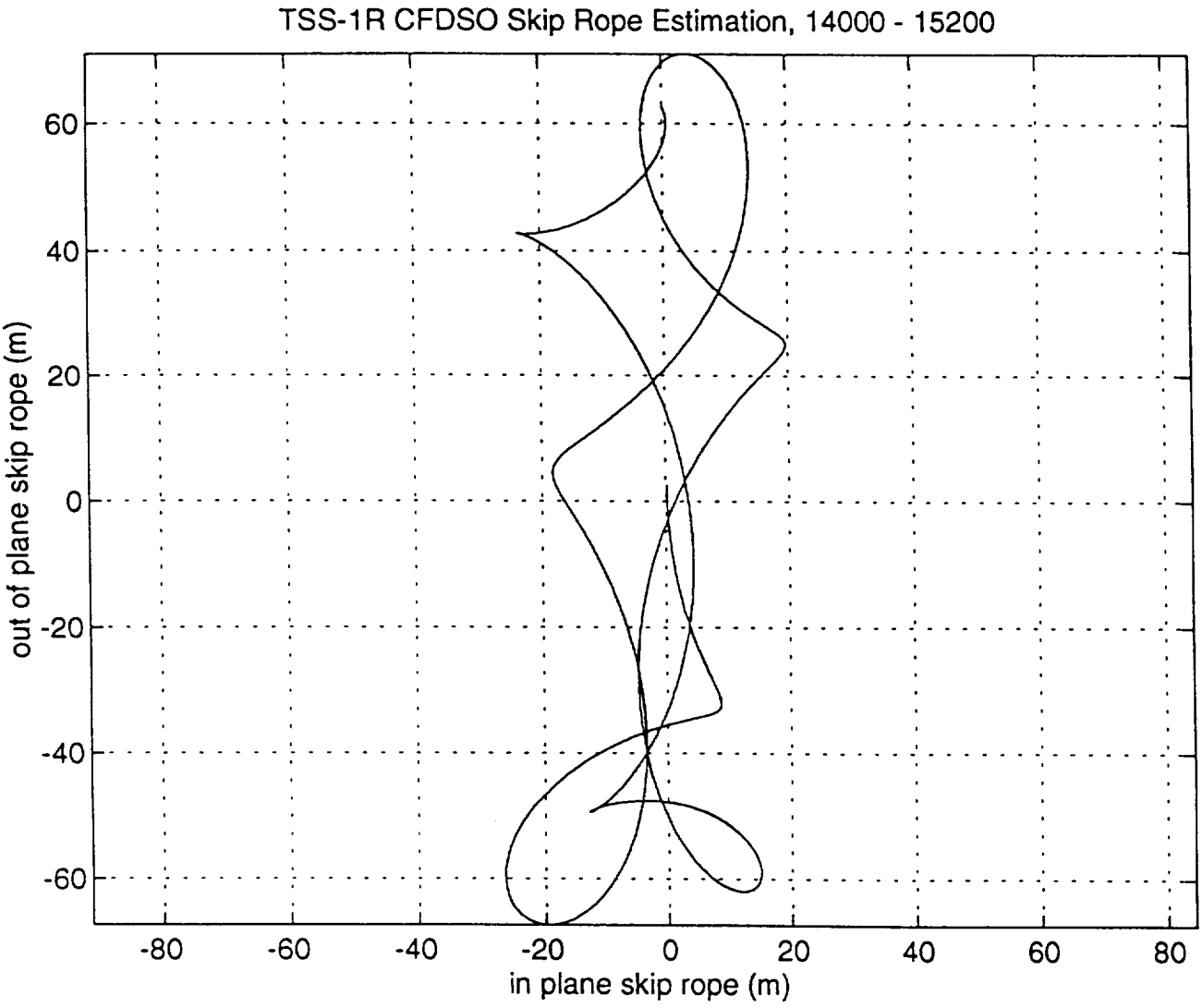
TSS-1R CFDSO Skip Rope Estimation, 14000 - 15200
out of plane skip rope (m)
in plane skip rope (m)
60
40
20
0
-20
-40
-60
-80
-60
-40
-20
0
20
40
60
80

Figure 4.24

The final interval covers 15600-17000, the period just prior to the tether cut. The deployment rate is slowing during this interval and the CFDSO performance should be improving. This data is shown in Figures 4.25-4.27. Note that the amplitude has reduced to approximately 35 m in plane and 30 m out of plane. The SR motion has acquired more angular momentum. The effects of current flowing is beginning to be more evident.

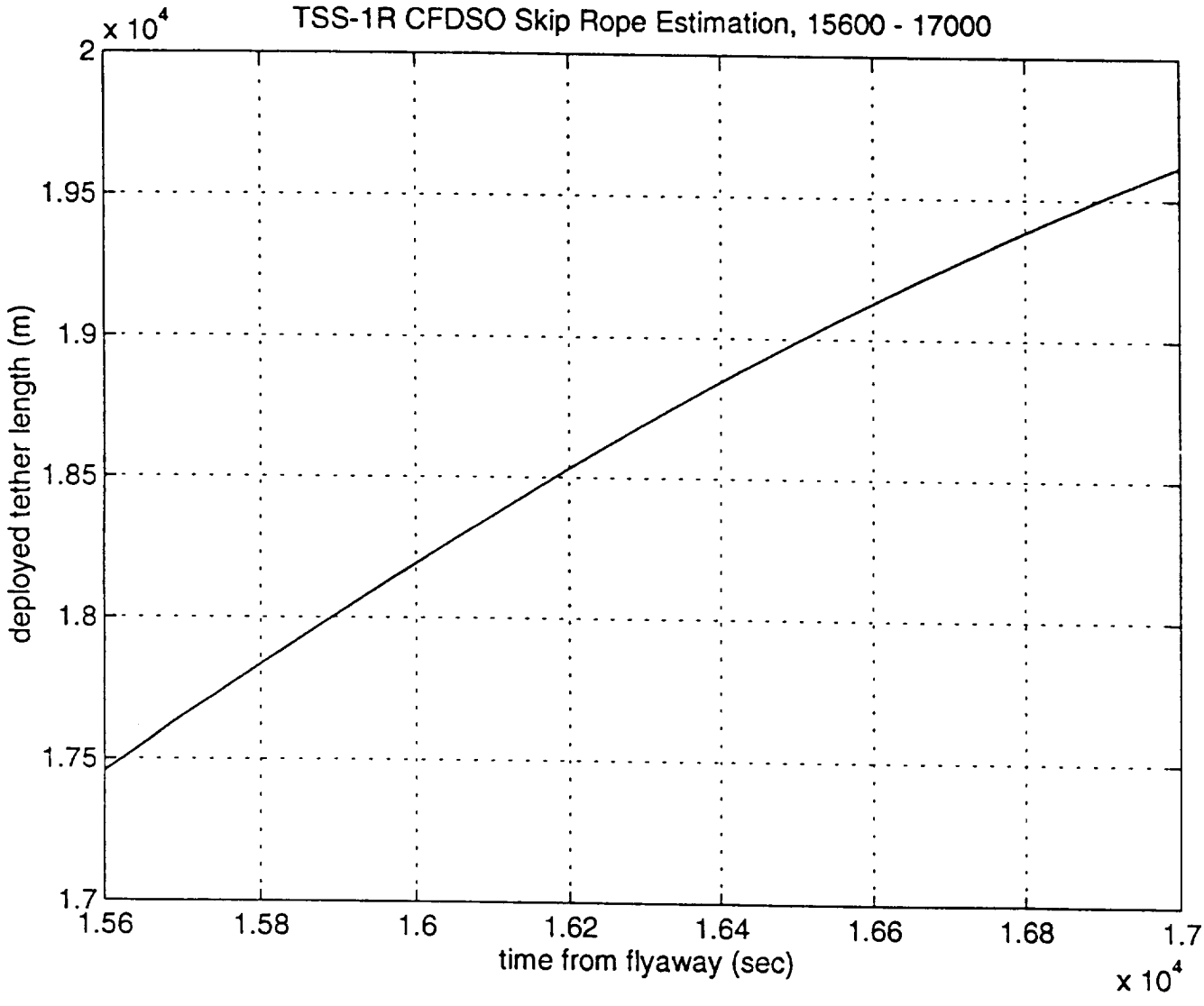

Figure 4.25

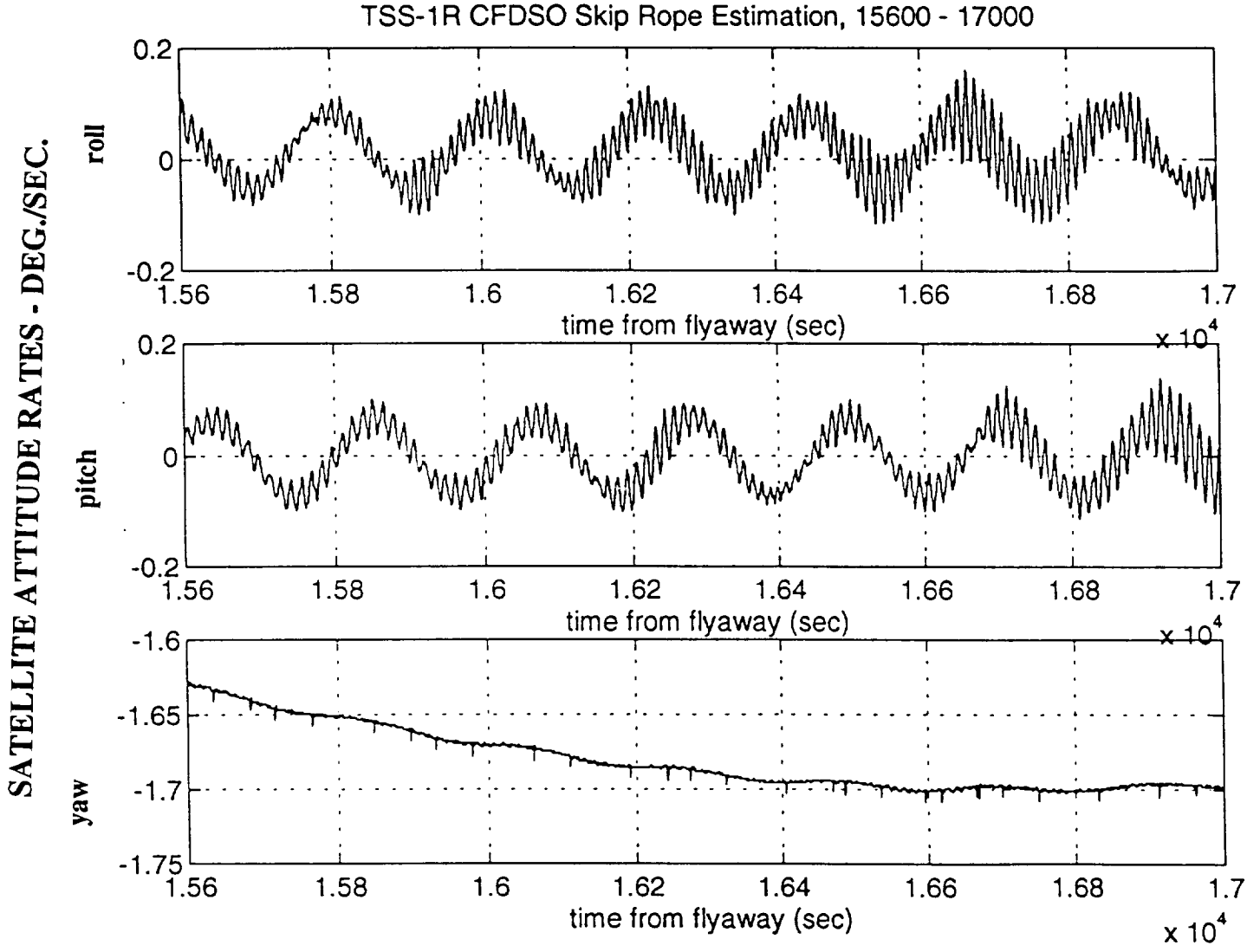
TSS-1R CFDSO Skip Rope Estimation, 15600 - 17000
SATELLITE ATTITUDE RATES - DEG./SEC.
roll
pitch
yaw
0.2
0
-0.2
-1.6
-1.65
-1.7
-1.75
1.56
1.58
1.6
1.62
1.64
1.66
1.68
1.7
time from flyaway (sec)
x 10^4

Figure 4.26

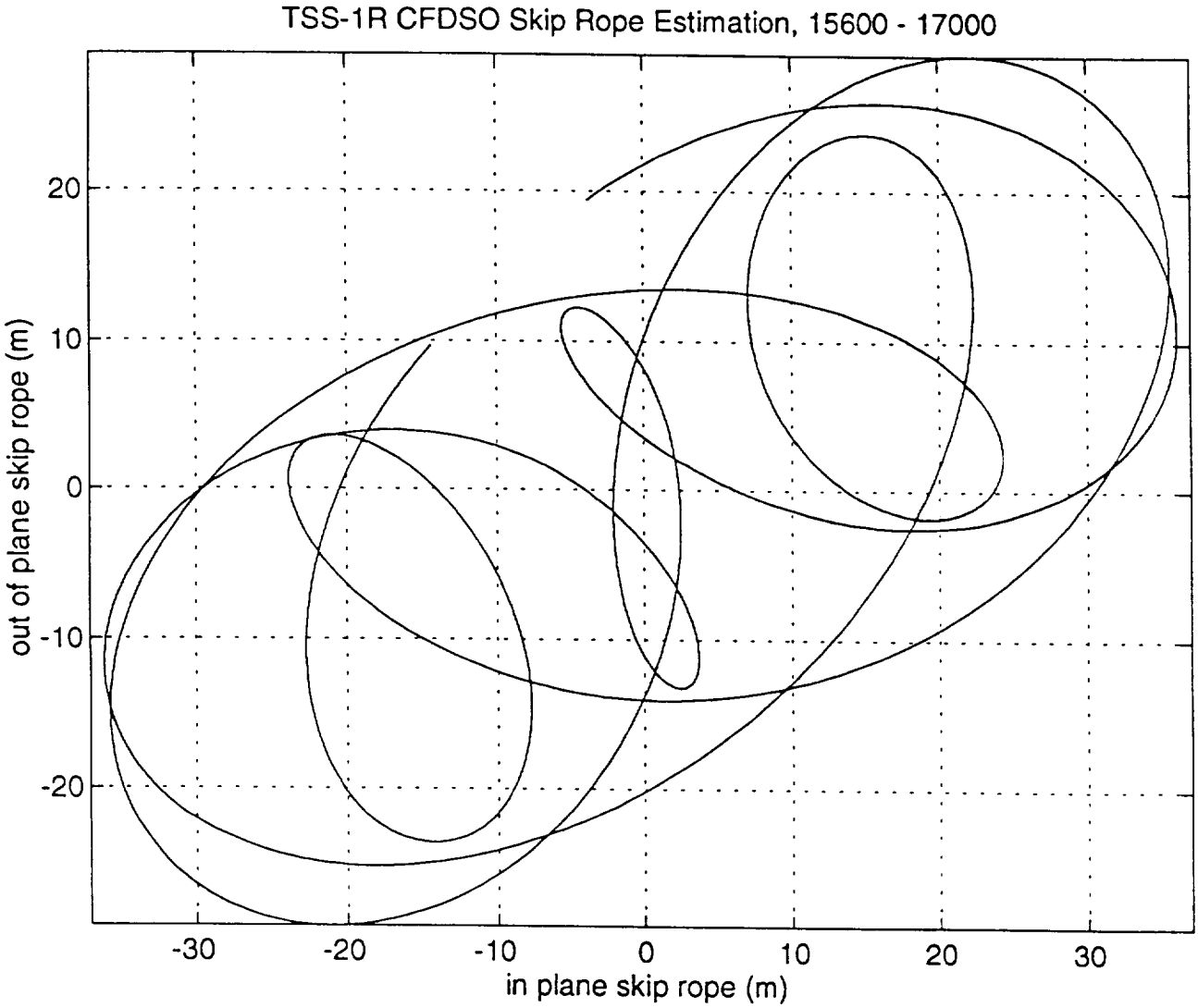
TSS-1R CFDSO Skip Rope Estimation, 15600 - 17000
out of plane skip rope (m)
in plane skip rope (m)
20
10
0
-10
-20
-30
-20
-10
0
10
20
30

Figure 4.27

Overall the performance of the CFDSO during this period appears to be reasonable. Comparisons between SRO's (time domain skip rope observer (TDSO) and CFDSO have shown approximate matches in amplitude but disagreement in phase. Thus, the results summarized in this discussion with the accompanying plots represents a good estimate of SR behavior over the period of the tether deployment for TSS-1R. More detailed analysis of the telemetry data including better estimates of satellite attitude as well as video data showing the tether may allow better determination of tether skip rope motion.

5.0 AUTO RATE DAMPING PERFORMANCE

The auto rate damping (ARD) mode was tested during the period from 3427-5162 following flyaway. Figure 5.1 shows the satellite roll and pitch rates during this period. The ARD tests are indicated by the increases in rates followed by the reductions back to previous levels. The performance of the ARD system is indicated by the rapid reduction of the satellite rates back to levels within the deadband levels set for the ARD which were typically 0.5 degrees/second. This reduction was accomplished with 1 to 2 thruster shots. Thus, the ARD system was shown to perform its function quite well.

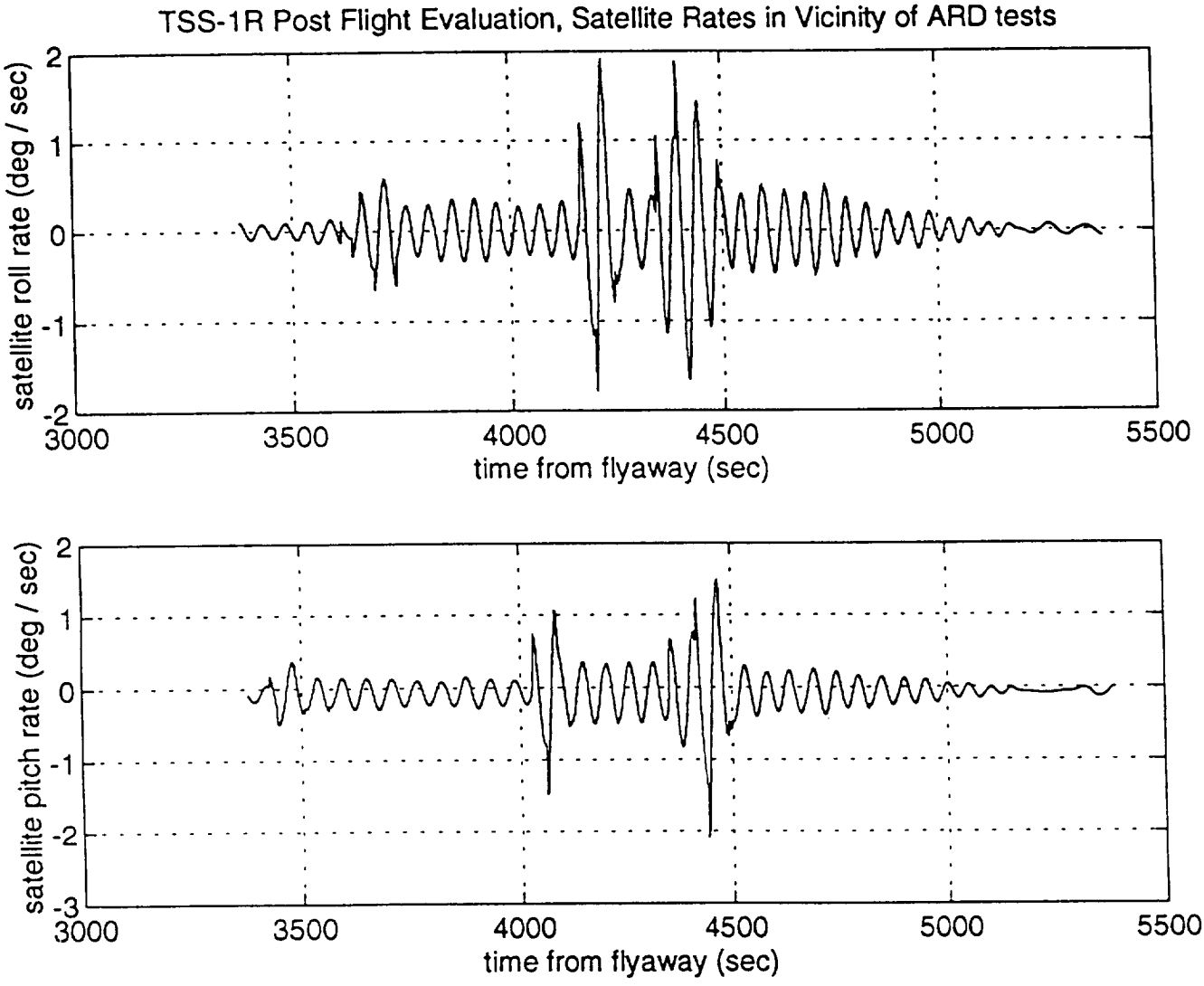
TSS-1R Post Flight Evaluation, Satellite Rates in Vicinity of ARD tests
satellite roll rate (deg / sec)
2
1
0
-1
-2
3000
3500
4000
4500
5000
5500
time from flyaway (sec)
satellite pitch rate (deg / sec)
2
1
0
-1
-2
-3
3000
3500
4000
4500
5000
5500
time from flyaway (sec)

Figure 5.1

6.0 TETHER VOLTAGE AND CURRENT TIME HISTORIES

The tether voltage vs time curve is shown in Figure 6.1. Scale changes which occur at discrete times during the deployment are not properly accounted for in the conversion algorithm. These show up as abrupt changes in voltage level. Each scale change is a factor of 10.

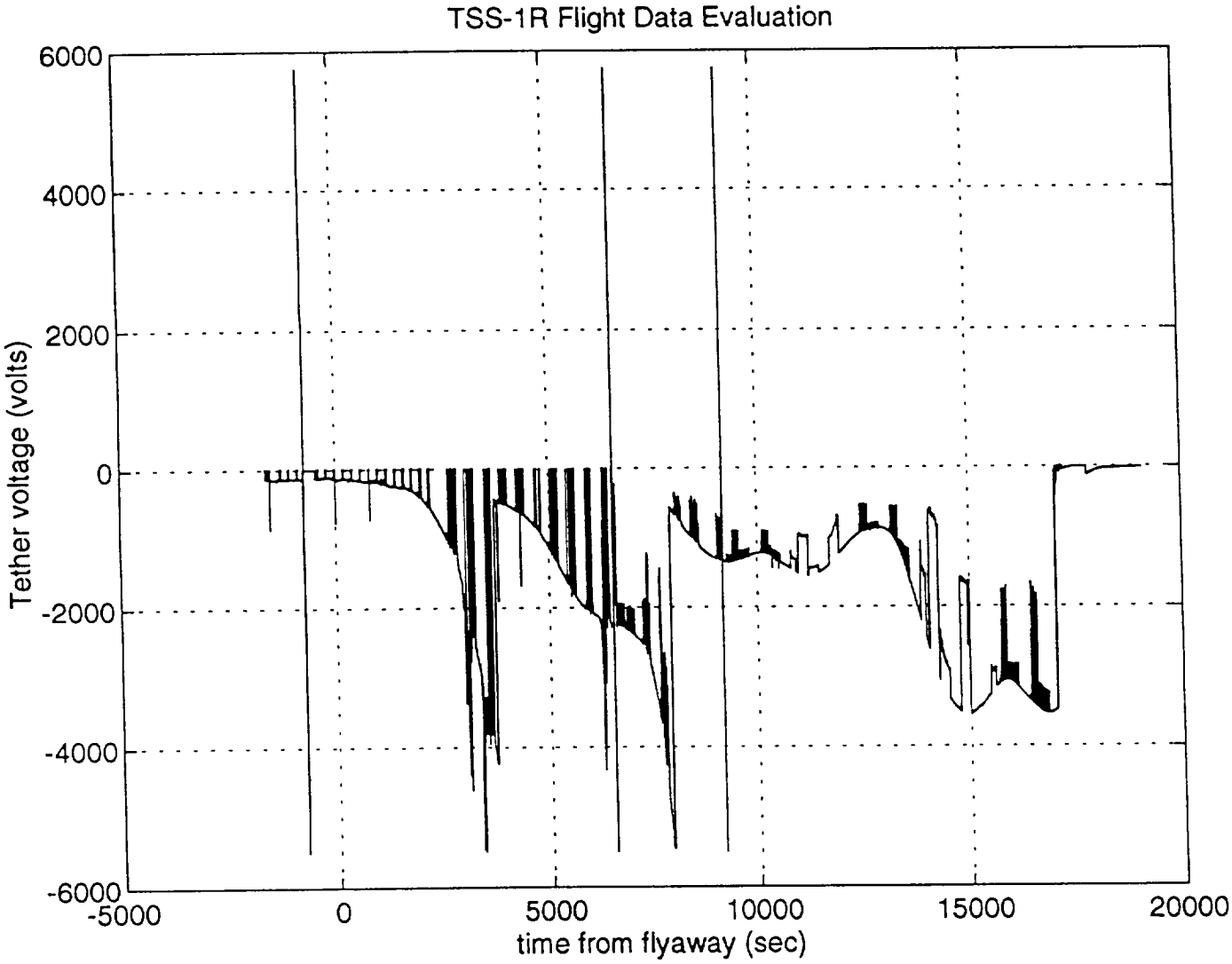

Figure 6.1

The final scale is 1.0 so that voltage levels after approximately 8000 seconds after flyaway are correct. Figure 6.2 shows tether current vs time. The vertical lines apparently represent spurious noise peaks which were not eliminated by the processing algorithm. It is to be noted that no currents above 0.5 Amperes were measured (disregarding the noise spikes). The current which caused the tether to break apparently bypassed the ammeter location. This is reasonable since ammeter was on the deployer side of the tether and hence would be bypassed by the arcing current. No conclusions are reached with respect to voltage and current except that they were both within expected ranges and behaved as expected prior to the tether break.

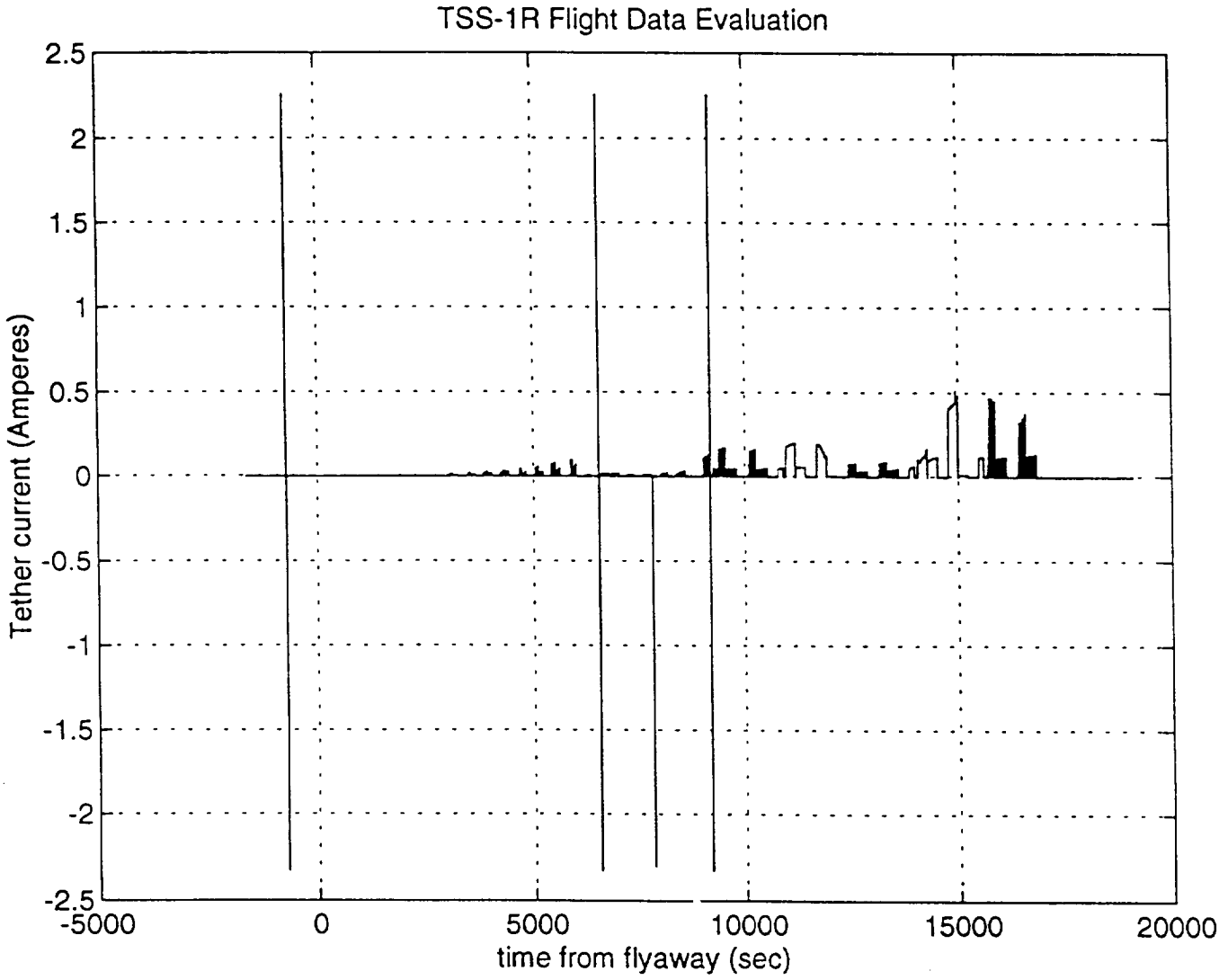

Figure 6.2

7.0 SATELLITE MAGNETIC FIELD TIME HISTORY

The tethered satellite measured magnetic (Temag) field data was used as part of the information set processed by the SRO's. There were questions prior to the flight of TSS-1R whether the understanding of the coordinate axes in which these were defined were properly handled by the SRO's and the SRO pre-processor logic. The pre-processor logic calculated an estimate of the earth magnetic field appropriate to the satellite altitude and latitude and longitude. This was converted to the local vertical, local horizontal (LVLH) reference frame and compared with Temag to calculate a yaw angle and provide additional information to the Kalman filter process in the TDSO. Figure 7.1 shows the Temag and estimation model x component of the magnetic field. The Temag data is the rapidly varying data and the model is the slow varying data. This behavior results because the time interval covered here is the period during which the satellite is spinning and no attempt has been made to transform the Temag data to a non-spinning frame aligned with LVLH.

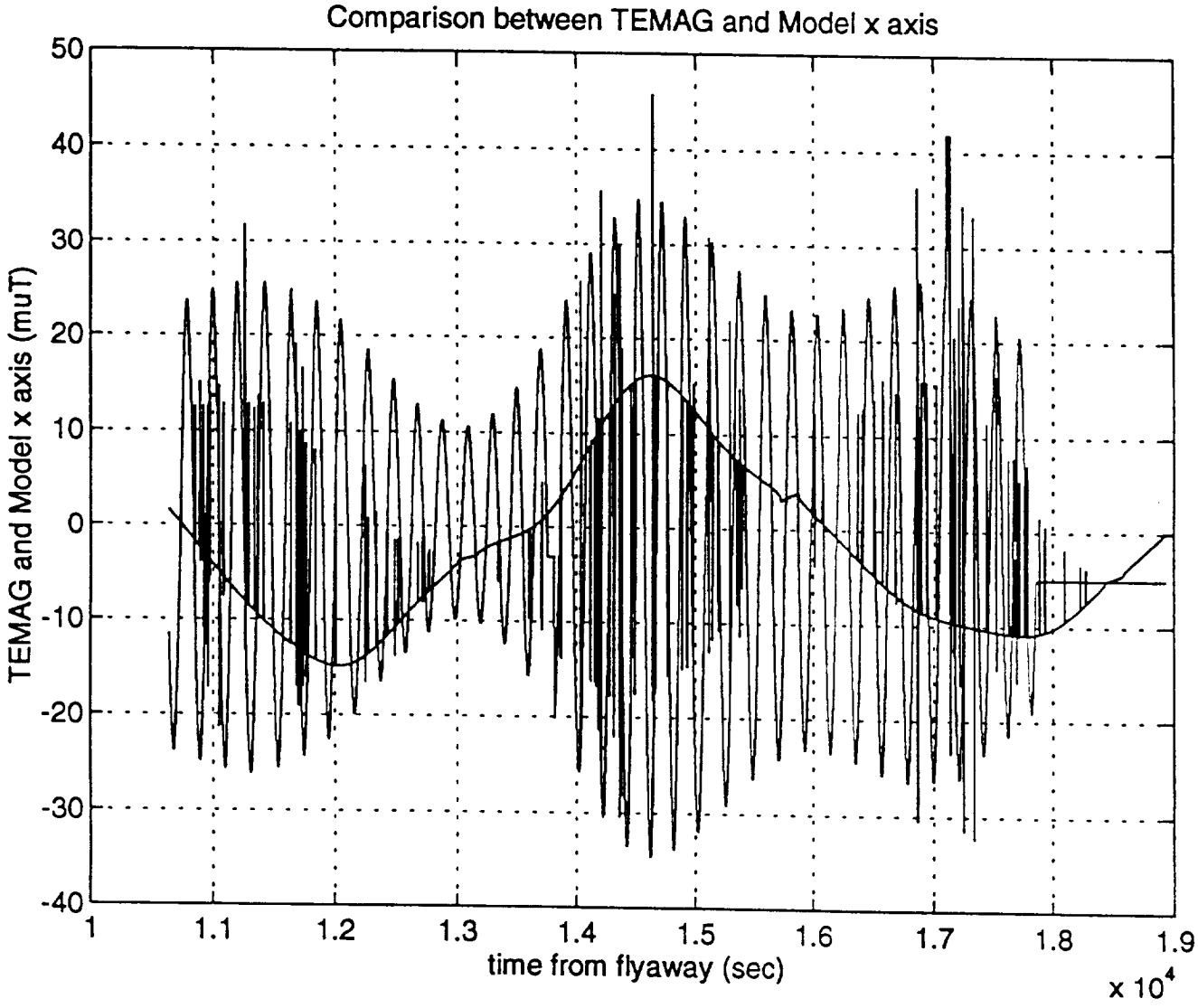
Comparison between TEMAG and Model x axis
TEMAG and Model x axis (muT)
50
40
30
20
10
0
-10
-20
-30
-40
1
1.1
1.2
1.3
1.4
1.5
1.6
1.7
1.8
1.9
time from flyaway (sec)
x 10^4

Figure 7.1

Figure 7.2 shows a similar plot for the y axis and similar comments apply. Figure 7.3 shows the RSS of the Temag x and y (solid) and the model x and y (dotted) data. Figure 7.4 shows Temag and model for the z axis. The model z axis is the smoother curve. From the preceeding discussion, it can be seen there is excellent agreement between the model and the Temag measurements. It should be noted that the libration angle over this time interval is approximately 5 degrees so that the LVLH and satellite z axes are 5 degrees apart. This does not seem to affect the agreement between model and Temag z axes. Calculations made prior to flyaway using telemetry data and satellite attitude relative to LVLH confirmed that the coordinate frames were being properly converted in the pre-processor logic. Thus, Temag is validated as a useful source of SRO data.

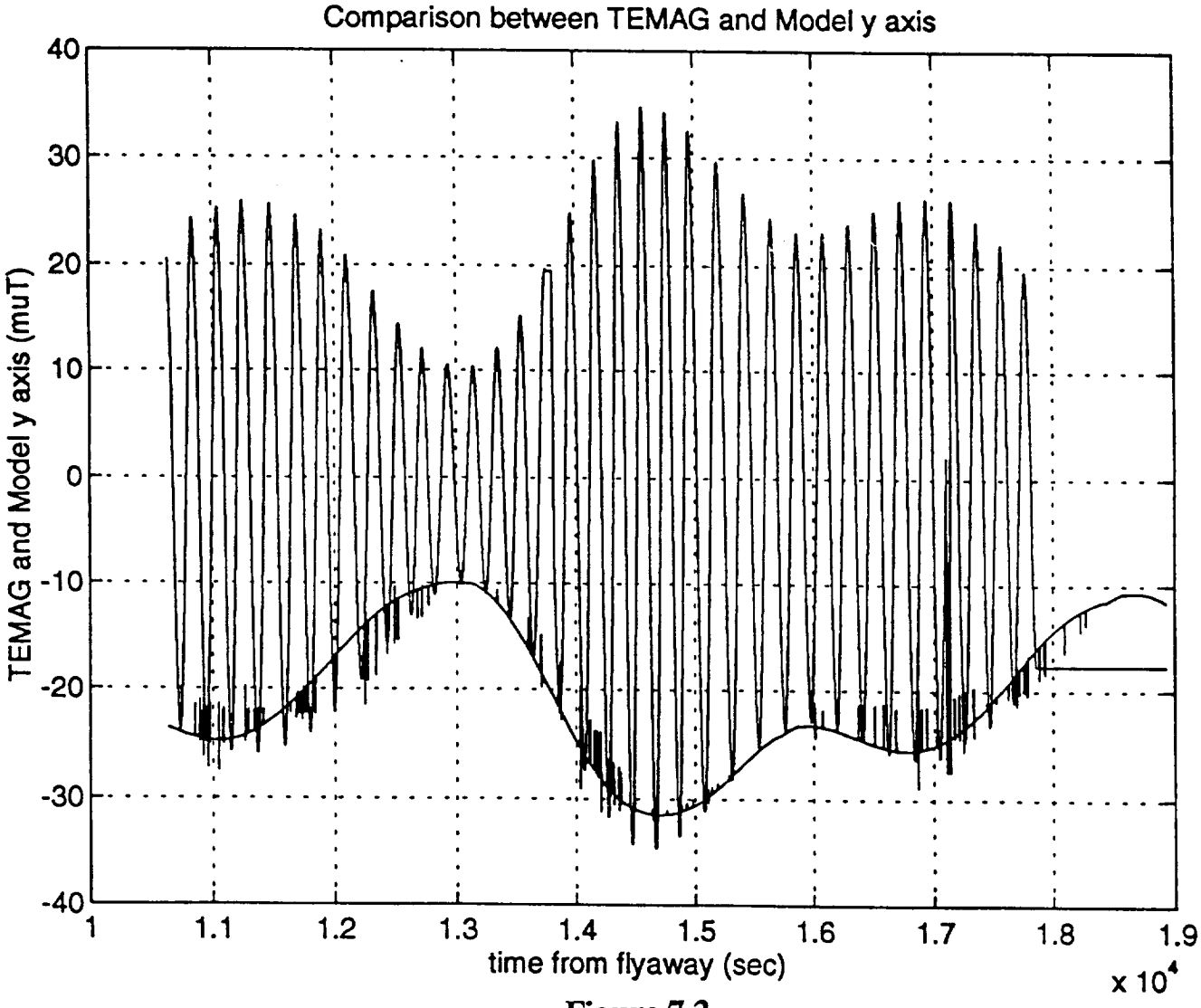

Figure 7.2

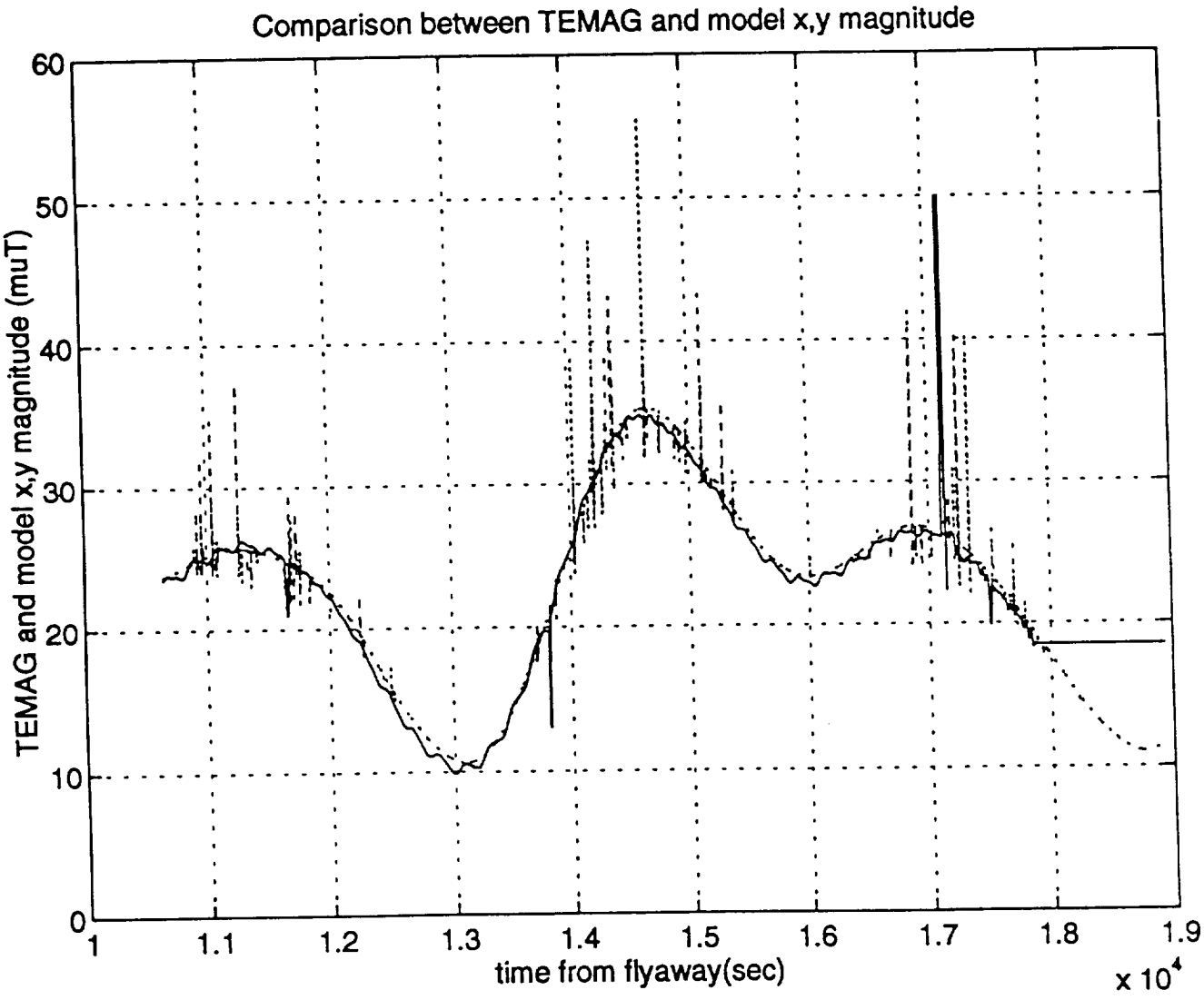
Comparison between TEMAG and model x,y magnitude
TEMAG and model x,y magnitude (muT)
time from flyaway(sec)
x 10^4
0
10
20
30
40
50
60
1
1.1
1.2
1.3
1.4
1.5
1.6
1.7
1.8
1.9

Figure 7.3

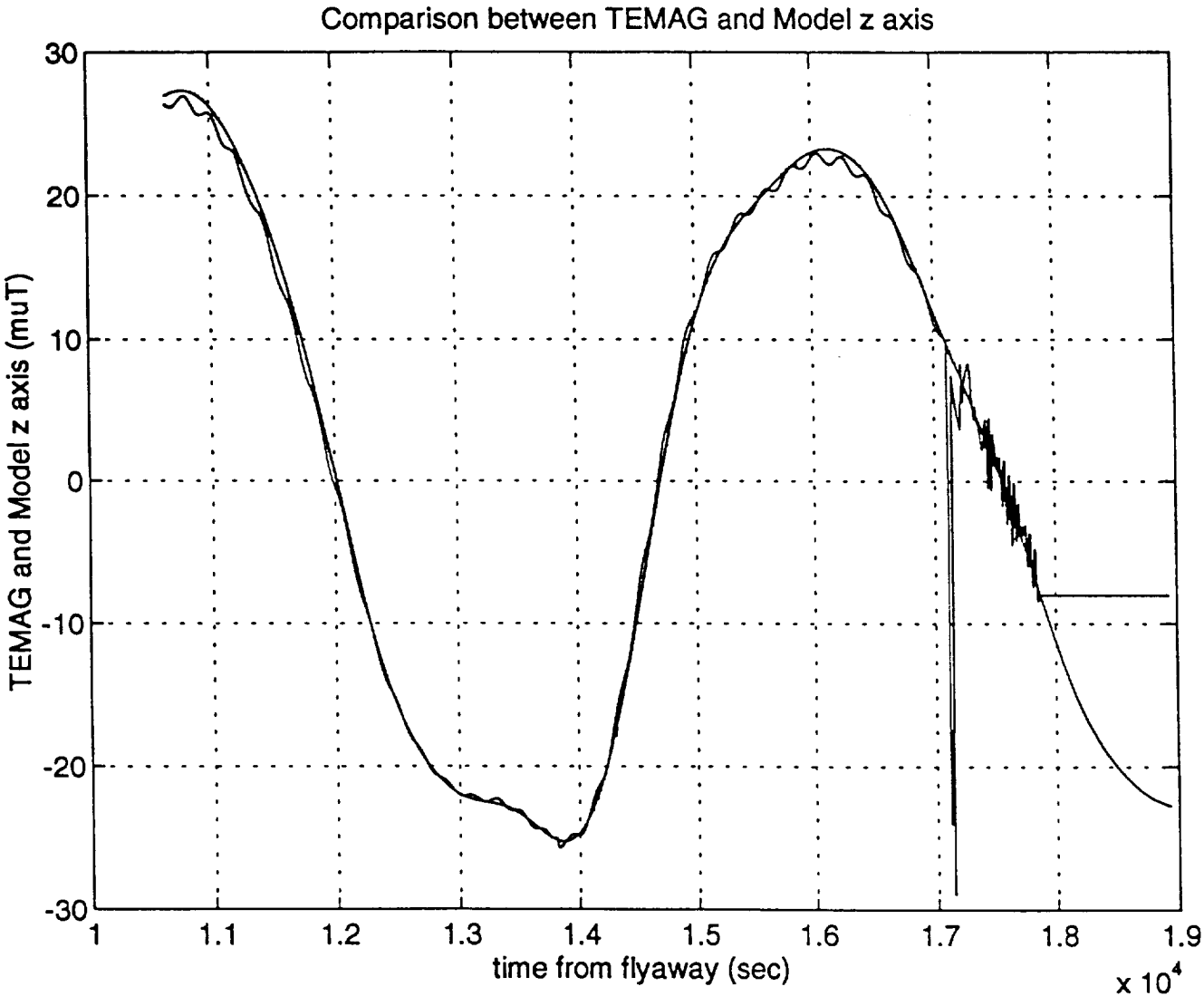
Comparison between TEMAG and Model z axis
TEMAG and Model z axis (muT)
30
20
10
0
-10
-20
-30
1
1.1
1.2
1.3
1.4
1.5
1.6
1.7
1.8
1.9
time from flyaway (sec)
x 10^4

Figure 7.4

8.0 SATELLITE ATTITUDE BEHAVIOR AROUND FLYAWAY

The satellite attitude just prior to and just after flyaway is shown in the three plots in Figures 8.1-8.3. These angles define the satellite attitude determined by the attitude measurement and control system (AMCS) and represent an Euler angle set in a yaw, pitch, roll sequence. There is a significant transient in attitude which occurs shortly after flyaway. Much speculation has been focused toward this transient and there is not currently a consensus toward the cause. Of course, the satellite attitude control is not active for the first 3 minutes and 40 seconds after flyaway and there is no roll or pitch control for considerably longer. There is a loss of data for several seconds shortly after flyaway. One likely source of this transient is the passive damper. The satellite remains in contact with the passive damper for 1-2 minutes after flyaway or until the satellite has deployed approximately 0.5 m. Also, the in line thruster nozzles are arranged in a rectangular pattern while the passive damper ferrule or centerpiece has three spokes corresponding to the 3 negator motors. It is likely the nitrogen gas plume from the firing in line thrusters is reflected by the centerpiece in a non symmetric fashion and may cause the satellite to be pushed to the side until the satellite if sufficiently far away from the centerpiece for this effect to be minimized. This hypothesis has not yet been tested or thoroughly explored.

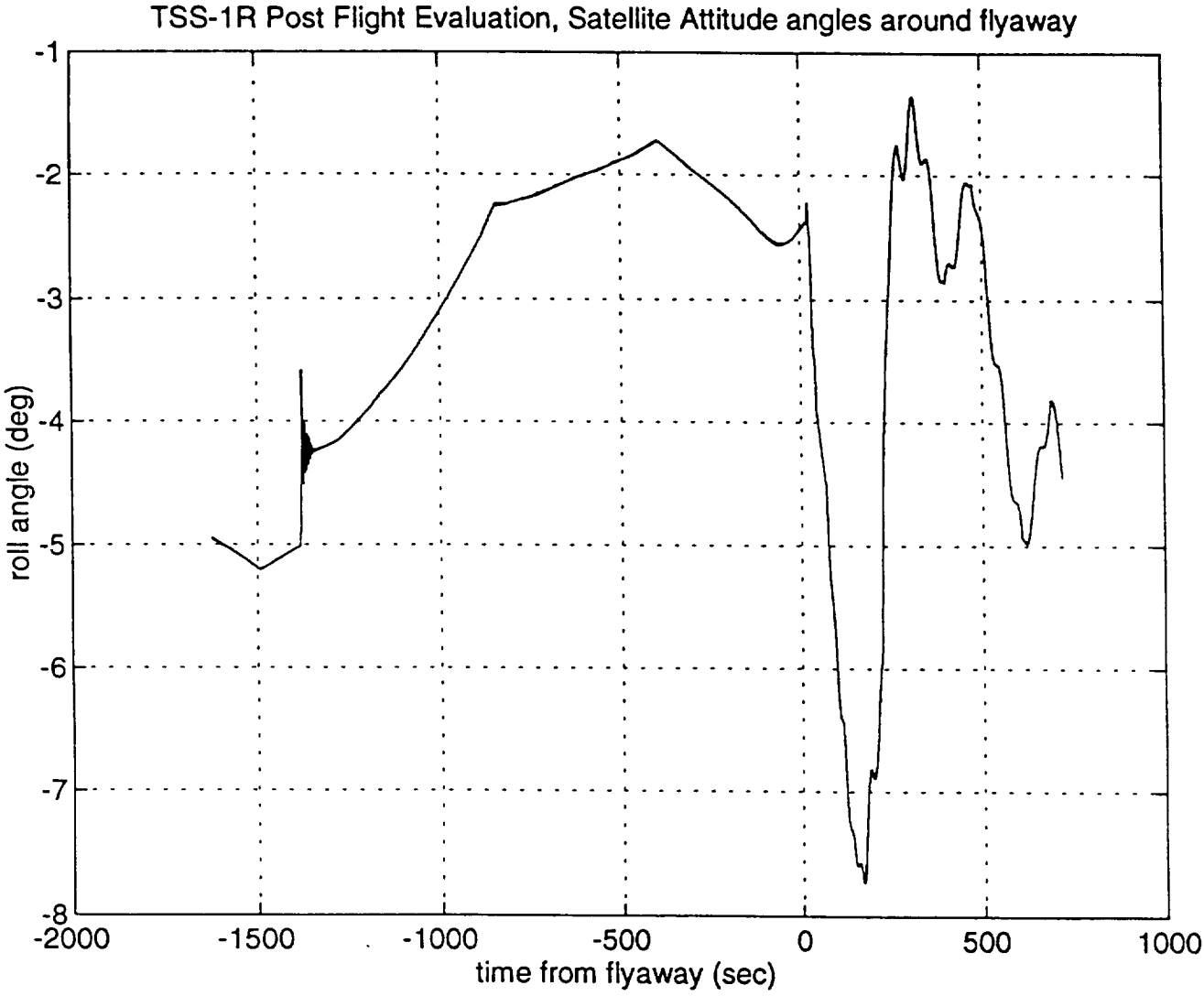
TSS-1R Post Flight Evaluation, Satellite Attitude angles around flyaway
roll angle (deg)
-1
-2
-3
-4
-5
-6
-7
-8
-2000
-1500
-1000
-500
0
500
1000
time from flyaway (sec)

Figure 8.1

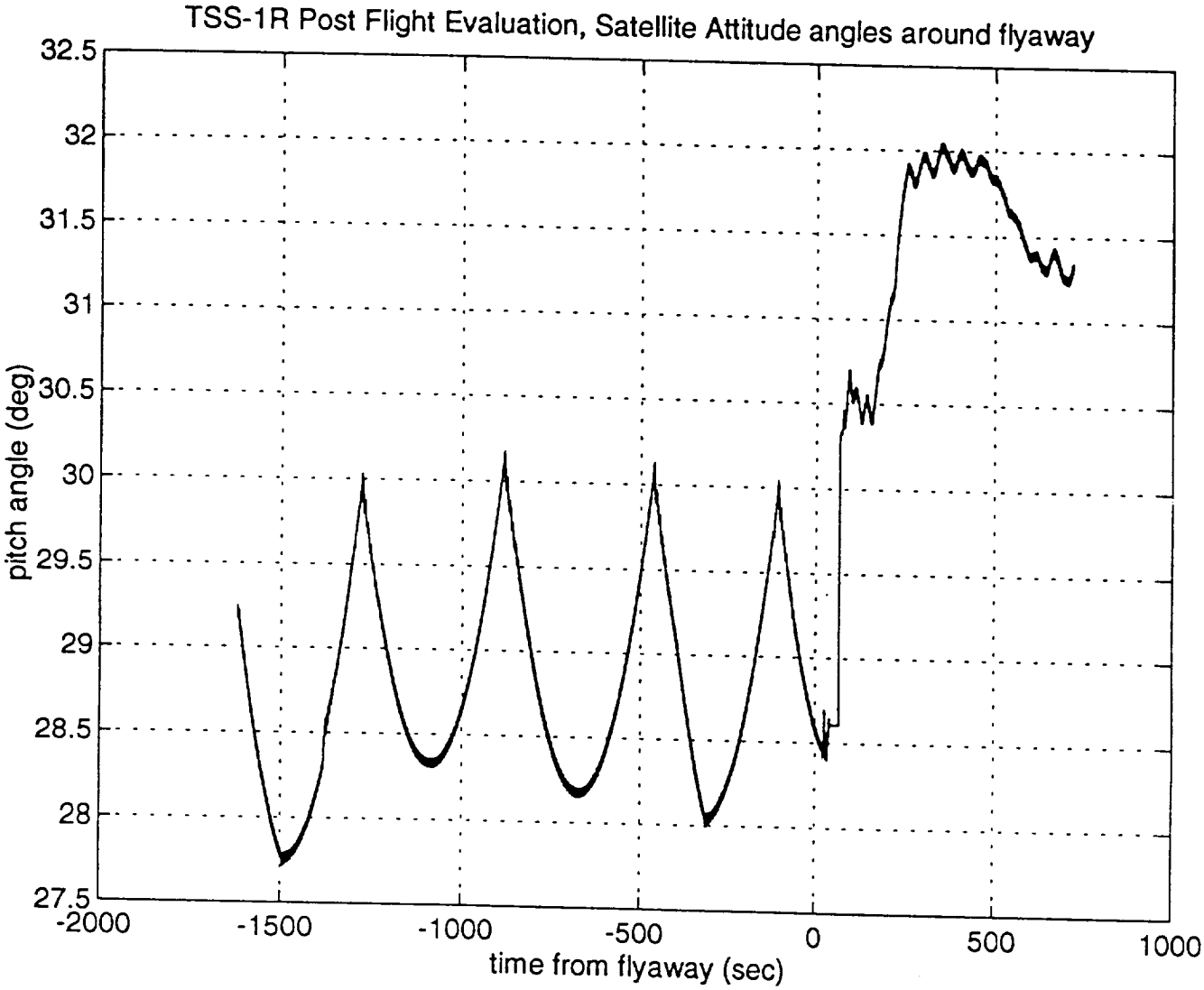
TSS-1R Post Flight Evaluation, Satellite Attitude angles around flyaway
pitch angle (deg)
32.5
32
31.5
31
30.5
30
29.5
29
28.5
28
27.5
-2000
-1500
-1000
-500
0
500
1000
time from flyaway (sec)

Figure 8.2

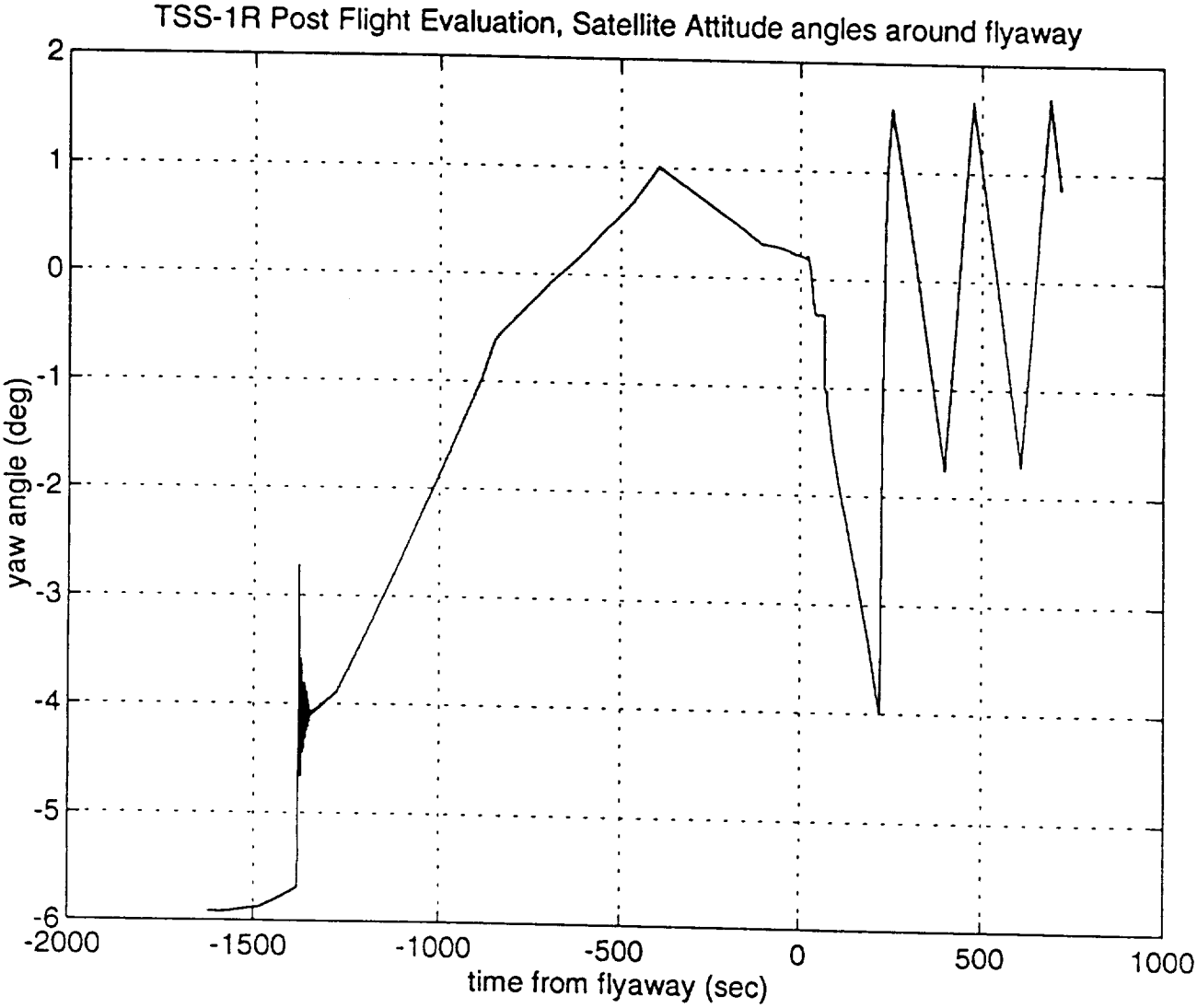
TSS-1R Post Flight Evaluation, Satellite Attitude angles around flyaway
yaw angle (deg)
time from flyaway (sec)
2
1
0
-1
-2
-3
-4
-5
-6
-2000
-1500
-1000
-500
0
500
1000

Figure 8.3

9.0 SATELLITE THRUSTER FIRING HISTORIES

The satellite has several sets of thrusters. For initial deployment and final retrieval at short distances where gravity gradient forces are insufficient to maintain sufficient tension the satellite has in line thrusters whose thrust vectors are aligned with the satellite z axis so that a thrust force is applied to the satellite along the negative z axis. For yaw axis, attitude and spin rate control, the satellite yaw thrusters are provided. For roll and pitch attitude control, the lateral thrusters have been re-directed and are now adapted for this purpose. The ARD control mode was provided to damp satellite pitch and roll rates. Figure 9.1 shows valve open or closed status for the roll and pitch thrusters for the ARD and manual roll and pitch control. This provides the history of the thruster activity for these thrusters. Figure 9.2 shows the activity for the yaw axis thrusters. These figures provide an overview of the times when thruster firings were most and least frequent. The ARD tests show clearly for the roll and pitch thrusters. The passive and active yaw attitude and spin control phases are clearly shown for the yaw thrusters.

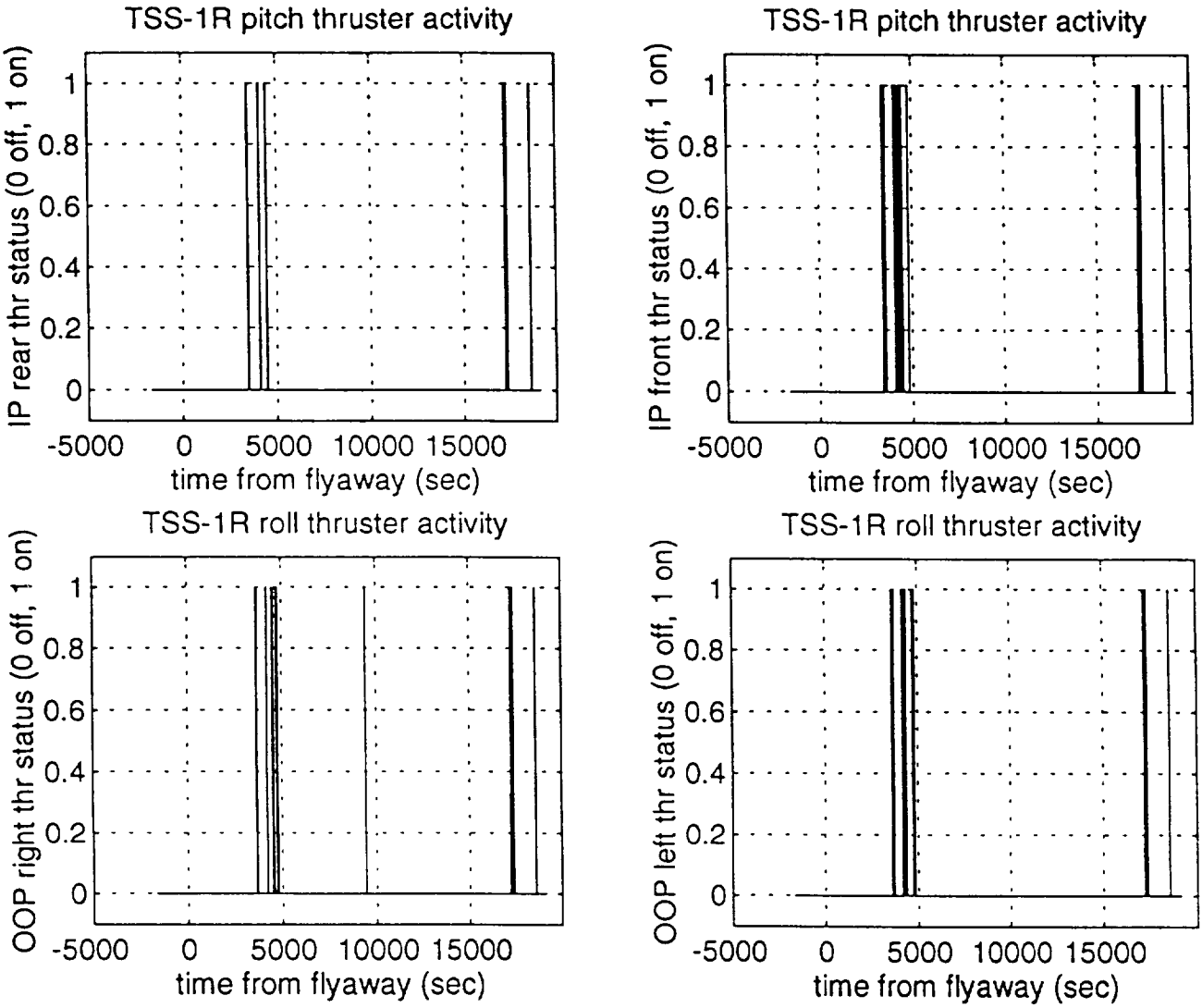
TSS-1R pitch thruster activity
IP rear thr status (0 off, 1 on)
time from flyaway (sec)
TSS-1R pitch thruster activity
IP front thr status (0 off, 1 on)
time from flyaway (sec)
TSS-1R roll thruster activity
OOP right thr status (0 off, 1 on)
time from flyaway (sec)
TSS-1R roll thruster activity
OOP left thr status (0 off, 1 on)
time from flyaway (sec)

Figure 9.1

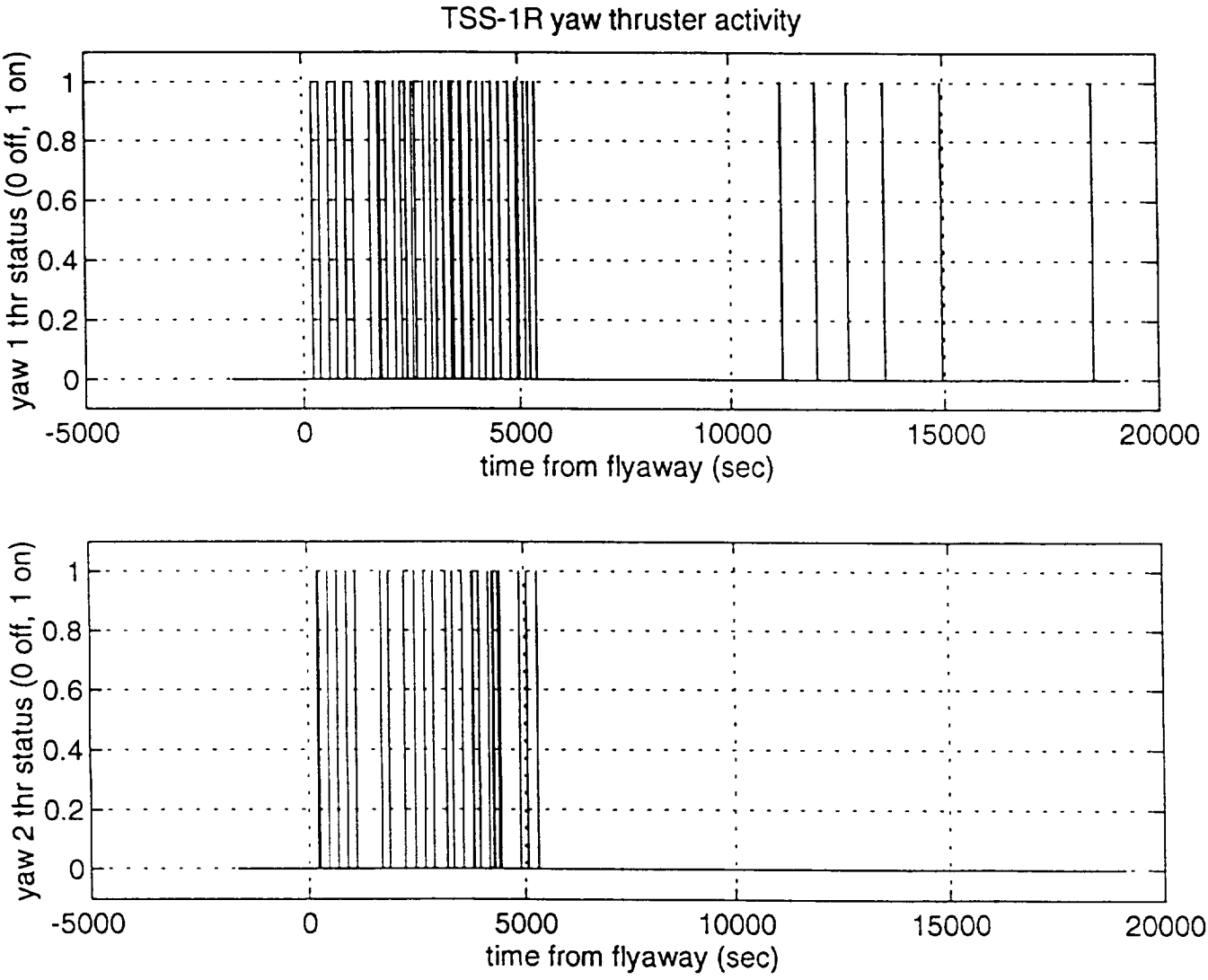
TSS-1R yaw thruster activity
yaw 1 thr status (0 off, 1 on)
1
0.8
0.6
0.4
0.2
0
-5000
0
5000
10000
15000
20000
time from flyaway (sec)
yaw 2 thr status (0 off, 1 on)
1
0.8
0.6
0.4
0.2
0
-5000
0
5000
10000
15000
20000
time from flyaway (sec)

Figure 9.2

10.0 TETHER TENSION

The tension in the TSS-1R tether was measured at two locations. The outboard tension or tension in the deployed tether outside of the deployer boom was measured at a point in the UTCM just before the tether passes through the bugle which is the tether exit from the deployer boom and into free space. There is a coarse and fine tensiometer at this location. The fine tensiometer saturates at approximately 9 N. The coarse tensiometer saturates at a much higher level and is capable of measuring higher levels covering the expected range in excess of the nominal 50 N at the fully deployed length of 20.7 km. The gravity gradient tension levels vary approximately linearly with tether length. The in line thrusters also contribute to the tension levels until they are switched off during the early stages of the deployment. The inboard tensiometer is located in the LTCM and measures the tension in the tether segment between the tether reel and the vernier motor grip pulley. This tension is maintained by the reel controller. The vernier motor applies a tension to the tether pulling it off the reel and through the LTCM and UTXM pulleys and their inherent friction. It's purpose is to overcome the internal friction of the deployer boom and guide pulleys. When it is powered, after its 3 minute ramp up, it is fully powered. Deployment control is exercised by the reel motor and the data acquisition and control assembly (DACA) computer. The control law is length based and is defined to follow a desired deployment profile. Figure 10.1 shows a comparison plot of the inboard and coarse outboard tensiometers. The difference between the two is primarily due to the internal friction in the guide pulleys, tensiometers, the vernier motor and the exit bugle. There is also a bias apparent in the readings of the two tensiometers. This is evident in the difference which shows in the period after the tether has broken. Several discrete events occur during the deployment which cause level shifts in the measured tension that are evident in both tension measurements. The first is in line thruster 1 (IL1) which cuts off 188 seconds after flyaway. The second is IL2 which cuts off 5162 seconds after flyaway. Other events are caused by deployment profile segment changes.

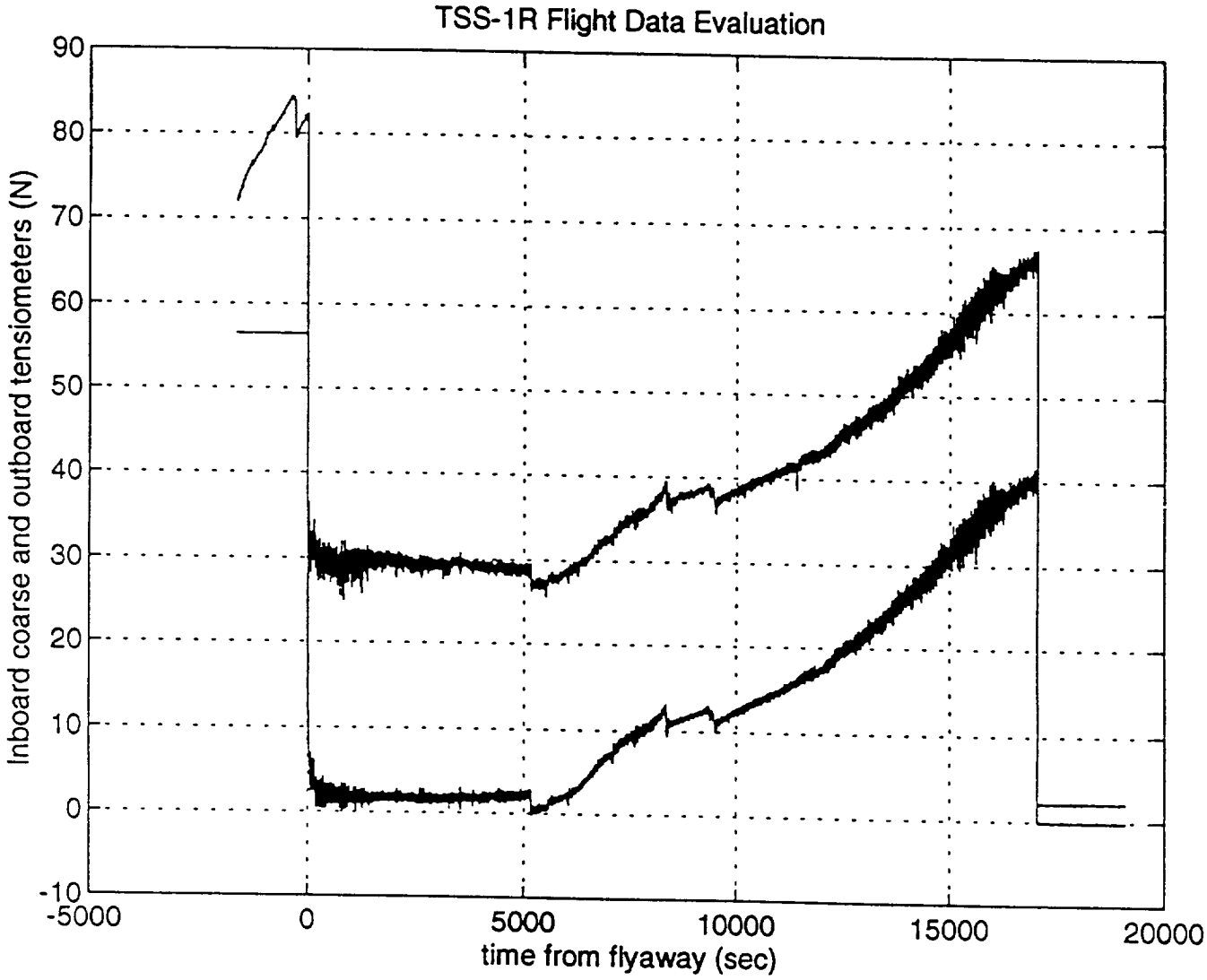
TSS-1R Flight Data Evaluation
Inboard coarse and outboard tensiometers (N)
time from flyaway (sec)
90
80
70
60
50
40
30
20
10
0
-10
-5000
0
5000
10000
15000
20000

Figure 10.1

Figure 10.2 shows the satellite z axis accelerometer multiplied by the satellite mass and converted in sign as appropriate to compare with the outboard coarse tensiometer. The interesting points are that the in line thrusters increase in tension shows up in the tension measurement but not in the accelerometer reading. This is expected since the in line thrust is balanced by the tension force so that no net change in satellite acceleration occurs. The event at approximately 9000 seconds is apparently due to a profile segment change although it is unclear why it does not show up on the accelerometer profile on the satellite.

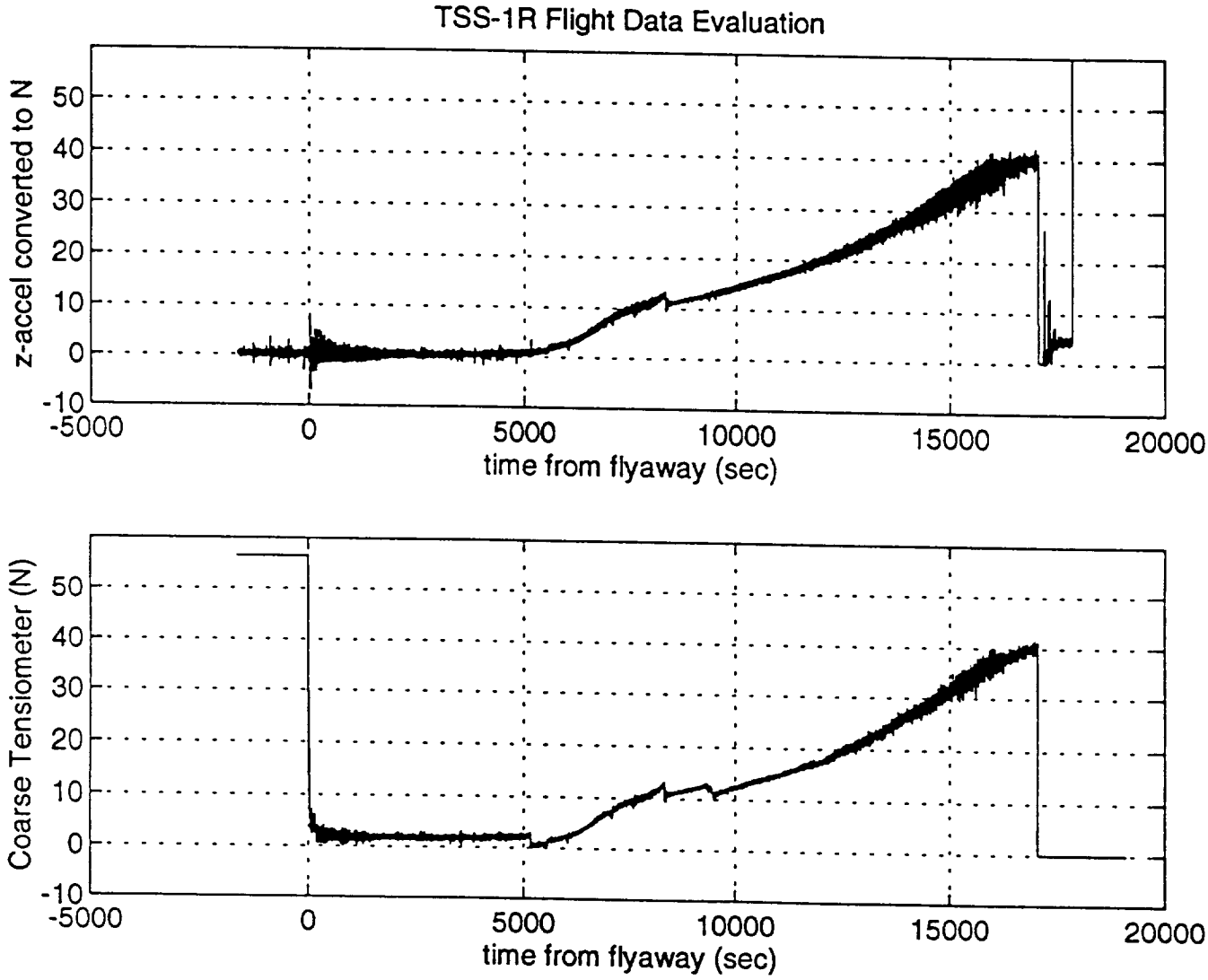

Figure 10.2

A review of Figure 10.1 reveals that this event shows up on both outboard and inboard tensiometers. In a deployment profile segment change the acceleration of the tether changes discontinuously resulting in a tension change. This should also result in an acceleration change on the satellite. The fact that this does not show up on the satellite accelerometer is somewhat of a mystery at this point. We have not reviewed simulation data at this point to determine whether this result is consistent with simulation.

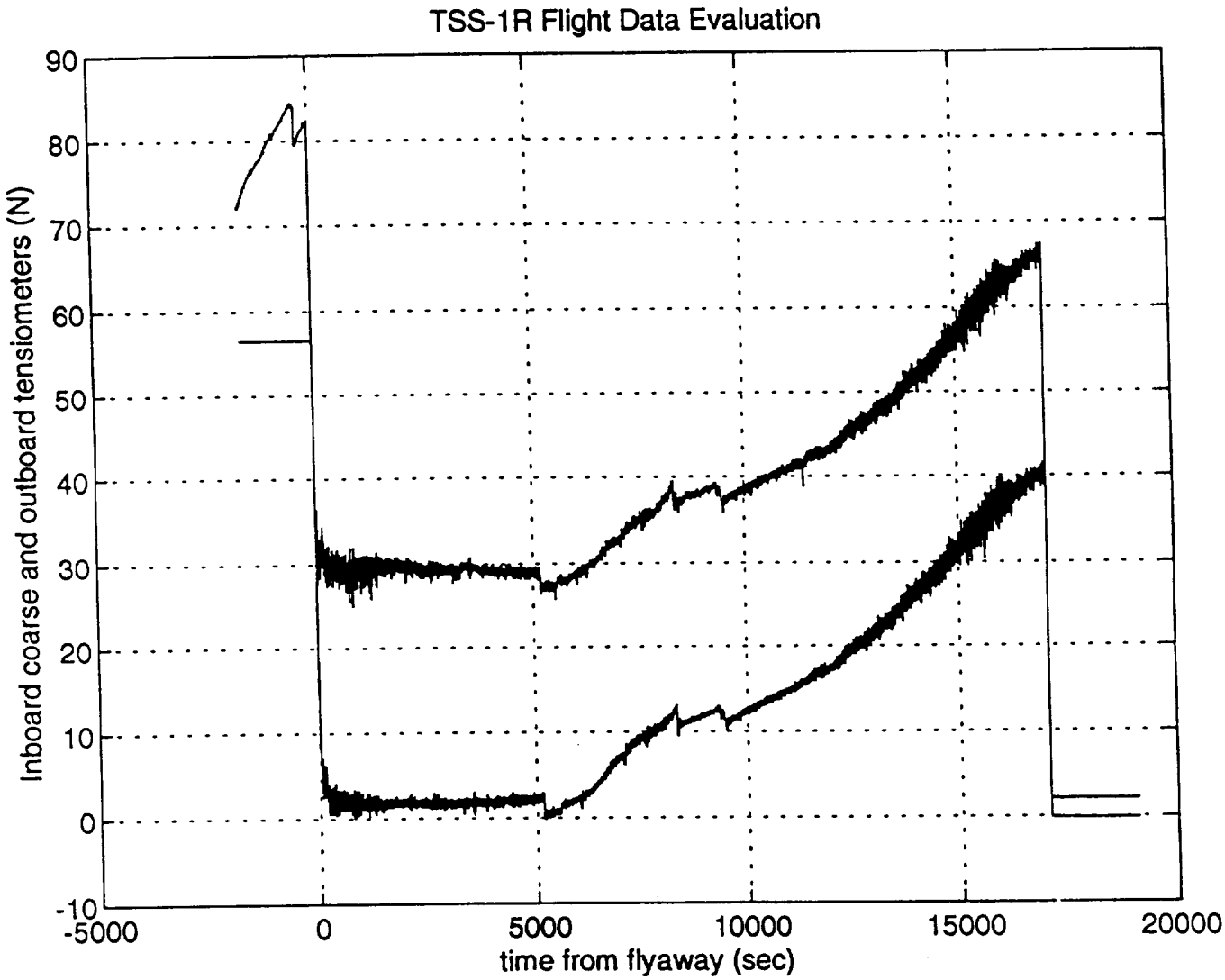

Figure 10.1

As stated previously, neither the satellite accelerometer or either tensiometer on the deployer showed a significant or even observable tension increase at the time of the tether break. Tension levels simply dropped to zero at the time of the break Charring observed on the tether also reinforces that arcing caused the tether break. The evaluation of the tether dynamics of TSS-1R has not revealed any anomalous behavior. The observations made and shown previously are consistent with pre-flight simulations and support the conclusions that tether dynamics associated with the TSS mission is well modeled and understood. It is clear that the events associated with the break in the TSS-1R tether were not related to any tether dynamics anomaly but were associated with the electrodynamics of the current flow and plasma physics of the TSS experiments.

11.0 CONCLUSIONS

The evaluation of the tether dynamics of TSS-1R has not revealed any anomalous behavior. The observations made and shown previously are consistent with pre-flight simulations and support the conclusions that tether dynamics associated with the TSS mission is well modeled and understood. It is clear that the events associated with the break in the TSS-1R tether were not related to any tether dynamics anomaly but were associated with the electrodynamics of the current flow and plasma physics of the TSS experiments.

NASA **Report Documentation Page**

1. Report No.	2. Government Accession No.	3. Recipient's Catalog No.
Final Report		

4. Title and Subtitle	5. Report Date
Tethered Satellite System (TSS) Dynamics Assessments and Analysis, TSS-1R Post Flight Data Evaluation	14 June 1996

7. Author(s)	6. Performing Organization Code
Dr. John R. Glaese	
	8. Performing Organization Report No.

9. Performing Organization Name and Address	10. Work Unit No.
Control Dynamics, A Division of bd Systems, Inc. 600 Boulevard South, Suite 304 Huntsville, Alabama 35802	
	11. Contract or Grant No. NAS8-39880

12. Sponsoring Agency Name and Address	13. Type of Report and Period Covered
National Aeronautics and Space Adminstration George C. Marshall Space Flight Center Marshall Space Flight Center, Alabama 35812	Final 02/01/94 - 06/14/96
	14. Sponsoring Agency Code NASA/MSFC - GP32

15. Supplementary Notes

16. Abstract

This Final report summarizes the work performed under contract NAS8-39880 for TSS 1-R Post Flight Data Evaluation in support of the Marshall Space Flight Center.

17. Key Words (Suggested by Author(s))	18. Distribution Statement
1. Tethered Satellite System (TSS) 2. Tether Dynamics 3. Post Flight Data Evaluation	

19. Security Classif. (of this report)	20. Security Classif. (of this Page)	21. No. of pages	22. Price
Unclassified	Unclassified	66	